ERDC/EL SR-00-9

Environmental Laboratory

US Army Corps of Engineers®
Engineer Research and Development Center

Water Quality Modeling of J. Percy Priest Reservoir Using CE-QUAL-W2

James L. Martin and Thomas M. Cole

August 2000

Approved for public release; distribution is unlimited.

ERDC/EL SR-00-9
August 2000

Water Quality Modeling of J. Percy Priest Reservoir Using CE-QUAL-W2

by James L. Martin, Thomas M. Cole

Environmental Laboratory
U.S. Army Engineer Research and Development Center
3909 Halls Ferry Road
Vicksburg, MS 39180-6199

Final report

Approved for public release; distribution is unlimited

Prepared for U.S. Army Engineer District, Nashville
Nashville, TN

Engineer Research and Development Center Cataloging-in-Publication Data

Martin, James L.
Water quality modeling of J. Percy Priest Reservoir using CE-QUAL-W2 / by James L. Martin, Thomas M. Cole ; prepared for U.S. Army Engineer District, Nashville.
106 p. : ill. ; 28 cm. -- (ERDC/EL ; SR-00-9)
Includes bibliographic references.
1. Water quality -- Tennessee -- J. Percy Priest Reservoir -- Mathematical models. 2. Water temperature -- Tennessee -- J. Percy Priest Reservoir -- Mathematical models. 3. Hydraulic structures -- Tennessee -- Mathematical models. I. Martin, James L. II. Cole, Thomas M. III. United States. Army. Corps of Engineers. Nashville District. IV. U.S. Army Engineer Research and Development Center. V. Environmental Laboratory (U.S.) VI. Title. VII. Series: ERDC/EL SR ; 00-9.
TA7 E8 no. ERDC/EL SR-00-9

REPORT DOCUMENTATION PAGE

Form Approved
OMB No. 0704-0188

Public reporting burden for this collection of information is estimated to average 1 hour per response, including the time for reviewing instructions, searching existing data sources, gathering and maintaining the data needed, and completing and reviewing this collection of information. Send comments regarding this burden estimate or any other aspect of this collection of information, including suggestions for reducing this burden to Department of Defense, Washington Headquarters Services, Directorate for Information Operations and Reports (0704-0188), 1215 Jefferson Davis Highway, Suite 1204, Arlington, VA 22202-4302. Respondents should be aware that notwithstanding any other provision of law, no person shall be subject to any penalty for failing to comply with a collection of information if it does not display a currently valid OMB control number. **PLEASE DO NOT RETURN YOUR FORM TO THE ABOVE ADDRESS.**

1. REPORT DATE *(DD-MM-YYYY)*
August 2000

2. REPORT TYPE
Final Report

3. DATES COVERED *(From - To)*

4. TITLE AND SUBTITLE
Water Quality Modeling of J. Percy Priest Reservoir Using CE-QUAL-W2

5a. CONTRACT NUMBER

5b. GRANT NUMBER

5c. PROGRAM ELEMENT NUMBER

6. AUTHOR(S)
James L. Martin, Thomas M. Cole

5d. PROJECT NUMBER

5e. TASK NUMBER

5f. WORK UNIT NUMBER

7. PERFORMING ORGANIZATION NAME(S) AND ADDRESS(ES)

U.S. Army Engineer Research and Development Center
Environmental Laboratory
3909 Halls Ferry Road
Vicksburg, MS 39180-6199;

8. PERFORMING ORGANIZATION REPORT NUMBER
ERDC/EL SR-00-9

9. SPONSORING / MONITORING AGENCY NAME(S) AND ADDRESS(ES)
U.S. Army Engineer District, Nashville
Nashville, TN

10. SPONSOR/MONITOR'S ACRONYM(S)

11. SPONSOR/MONITOR'S REPORT NUMBER(S)

12. DISTRIBUTION / AVAILABILITY STATEMENT
Approved for public release; distribution is unlimited.

13. SUPPLEMENTARY NOTES

14. ABSTRACT

The U.S. Army Engineer District, Nashville (CELRN), plans to apply the two-dimensional hydrodynamic and water quality model CE-QUAL-W2 to all Corps of Engineers reservoirs in the Cumberland basin to provide a tool capable of simulating temperature and water quality related issues that currently exist or may arise in the future. One of the planned applications was to the J. Percy Priest Reservoir located near Nashville, TN. The CELRN requested the assistance of the Water Quality and Contaminant Modeling Branch at the U.S. Army Engineer Research and Development Center to develop and apply CE-QUAL-W2 to this reservoir.

The objective of this study is to provide a calibrated temperature and water quality model for J. Percy Priest Reservoir suitable for addressing a variety of management related issues.

CE-QUAL-W2 (Version 2), a two-dimensional, longitudinal and vertical hydrodynamic and water quality model, was chosen for the study. The model is recognized as the state-of-the-art reservoir hydrodynamic and water quality model and has been successfully applied to over 100 different systems in the United States and throughout the world. It is the reservoir model of choice for TVA, USBR, USGS, USACE, and USEPA.

(Continued)

15. SUBJECT TERMS

CE-QUAL-W2	Euthropication	Reservoir
Dissolved oxygen	Model	Temperature

16. SECURITY CLASSIFICATION OF:			17. LIMITATION OF ABSTRACT	18. NUMBER OF PAGES	19a. NAME OF RESPONSIBLE PERSON
a. REPORT	b. ABSTRACT	c. THIS PAGE			19b. TELEPHONE NUMBER *(include area code)*
UNCLASSIFIED		UNCLASSIFIED		106	

14. (Concluded)

The model consists of a hydrodynamic module that predicts water surface elevations, horizontal/vertical velocities, and temperature. The hydrodynamics are influenced by variable water density resulting from variations in temperature, total dissolved solids, and suspended solids. Twenty-two water quality state variables, including temperature, and their kinetic interactions are included in the water quality module.

Any combination of these state variables can be included in a simulation, but care must be taken to ensure that all relevant variables are included. Twelve state variables, including temperature, were simulated in this application. These included all relevant variables for computing algal/nutrient/DO interactions and their effects on water quality within the reservoir. In addition, the model was modified to simulate water age as a state variable, which can be used to evaluate the retention time of the reservoir or portions thereof.

A calibrated CE-QUAL-W2 model of J. Percy Priest has been developed suitable for addressing a variety of management related issues. The water quality model, while only a simplified description of what in reality is a very complex system, generally accurately predicted variations in temperature, dissolved oxygen concentrations, iron and nutrients, in comparison to observed data for the 5 years of simulation (1976-1978, 1981 and 1994). The 5 years represented hydrologic conditions ranging from dry (1981) to wet (1994). The model was then used to demonstrate two potential management related issues: an additional wastewater discharge to the reservoir, and a dissolved oxygen injection system. For the later scenario, the model was modified based upon a previous application to Richard B. Russell Reservoir.

For this application, none of the kinetic coefficients were varied between simulation years. Rather, a considerable portion of the effort required for the application consisted of determining a consistent set of kinetic coefficients for all years simulated. However, it is not entirely reasonable to assume that algal populations, sediment release rates, and other processes would be constant over the 18-year time span between the 1976 and 1994 applications. The collection of more recent data may provide a basis for additional calibration to present conditions.

While model predictions were in reasonable agreement with observed data, predictions were responsive to changes in loadings. However, inflows and loadings to the system were generally based on estimated, rather than measured, values. Errors in loadings were potentially greatest for the 1981 and 1994 simulation years, since the methods used to estimate the loadings were developed using data collected in the 1970's. Until such time as more recent data are collected, it is suggested that the best use of the model as a management tool would be to assess relative rather than absolute impacts of alternative management scenarios.

Contents

Preface v

1—Introduction 1

Background 1
Objective 1
Approach 1
Site Description 3

2—Data Analysis 7

3—Input Data 10

Bathymetry 10
In-Pool Data 12
Boundary Conditions 12
Meteorology 12
Tributary boundary conditions 12
Point sources 17
Outflows 17

4—Model Evaluation 20

Application to 1976-1978 23
Water surface elevations 24
Water age 24
Temperature 25
Dissolved oxygen 27
Nutrients 28
Algae 33
Iron 36
Application to 1981 38
Water surface elevations 38
Water age 38
Temperature 38
Dissolved oxygen 41
Nutrients 42

Algae 44
Iron 47
Application to 1994 47
Water surface elevations 48
Water age 48
Temperature 49
Dissolved oxygen 51
Nutrients 52
Algae 55
Iron 57

5—Evaluation of Model Scenarios 58

Wastewater Treatment Plants 58
Dissolved Oxygen Injection 61
Model theory 61
Implementation in CE-QUAL-W2 62

6—Conclusions and Recommendations 66

References 67

Appendix A: A1

Appendix B: B1

Appendix C: C1

Preface

This report presents results of a CE-QUAL-W2 Water Quality Modeling Study for J. Percy Priest Reservoir. This report was prepared in the Environmental Laboratory (EL), U.S. Army Engineer Research and Development Center (ERDC), Vicksburg, MS. The study was sponsored by the U.S. Army Engineer District, Nashville (CELRN-EP-H), and was funded under the Military Interdepartmental Purchase Request No.W38XDD90841781 dated 25 March 1999.

The Principal Investigators of this study were Dr. James L. Martin, P. E., and Mr. Thomas M. Cole, Water Quality and Contaminant Modeling Branch (WQCMB), Environmental Processes and Effects Division, EL. This report was prepared by Dr. Martin and Mr. Cole under the direct supervision of Dr. Mark Dortch, Chief, WQCMB, and under the general supervision of Dr. Richard Price, Chief, Environmental Processes and Effects Division (EPED), and Dr. John Keeley, Acting Director, EL. Technical reviews by Dr. Barry W. Bunch and Ms. Dorothy H. Tillman are gratefully acknowledged.

At the time of publication of this report, Director of ERDC was Dr. James R. Houston, and Commander was COL James S. Weller, EN.

This report should be cited as follows:

> Martin, James L., and Cole, Thomas M. (1999). "Water Quality Modeling of J. Percy Priest Reservoir Using CE-QUAL-W2," ERDC/EL SR-00-9, U.S. Army Engineer Research and Development Center, Vicksburg, MS.

1 Introduction

Background

The U.S. Army Engineer District, Nashville (CELRN), plans to apply the two-dimensional hydrodynamic and water quality model CE-QUAL-W2 to all Corps of Engineers reservoirs in the Cumberland basin to provide a tool capable of simulating temperature and water quality related issues that currently exist or may arise in the future. One of the planned applications was to the J. Percy Priest Reservoir located near Nashville, TN. The CELRN requested the assistance of the Water Quality and Contaminant Modeling Branch at the U.S. Army Engineer Research and Development Center to develop and apply CE-QUAL-W2 to this reservoir.

Objective

The objective of this study is to provide a calibrated temperature and water quality model for J. Percy Priest Reservoir suitable for addressing a variety of management related issues.

Approach

CE-QUAL-W2 (Version 2), a two-dimensional, longitudinal and vertical hydrodynamic and water quality model, was chosen for the study. The model is recognized as the state-of-the-art reservoir hydrodynamic and water quality model and has been successfully applied to over 100 different systems in the United States and throughout the world. It is the reservoir model of choice for TVA, USBR, USGS, USACE, and USEPA.

The model consists of a hydrodynamic module that predicts water surface elevations, horizontal/vertical velocities, and temperature. The hydrodynamics are influenced by variable water density resulting from variations in temperature, total dissolved solids, and suspended solids. Twenty-two water quality state variables (including temperature) and their kinetic interactions are included in the water quality module. They are:

1. conservative tracer
2. suspended solids
3. coliform bacteria
4. total dissolved solids or salinity
5. labile dissolved organic matter
6. refractory dissolved organic matter
7. phytoplankton
8. Labile particulate organic matter
9. phosphate phosphorus
10. ammonia nitrogen
11. nitrate + nitrite nitrogen
12. dissolved oxygen
13. organic sediments
14. total inorganic carbon
15. alkalinity
16. pH
17. carbon Dioxide
18. bicarbonate
19. carbonate
20. total iron
21. BOD

Any combination of these state variables can be included in a simulation, but care must be taken to ensure that all relevant variables are included. The state variables included for this study were variables 1, 2, 5-12, 20, and water temperature. These included all relevant variables for computing algal/ nutrient/DO interactions and their effects on water quality within the reservoir. In addition, the model was modified to simulate water age as a state variable, which can be used to evaluate the retention time of the reservoir or portions thereof.

Site Description

J. Percy Priest Reservoir is located in the Stones River Basin in central Middle Tennessee. The Stones River flows into the Cumberland River at mile 205.9, which is about 15 river miles upstream of Nashville. Most of the basin lies within Rutherford County (60%) with significant portions lying in Wilson (18%), Cannon (14%), and Davidson (8%) Counties.

The project lies within the Central or Nashville Basin region of the Central Highland Province, and the area is characterized by topographic features varying from gentle slopes to bluffs with slopes in excess of 20 percent. Sinkholes and other karst features are found throughout the project which resulted from the action of groundwater on the predominantly limestone formations. J. Percy Priest Reservoir lies in the Stones River watershed (Hydrologic Unit Code 0513023), with a total area of 926 square miles. There are a total of 13 rivers and streams in the watershed with a total of 879.3 river miles and 642.2 perennial river miles. As of 1990, the total population in the watershed was approximately 200,000. The watershed is characterized by gently rolling hills. The limestone bedrock formations predominant throughout this area are of Ordovician age, consisting of Lebanon and Hermitage formations. Some of the limestone formations are rich in organic phosphates, and commercial mining operations for these materials have been conducted in the basin. The area is also characterized by karst topography from the formation and collapse of soluble limestone caverns, which creates many small landforms around the project such as sinkholes. The lower end of the lake is characterized by heavily forested areas, while the middle and upper regions of the lake are characterized by cedar glades, forested areas, and agricultural lands developed for wildlife management purposes. For the most part, soils along the shoreline are thin and rocky and large sections of exposed bedrock are common. Forests in the area have been repeatedly cut and are comprised mostly of oak, hickory, and eastern red cedar. Cedar glades are common throughout the area, and contain several rare and endangered plants (CELRN 1978, 1999)

J. Percy Priest Reservoir was created by the impoundment of the Stones River. J. Percy Priest has 213 miles of shoreline at summer pool elevation 490.0 feet above mean sea level, and extends approximately 42 miles at this elevation. J. Percy Priest has an average depth of 28.7 feet, with a 90-foot depth at the dam.

Initially, the project was authorized as Stewarts Ferry Reservoir in 1946, but was changed to J. Percy Priest Reservoir in honor of the late Congressman from Tennessee. Acquisition of lands for the reservoir began in 1963, and construction of the dam began in June 1963. The dam is a combination rolled earthfill and concrete gravity, with a length of about 2,000 feet. The spillway is a controlled ogee type, concrete gravity spillway with a gross length of crest of 213 feet, surmounted by four tainter gates, 45 feet by 41 feet. The powerplant has one unit with a capacity of 28,000 kw. The dam was closed on 18 September 1967 and the pool allowed to fill during the next several months. The normal summer pool elevation was first reached in June 1968. The generator was placed in commercial operation in February 1970 (CELRN 1978, 1999).

As a unit of the comprehensive development plan for the Cumberland River Basin in Tennessee and Kentucky, J. Percy Priest Lake furnishes hydroelectric power which is marketed by the Southeastern Power Administration, most of which is sold to the Tennessee Valley Authority. In addition to hydroelectric power production, other project purposes include flood control, recreation, water quality, fish, forest, and wildlife conservation deemed necessary in the public interest.

The reservoir is thermally stratified for about 7-8 months of the year and anaerobic conditions in the hypolimnion exist for at least five of these months. During the period when the hypolimnion is anaerobic, the concentrations of ammonia, phosphorus, hydrogen sulfide, iron and manganese increase significantly in the deep layers. Power generation during the summer and fall results in the release of water with undesirably high concentrations of these parameters and a low dissolved oxygen concentration (CELRN 1999)

In general, the overall quality of waterbodies within the Stones River watershed are reported to be good. According to the USEPA's Index of Water Quality Indictors, the IWI score of the watershed is "2." This IWI score results in a watershed classification of "Better Water Quality", indicating that designated uses are largely met and other indicators of watershed condition show few problems (see score at http://www.epa.gov/iwi/hucs/05130203/score.html). The watershed is also classified as a high vulnerability area with significant pollution and other stressors and, therefore, a higher vulnerability to declines in aquatic health, requiring action to protect quality and prevent decline. A number of waterbodies within the watershed do not meet their designated use and are included on the 1998 303(d) list of impaired waterbodies. These waterbodies are listed in Table 1 and the locations illustrated in Figure 1.

Table 1. 303(d) List of Impaired Waterbodies for 1998 (From USEPA TMDL Web Site: http://www.epa.gov/owow/tmdl/)

Waterbody	Parameter Of Concern	Priority For TMDL Development	Potential Sources Of Impairment
Stones River	Other Inorganics, Flow Alterations, Organic Enrichment/Low Do, Taste And Odor	Low	Upstream Impoundment
McCrory Creek	Habitat Alterations, Pathogens	Low	Urban Runoff/Storm Sewers, Collection System Failures
Finch Branch	Habitat Alterations, Organic Enrichment/Low Do, Pathogens	Low	Collection System Failure, Riparian Loss, Land Development
Stewarts Creek	Flow Alterations, Habitat Alterations, Siltation	Low	Land Development,Urban Runoff/Storm Sewers
Overall Creek	Habitat Alterations, Organic Enrichment/Low Do	Low	Pastureland
West Fork Stones River	Organic Enrichment/Low Do	High	Land Development, Municipal Point Source
Lytle Creek	Habitat Alterations, Oil And Grease, Siltation	Low	Riparian Loss, Urban Runoff/Storm Sewers
Bear Branch	Habitat Alterations, Organic Enrichment/Low Do, Siltation	Low	Land Development, Pastureland, Riparian Loss
Wades Branch	Siltation, Other Habitat Alterations	Low	Pastureland, Habitat Modification
Cripple Creek	Habitat Alterations, Siltation	Low	Pastureland, Riparian Loss
East Fork Stones	Habitat Alterations	Low	Habitat Modification
East Fork Stones Tributaries	Other Habitat Alterations	Low	Agriculture, Riparian Loss
Bradley Creek	Habitat Alterations, Organic Enrichment/Low Do, Siltation	Low	Pastureland, Riparian Loss
Fall Creek	Siltation	Low	Pastureland, Riparian Loss
Stoners Creek	Oil And Grease, Pathogens, Siltation	Low	Spills, Collection System Failure, Industrial Permitted Runoff, Land Development
Hurricane Creek	Nutrients, Organic Enrichment/Low Do, Siltation Thermal Modifications	Low	Channelization, Industrial Point Source, Land Development, Riparian Loss
East And West Fork Hamilton Creek	Pathogens Organic Enrichment/Low Do	Low	Collection System Failure,

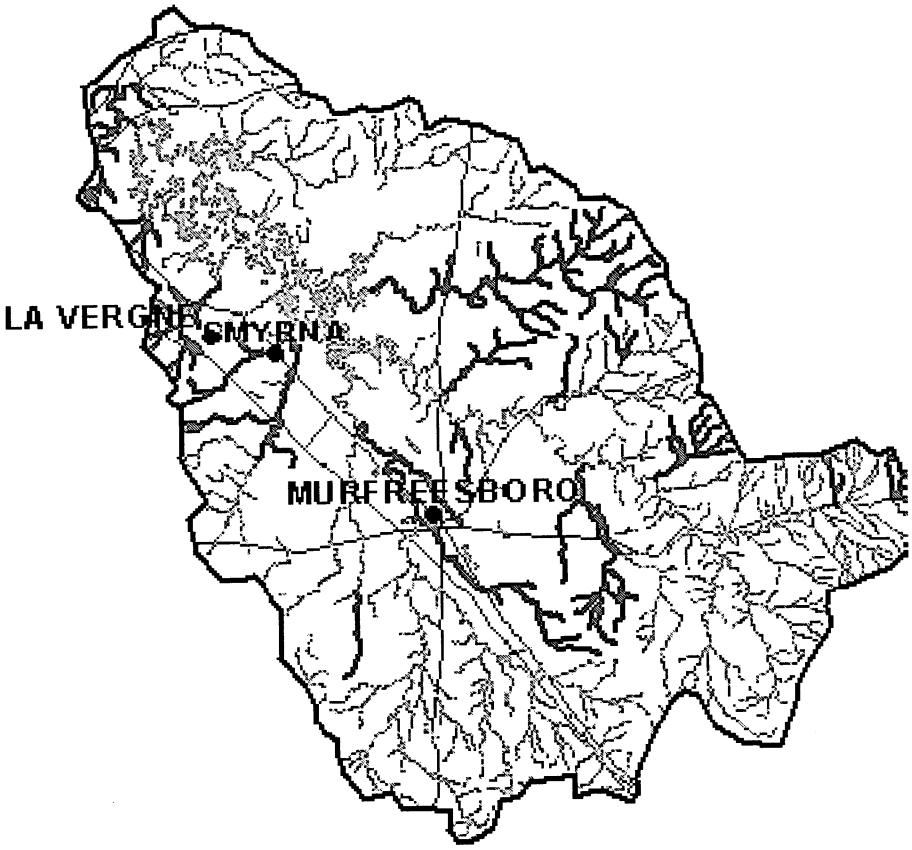

Figure 1. Locations of Impaired Waterbodies in the Stones Basin (from USEPA TMDL web site: http://www.epa.gov/owow/tmdl/).

2 Data Analysis

The first task in this study was to analyze all existing data to determine the years for the model application. ACCESS files containing all Corps of Engineers (CE) water quality data from the J. Percy Priest project were supplied by CELRN, along with an interface providing access to the data. The data included area and capacity curves, measured water surface elevations, measured outflows, computed inflows, and all water quality data collected. The locations of water quality stations evaluated are illustrated in Figure 2. Log sheets indicated the sampling dates for each water quality station were also provided for the period of 1970-1998.

A minimum of four years were to be selected to represent conditions classified as wet, dry and normal, as well as an additional year for model evaluation. The data were analyzed, collaboratively by WES and CELRN, based upon rates of flows and the sufficiency of data for model forcings (boundary conditions) and in-pool data for comparison with model predictions.

Although J. Percy Priest reservoir was impounded in 1968, data were not collected until 1970. The period of consideration, as specified by CELRN was 1970-1998. Based upon available data, the WES and CELRN categorized these years as wet, dry, normal, or mixed, as shown in Table 2.

Table 2. Classification of Hydrologic Conditions for 1970-1998

Wet Years	Dry years	Normal Years	Mixed Years
1970	1981	1971	1972
1973	1985	1976	1974
1975	1987	1991	1977
1979	1988	1993	1978
1984	1990	1995	1980
1989			1982
1994			1983
1996			1986
			1992
			1997
			1998

The analysis of available water quality data indicated that chlorophyll *a* data were not collected prior to 1975, eliminating 1970-1975 from consideration. In addition, the following years had 3 or less sampling trips during those years, and

were removed from consideration: 1970, 1980, 1984-1993, and 1995-1998. The data for the remaining years was analyzed by both examining the number of dates for which data were available and graphical comparisons of all available data. The year 1976 had the most complete data set. However, dissolved oxygen concentrations during 1976 were consistently greater than saturation in surface waters at 3JPPS20002. The dissolved oxygen saturation was 170 percent in August at 3JPPS10015 but only 96 percent at 3JPPS10016. The years 1977 and 1978 also had reasonably complete data sets. The data for 1981 was limited, with boundary stations only collected once during the year. The data for 1994 were reasonably complete. However, for 1994 boundary stations were only sampled 5 times (March, May, July and twice in November). No BOD data were collected for the boundary stations during 1994, and only three samples were analyzed for iron. The principal calibration stations were sampled 6 times for temperature and DO (February, then March-November), and 5 times for nutrients, during 1994. The DO exceeded saturation in the early months of 1994.

The availability of data is summarized in Table 3.

Table 3. Summary of Available Data for all In-Reservoir and Boundary Stations.

Year	Condition	No. of dates for which in-pool data are available	No. of dates for which boundary data are available	Summary
1976	Normal	7	15-18	Most complete data set
1977	Mixed	3-5	10-14	Reasonably complete data set
1978	Mixed	3-8	2-5	Boundary data limited
1979	Wet	0-11	1-2	Few boundary data
1981	Dry	0-4	1	Few data
1982	Mixed	2-3	1	Few data
1983	Mixed	0-3	0-2	Few data
1994	Wet	5-6	0-5	Little data

Based upon the above analysis, the years 1976-1978 and 1994 contained the most available data, and were selected for the model application. The years 1976-1978 would be run continuously as a further test for the model application. However, these years did not include a dry year. Therefore, 1981 was selected as the dry year for the simulation, even though the available data for that year were very limited.

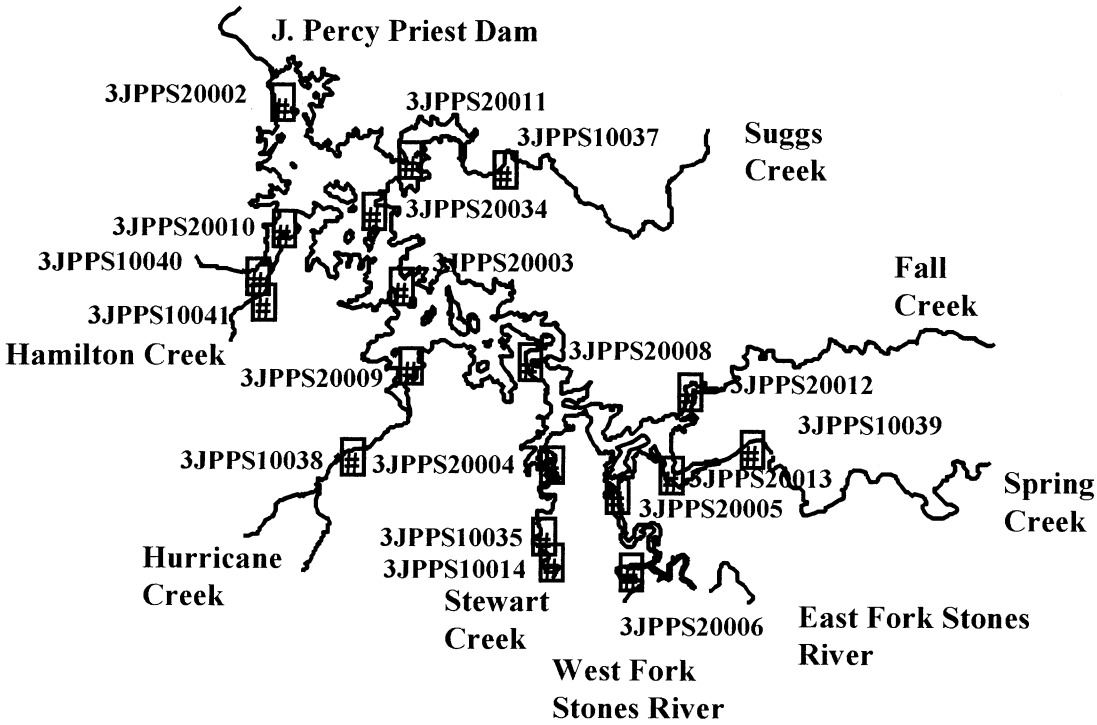

Figure 2. J. Percy Priest Reservoir and Sample Locations.

3 Input Data

Once the years for the application had been selected, the next task involved assembly and preparation of model input data. The following data are required for an application of CE-QUAL-W2:

1. initial conditions
   a. bathymetry
   b. water surface elevation
   c. temperature
   d. water quality constituents
2. boundary conditions
   a. inflow/outflow
   b. temperature
   c. water quality
   d. meteorology

These data are used to set initial conditions at the start of a model run and to provide time-varying inputs that drive the model during the course of a simulation. Additional data such as outlet descriptions, tributary and withdrawal locations, etc. are also required to complete the physical description of the prototype. In-pool data including water surface elevations, temperatures, and constituent concentrations are also required during model calibration in order to assess the performance of the model.

A clear distinction needs to be made regarding initial and boundary conditions and in-pool data. In-pool data have no effect on model performance - they are used only to assess model performance. Initial and boundary conditions are of greater importance because they directly affect model performance. Unfortunately, boundary conditions are rarely determined with a frequency that most modelers deem sufficient to accurately describe the forcing functions that are responsible for observed temperature and water quality conditions. Such is the case for J. Percy Priest as will be discussed below.

Bathymetry

CE-QUAL-W2 requires that the reservoir be discretized into longitudinal segments and vertical layers that may vary in length and height. An average width must then be defined for each active cell where an active cell is defined as

potentially containing water. Segment layer heights for J. Percy Priest were constant (1.0 m) while segment lengths varied. Once the segment lengths and layer heights were finalized, average widths were determined for each cell from bathymetric charts and sediment range data provided by the CELRN.

The J. Percy Priest grid consists of 10 branches comprising 95 active segments and a maximum of 39 layers. Segment lengths varied from 0.5 to 2.1 km. The main branch (Branch 1) represents the Stones River, extending into the West Fork of the Stones River. Branches 2-7 represent Hamilton Creek, Suggs Creek, Hurricane Creek, Stewart Creek, combined Spring and Fall Creeks, and the East Fork of Stones River, respectively (Figure 3). The remaining branches represent storage areas included to remove them from the main conveyance areas of the reservoir while still including them in simulations. These areas were considered to be outside of the main flow path through the reservoir. Including their conveyance areas in the main branch may have resulted in an underestimation of flow velocities and an overestimation of travel times through the reservoir.

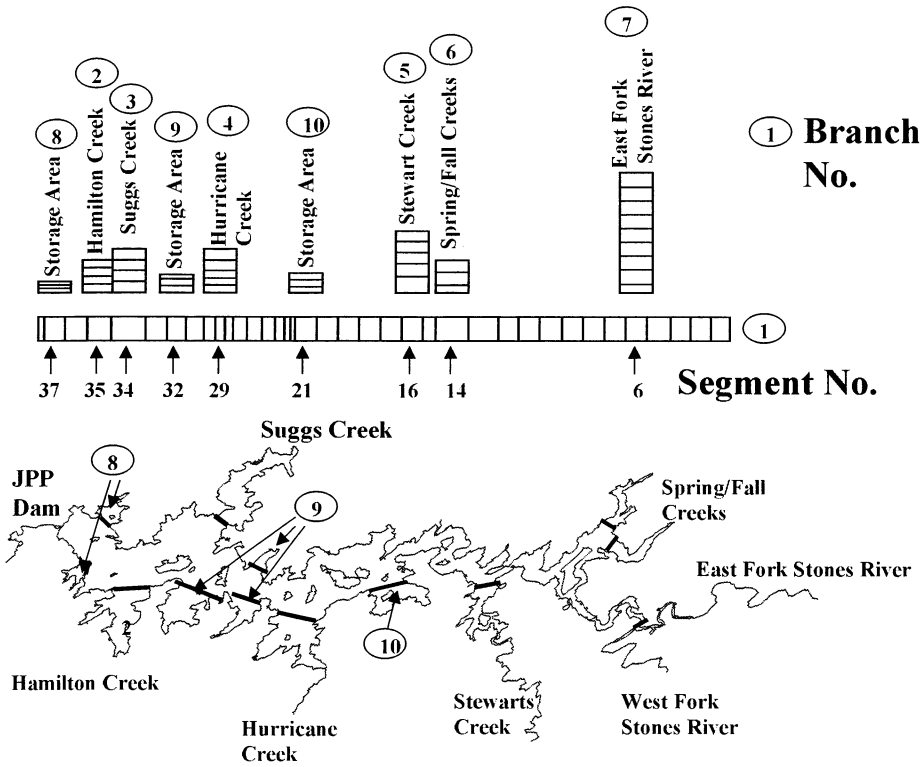

Figure 3. J. Percy Priest Model Grid (Plan View)

A comparison of computed volume-elevation curve and CELRN data is presented in Figure 4. The computed volume-elevation curve closely matches the CELRN data, with the exceptions of upper elevations, which were beyond the range of the sediment survey data provided. These elevations were above the maximum pool simulated.

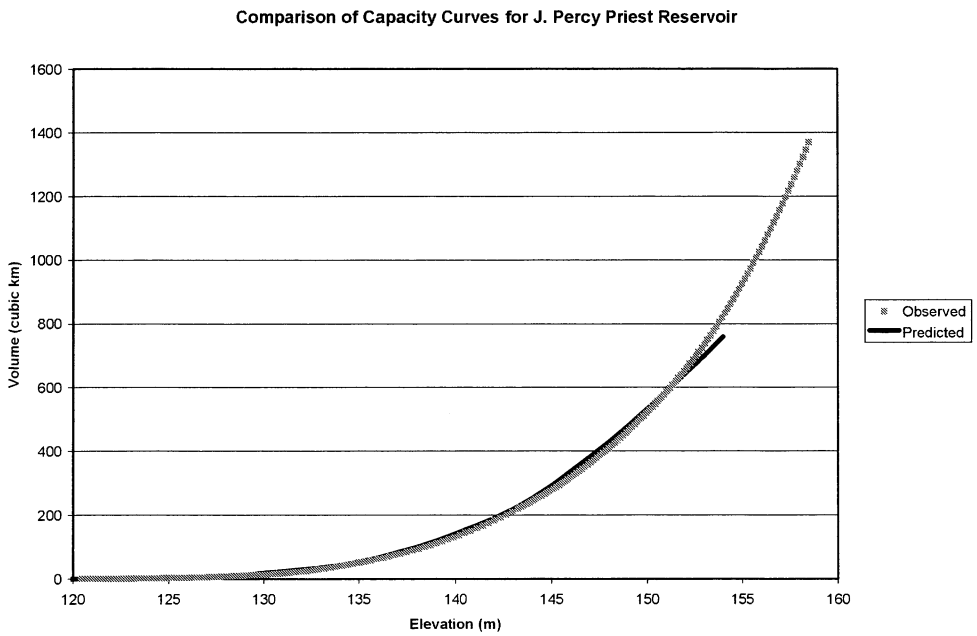

Figure 4. J. Percy Priest Volume-elevation Curve.

In-Pool Data

In-pool data for J. Percy Priest were provided in database format from CELRN. These data were, for the years selected, processed for comparison with model predictions. Data were typically collected as profiles and were generally available for comparisons of model predictions of temperatures, chlorophyll *a*, ammonia, nitrate-nitrogen, phosphate, dissolved oxygen and total iron.

Boundary Conditions

Meteorology

Hourly meteorology was obtained for the Nashville Airport, located 4 miles west of the J. Percy Priest dam, from the EarthInfo, Boulder, CO. Data required by CE-QUAL-W2 for surface heat exchange were air temperature, dew point temperature, wind speed and direction, and cloud cover.

Tributary boundary conditions

Inflow rates. Inflow rates were specified for each major tributary to J. Percy Priest. The total daily inflows to the reservoir were computed by CELRN for the period of 1970-1998 from continuity, based upon the known outflows, observed water surface elevations, and relationship between water surface elevations and reservoir volumes. Daily inflows for the period of simulation (1976-1978, 1981, and 1994) were extracted from this record. Data from the U.S. Geological

Survey stations on the West Fork of the Stones River near Smyrna (3428500) and East Fork of the Stones River near Lascassas (3427500) were also obtained. Based on previous studies by CELRN (1978), the flow for the East Fork was increased by a factor 1.137 to account for the ungaged portion of its watershed. In addition, local tributary inflows were estimated (CELRN 1978) to be 2/3 of the combined inflows for the East and West Forks of the Stones River. The local tributary flows were attributed to Fall/Spring, Suggs, Stewart, Hurricane, and Hamilton Creeks based upon ratios of their watershed areas to the total drainage area of the local tributaries (0.32, 0.10, 0.16, 0.03, and 0.03, respectively). The differences in the sum of the combined Stones River (East and West Fork) and estimated local tributary flows were then subtracted from the estimated total and attributed to distributed inflows.

Inflow temperatures. Inflow temperature data were limited for all inflows to J. Percy Priest. Temperature data may have been available from sources other than the CE routine data collection, but were not surveyed as part of this study. For 1976-1978, observed data were at an approximately monthly frequency were specified for model temperature boundaries. For 1981 and 1994, hourly inflow temperatures were estimated using a program that uses equilibrium temperatures based on meteorological data and stream depth to calculate water temperatures. The program used was the Response Temperature Calculator (RTC), developed by J.E. Edinger Associates. The inflows for all tributaries were assumed to be equal.

Inflow constituent concentrations. Water quality inflow concentrations for other constituents were also very limited. It was necessary to estimate the inflow concentrations from available data. The estimates were based upon an analysis of the relationship between flows and inflow concentrations completed by CELRN (1978), where total and dissolved phosphorus, nitrate+nitrite, ammonia, and volatile suspended solids were regressed against flow. The relationships are provided in Table 4, where the flow is considered rising if the value is 10 percent or more greater than the previous days flow. Flows within 10 percent of the previous days flow are considered stable, and the remainder considered to be falling.

Comparisons of concentrations predicted using the formulations in Table 4 are compared to observed nutrient concentrations in Figure 5-Figure 8.

The inflows for the local tributaries were also estimated. The inflow concentrations were based upon ratios of tributary concentrations to concentrations for the East Fork of the Stones River. The ratios, as computed by CELRN (1978), are provided in Table 5.

Table 4. Relationships Used to Compute Boundary Concentrations for the Stones River (CELRN 1978).

Constituent	West Fork of the Stones River		East Fork of the Stones River	
	Condition	Equation	Condition	Equation
Total P (μg/l)	Q < 2000	C = 111.2 + 40869.8/Q	Q ≤ 400	108.8-0.1116 Q
	2000 ≥ Q ≤ 14000	C = -20.2 + 0.0759 Q	Q > 400 (stable & falling)	121.0 + 0.04 Q
	Q > 14000	C = 1000.	Q > 400 (rising)	120.6 + 0.0528 Q
Ratio of dissolved to total P	Q < 14000	R =0.7978 exp (-0.000102 Q)	Q ≤ 8800	R = 0.610 exp (-0.000044Q)
	Q ≥ 14000	R =0.2	Q > 8800	R = 0.25
Nitrate+nitrite (mg/l)	Q ≤ 90	C = 1.98	Q ≤ 100	C = 0.34
	90 < Q < 14000	C = 1/[0.9594+0.00011Q)	100 < Q < 4500	C = 0.61
	Q ≥ 14000	0.40	4500 ≤ Q ≤ 18400	C = 0.714-0.0000225Q
			Q > 18400	C = 0.3
Ammonia (mg/l)	Q ≤ 175	C = 0.11	Q ≤ 150	C = 0.09
	Q > 175	C = 0.05	Q > 150	C = 0.03
Volatile Suspended Solids		C = 5.7 + 0.004 Q		C = 5.4 + 0.0019 Q

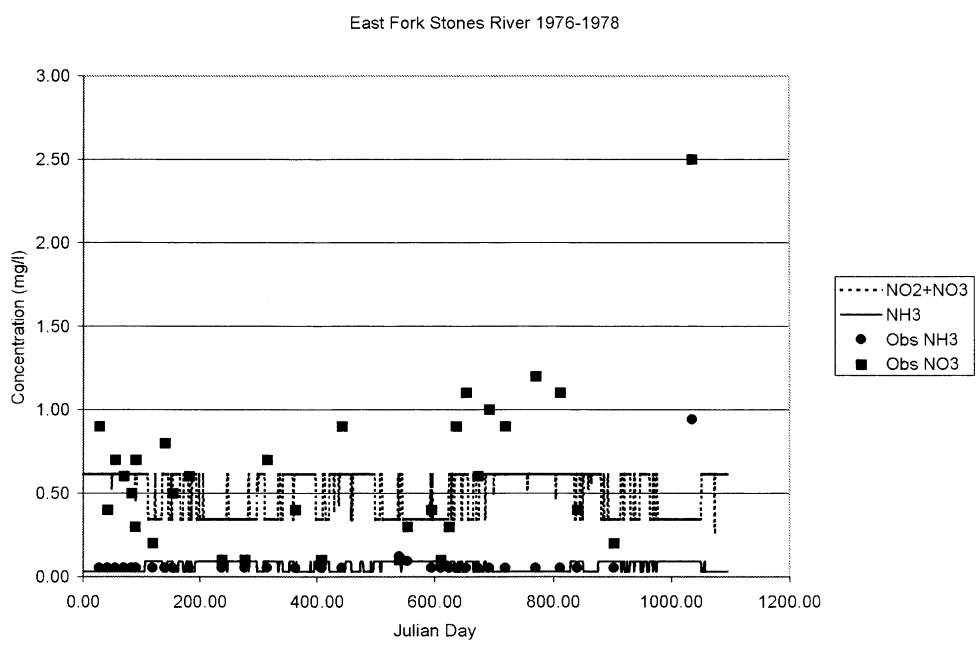

Figure 5. Comparison of Measured and Predicted Nitrogen Concentrations for the East Fork of the Stones River for 1976-1978.

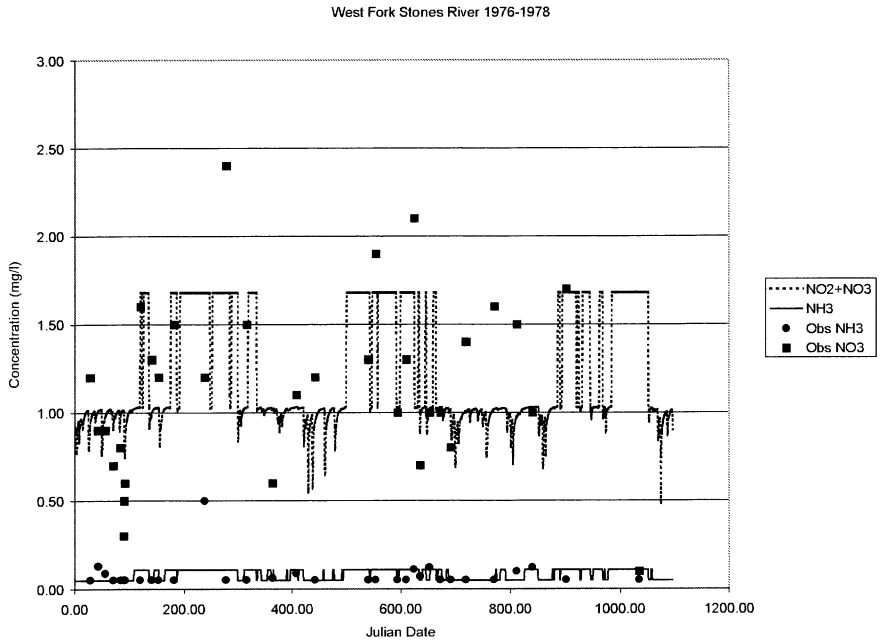

Figure 6. Comparison of Measured and Predicted Nitrogen Concentrations for the West Fork of the Stones River for 1976-1978.

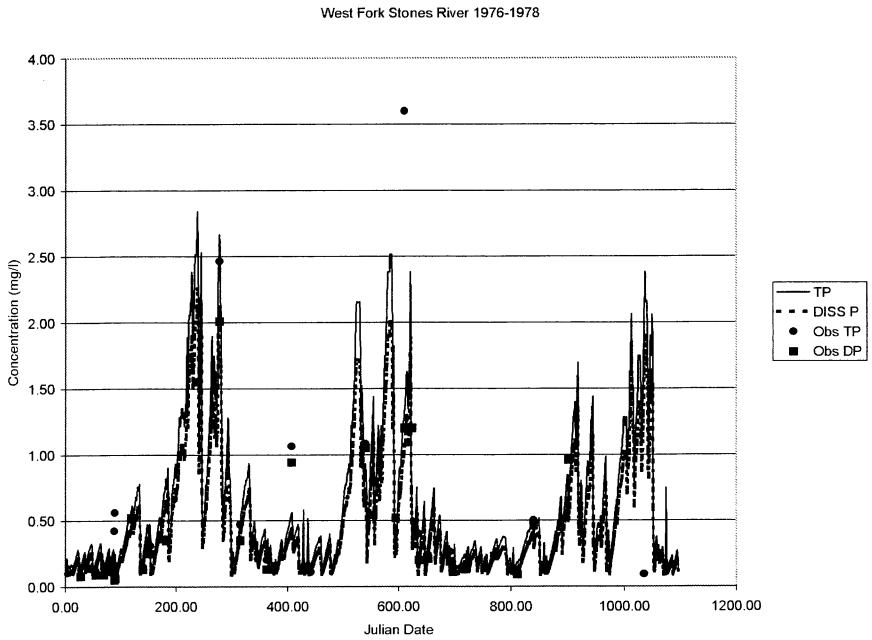

Figure 7. Comparison of Measured and Predicted Phosphorus Concentrations for the West Fork of the Stones River for 1976-1978.

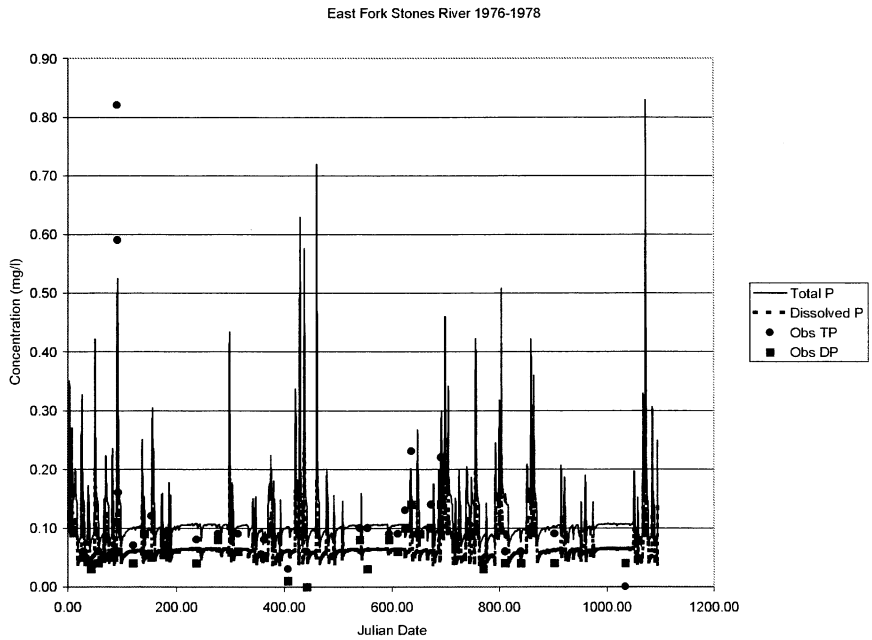

Figure 8. Comparison of Measured and Predicted Phosphorus Concentrations for the East Fork of the Stones River for 1976-1978.

Table 5. Local Tributary Multiplication Factors (CELRN 1978)

Local Tributary	Total P	Dissolved P	NO_2+NO_3	Ammonia	VSS
Suggs Creek	1.33	1.25	1.02	1.15	1
Hamilton Creek	1.64	1.8	0.75	0.98	1
Hurricane Creek	1.41	1.51	0.52	0.97	1
Spring/Fall Creek	0.42	0.56	0.33	1.05	1
Stewart Creek	1.33	1.25	1.02	1.15	1

The concentrations for state variable for detritus in CE-QUAL-W2 was assumed to equal volatile suspended solids concentrations.

The remaining parameters required for boundary conditions included labile and refractory dissolved organic matter (DOM), suspended solids, iron, algae and dissolved oxygen. For the years 1976-1978, these concentrations were taken from measured data interpolated to produce daily values. Labile and refractory DOM were taken to be 0.25 and 0.75 percent, respectively, of the measured dissolved volatile solids concentrations. Inflow algal biomass concentrations were assumed to be 0.01 mg/l, based on the assumption that few of the organisms in river waters were adaptable to the lake environment (approximately zero in inflows). Local tributary concentrations were assumed equal to concentrations for the East Fork of the Stones River.

For the years 1981 and 1994, suspended solids, dissolved volatile solids, algae and total iron were assumed to be constant with concentrations of 12, 70, 0.01 and 0.90 mg/l, respectively. This assumption was necessitated by the lack

of available data for these years. The assumed concentrations were based upon average values from 1976-1978. Dissolved oxygen concentrations were assumed to be 90 percent of the saturation concentration.

Point sources

A number of industrial and municipal point sources discharge either directly to J. Percy Priest or its tributaries. The point sources with current National Pollution Discharge Elimination System (NPDES) permits are listed in Table 6 some of which, as indicated, are presently inactive. This information was based upon information obtained from the EPA Region 4 Office and a Point Source Compliance (PCS) search from EPA databases. The approximate locations of the permitted discharges for the vicinity of J. Percy Priest are shown in Figure 9, taken from databases in EPA's BASINS software. Additional dischargers (numbers 29-35 in Table 6) are located in the upper watershed and not shown in Figure 9.

The inflow concentrations for the inflows for the East and West Forks of the Stones River were estimated, as described in the preceding section, and included the effects of the Woodbury and Murfreesboro sewage treatment plants. Therefore the impact of these plants are included in the estimated model boundary conditions. However, the estimated local tributary concentrations do not include the impact of effluents from local treatment plants. A Permit Compliance System (PCS) retrieval of data for the remaining dischargers was completed by the U.S. EPA Region 4 (Thomas McGill). Data were not available prior to 1990. In addition, for the dischargers actively contributing to local inflows, sufficient data were only available for Smyrna (TN0020541) for model input. Evaluation of PCS information for other facilities suggested that their flows were minimal and could be neglected. Input data for the Smyrna facility were developed from the PCS retrieval for the 1994 simulation year. Input data 1976 to 1978 simulations were based on PCS data from 1991-1993. Comparison of flows for those years were comparable to the total effluent flows used in the 1978 simulations (CELRN 1978). Input data for the 1981 simulation were based on PCS data from 1991. Dissolved phosphate concentrations were not available and assumed to be 6.6 mg/l in the Smyrna effluent, using values from previous modeling studies (USACE 1978).

Outflows

CELRN provided daily average outflows 1976-1978 and 1981 for both the turbines and spillways. Hourly turbine and spillway flows were provided for 1994. Based on operation rules, CELRN also estimated hourly turbine and spillway flows for 1976-1978 and 1981.

Table 6. Permitted Discharges

No.	Facility Name	NPDES ID	County	Receiving Stream
1	Nashville Hamilton-Creek STP	TN0028550	DAVIDSON	HAMILTON
2	USA CE J. Percy Priest Anderson Road Package Plant	TN0021458	DAVIDSON	STONES RIVER
3	Bridgestone USA	TN0022039	RUTHERFORD	HURRICANE CREEK
4	Music City Union Oil	TN0028792	DAVIDSON	MILL CREEK
5	Bridgestone USA	TND065833196	RUTHERFORD	HURRICANE CREEK
6	Speedway 8454	TN0061301	RUTHERFORD	EAST BRANCH HURRICANE CREEK
7	TN Farmers Coop Lavergne	TN0002801	RUTHERFORD	BUCHANAN BRANCH
8	Lavergne Utility District WTP*	TN0024864	RUTHERFORD	HURRICANE CREEK
9	Smyrna (Industrial Facility), and Smyrna STP	TN0020541	RUTHERFORD	STEWARTS CREEK
10	Smyrna Airport*	TN0065331	RUTHERFORD	
11	Smyrna Airport STP*	TN0027642	RUTHERFORD	J. PERCY PRIEST
12	Nashville Hurricane Creek*	TN0024911	RUTHERFORD	HURRICANE CREEK
13	USA CE J. Percy Priest Jeff SP Package Plant	TN0021431	RUTHERFORD	STONES RIVER
14	Wright Brothers Construction	TN0071536	RUTHERFORD	OVERALL CREEK
15	Murfreesboro Sinking Creek STP	TN0022586	RUTHERFORD	WEST FORK STONES RIVER
16	General Electric	TN0004278	RUTHERFORD	STONES RIVER
17	Murfreesboro WTP*	TN0004391	RUTHERFORD	STONES RIVER
18	Hoover, Inc. Plant 608	TN0059455	RUTHERFORD	TRIBUTARY OF BUSHMANS CRK
19	Rutherford Co-Lascassas ES Package Plant	TN0067245	RUTHERFORD	BRADLEY CREEK
20	Hoover, Inc. Plant 637	TN0060771	RUTHERFORD	TRIB TO FALL CREEK
21	TDEC Hoovers of Lebanon STP	TN0058149	WILSON	
22	Wilson Co. Gladeville Package Plant	TN0057801	WILSON	SUGGS CREEK
23	USA CE J. Percy Priest Fate Sanders Package Plant	TN0021440	RUTHERFORD	STONES RIVER
24	USA CE J. Percy Priest Poole Knobs Package Plant	TN0024325	RUTHERFORD	J. PERCY PRIEST
25	USA CE J. Percy Priest 7 Points Picnic Package Plant	TN0028568	DAVIDSON	J. PERCY PRIEST
26	USA CE J. Percy Priest 7 Points Package Plant	TN0029319	DAVIDSON	J. PERCY PRIEST
27	USA CE J. Percy Priest Cooks Camp Package Plant	TN0021482	DAVIDSON	STONES RIVER
28	USA CE J. Percy Priest Cooks Rec. Package Plant	TN0021474	DAVIDSON	STONES RIVER
29	MAPCO Delta Express Station	TN0064599	RUTHERFORD	LYTLE CRK-STONES R.
30	Woodbury STP	TN0025089	CANNON	EAST FORK STONES
31	Woodbury WTP*	TN0005339	CANNON	STONES RIVER
32	Rutherford County Highway Quarry	TN0059561	RUTHERFORD	TRIB. To STONES R
33	Community Care of Rutherford Package Plant	TN0057771	RUTHERFORD	STONES RIVER
34	Runtherford County Kittrell ES Package Plant	TN0067253	RUTHERFORD	CRIPPLE CRK
35	Rutherford County Buchannan ES Package Plant	TN0057797	RUTHERFORD	STONES RIVER

* Inactive

Symbol	Facility Name
1	Nashville Hamilton-Creek STP
2	USA COE J. Percy Priest Anderson Road Package Plant
3	Bridgestone USA
4	Music City Union Oil
5	Bridgestone USA
6	Speedway 8454
7	TN Farmers Coop Lavergne
8	Lavergne Utility District WTP
9	Smyrna (Industrial Facility), and Smyrna STP
10	Smyrna Airport
11	Smyrna Airport STP
12	Nashville Hurricane Creek
13	USA COE J. Percy Priest Jeff SP Package Plant
14	Wright Brothers Construction
15	Murfreesboro Sinking Creek STP
16	General Electric
17	Murfreesboro WTP
18	Hoover, Inc. Plant 608
19	Rutherford Co- Lascassas ES Package Plant
20	Hoover, Inc. Plant 637
21	TDEC Hoovers of Lebanon STP
22	Wilson Co. Gladeville Package Plant
23	USA COE J. Percy Priest Fate Sanders Package Plant
24	USA COE J. Percy Priest Poole Knobs package Plant
25	USA COE J. Percy Priest 7 Points Picnic Package Plant
26	USA COE J. Percy Priest 7 Points Package Plant
27	USA COE J. Percy Priest Cooks Camp Package Plant
28	USA COE J. Percy Priest Cooks Rec. Package Plant

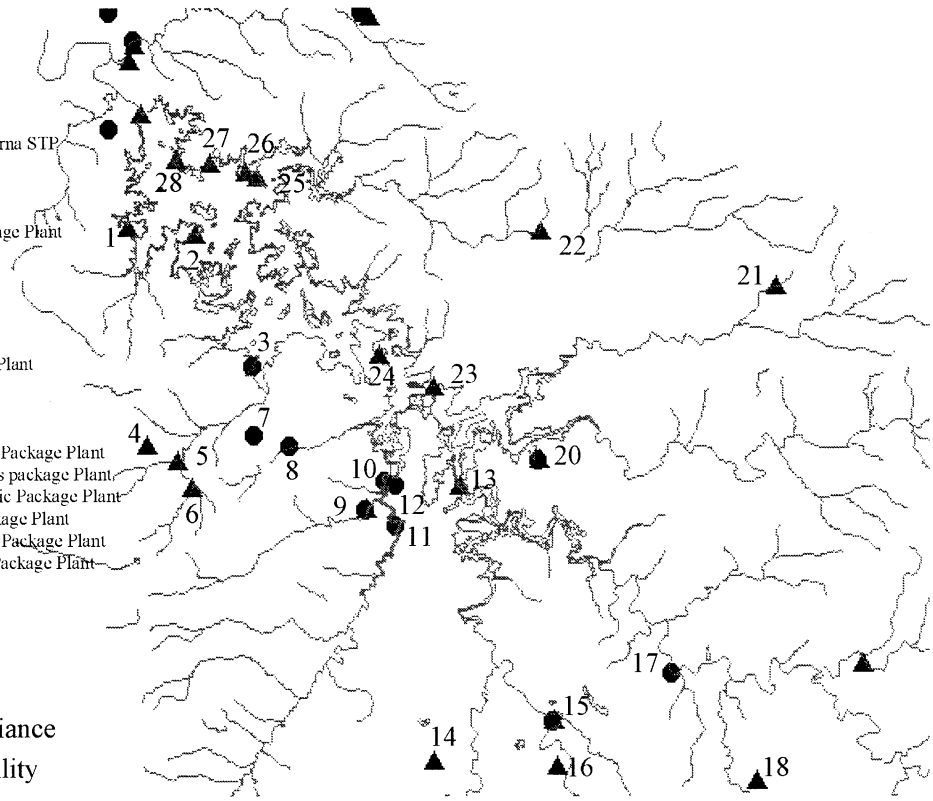

Figure 9. Approximate Location of Permitted Discharges to J. Percy Priest Basin.

4 Model Evaluation

The concept of calibration/verification of a model has changed in recent years. Previously, calibration was performed for a chosen year with coefficients being adjusted to give the best comparison between computed and observed data. Verification involved applying the model to another year without changing coefficients. In reality, if the results for the verification year were inadequate, both years were revisited and coefficients adjusted until an adequate fit of both years was achieved, essentially making both data sets calibration years. Including additional years for calibration further obscures the distinction between calibration and verification data sets.

Additionally, although not done in this application, there is no reason to expect that all water quality calibration parameters should remain constant from year to year. For example, sediment oxygen demand (SOD) and nutrient fluxes can and do change over time, otherwise, there would be no purpose in using a model to determine a system's response to changes in loadings. There is no reason to expect that SOD in 1976 would be the same as SOD in 1994 in J. Percy Priest reservoir. The only way to account for these changes would be to model all the years from 1976 to 1994 and hope that whatever changes in SOD and nutrient fluxes that occurred over the years would be captured by the model. Indeed, this would be the best way to gain confidence in a model's predictive ability. Clearly, however, this is not feasible as the data do not exist to drive the model for this period of time.

Successful model application requires calibrating the model to observed in-pool water quality. If at all possible, two or more years should be modeled with widely varying hydrology and/or water quality if corresponding water quality data are available. For J. Percy Priest, 1976-1978, 1981, and 1994 were used for calibration, representing hydrologic conditions ranging from dry to wet years. The period of 1976-1978 was run consecutively (a single model run).

Graphical and statistical comparisons of computed versus observed data were made to evaluate model performance. When interpreting temperature and water quality predictions from CE-QUAL-W2, several points need to be kept in mind. First, temperature and water quality predictions are averaged over the length, height, and width of a cell whereas observed data represent values at a specific point in the reservoir. Second, inflow temperatures were estimated from meteorological data. Third, measurement errors also exist with regards to measured depths, temperatures, and water quality. As a consequence, expecting the model to exactly match measured observations is unrealistic.

Six statistics were used to compare computed and observed in-pool observations. The Mean Error (ME), indicates how far, on the average, computed values are from observed values and is computed according to the following equation

$$ME = \frac{\sum \text{Predicted} - \text{Observed}}{\text{number observed}}$$

A ME of 0.5 °C means that the computed temperatures are, on the average, within ± 0.5 °C of the observed temperatures, and the sign of the ME indicates the direction of the error (above or below the observed values). The Mean Absolute Error (MAE) is computed similarly to the ME, but using the absolute value of the differences in observed and predicted values, and is computed according to the following equation:

$$MAE = \frac{\sum |\text{Predicted} - \text{Observed}|}{\text{number observed}}$$

The Relative Mean Absolute Error (RMAE) indicates the ratio of the absolute differences in observed and predicted values to the observed values (equivalent to the MAE divided by the observed mean), and is computed from

$$RMAE = \frac{\sum |\text{Predicted} - \text{Observed}|}{\sum \text{Observed}}$$

The root mean square error (RMS) indicates the spread of how far the computed values deviate from the observed data and is given by the following equation:

$$RMS = \sqrt{\frac{\sum (\text{Predicted} - \text{Observed})^2}{\text{number observed}}}$$

An RMS error of 0.5 °C means that 67 percent of the computed temperatures are within 0.5 °C of the observed temperatures. Finally, the means of the observed and predicted concentrations were computed for comparison using the following equations

$$\text{Mean Observed} = \frac{\sum \text{Observed}}{\text{number observed}}$$

$$\text{Mean Predicted} = \frac{\sum \text{Predicted}}{\text{number observed}}$$

Note that for all comparisons, predicted values were linearly interpolated to observed depths for comparison. Also, the mean predicted value only includes values at depths and times corresponding to the observed values.

Table 7 gives the final calibration values of all hydraulic and water quality parameters used in the model. It may seem like there are a large number of coefficients available for water quality calibration. However, of the 46 coefficients available for adjustment, 20 involve the temperature rate multiplier function used in the algal and nutrient compartments. Of the remaining 26, seven involve stoichiometric relationships that are basically fixed, leaving 19 coefficients for calibration. Experience has shown that the model provides good results with the default values for algal rates and half saturation coefficients. For nutrient calibration, the only coefficients adjusted are typically the sediment release rates for ammonium and phosphorus. For dissolved oxygen, the only coefficients usually adjusted are the zero-order SOD rates and possibly the organic matter decay rates. As a result, the amount of "curve fitting" has been kept to a minimum.

Table 7. Final Water Quality Coefficient Calibration Values (Continued).

Coefficient	**Variable**	**J. Percy Priest**
Hydraulic		
Horizontal eddy viscosity	AX	1.0 $m^2 s^{-1}$
Horizontal eddy diffusivity	DX	1.0 $m^2 s^{-1}$
Chezy bottom friction factor	CHEZY	70 $m^{½} s^{-1}$
Wind-sheltering	WINDSH	0.75
Fraction solar radiation absorbed at water surface	BETA	0.45
Light extinction for pure water	GAMMA	0.45 m^{-1}
Coefficient of bottom heat exchange	CBHE	7.0 * 10^{-8} °C $m^{-1} s^{-1}$
Water Quality		
Algae		
Growth rate	AG	2 day^{-1}
Mortality rate	AM	0.07 day^{-1}
Excretion rate	AE	0.04 day^{-1}
Respiration rate	AR	0.04 day^{-1}
Settling rate	AS	0.5 m s^{-1}
Phosphorus half-saturation for algal growth	AHSP	0.003 g m^{-3}
Nitrogen half-saturation for algal growth	AHSN	0.014 g m^{-3}
Light saturation intensity	ASAT	50 W m^{-2}
Fraction of algae to POM	APOM	0.8
Lower temperature for minimum algal rates	AT1	5 °C
Lower temperature for maximum algal rates	AT2	30 °C
Upper temperature for maximum algal rates	AT3	35 °C
Upper temperature for minimum algal rates	AT4	40 °C
Lower temperature rate multiplier for minimum algal rates	AK1	0.99
Upper temperature rate multiplier for minimum algal rates	AK2	0.99
Lower temperature rate multiplier for maximum algal rates	AK3	0.99
Upper temperature rate multiplier for maximum algal rates	AK4	0.99
Phosphorus to biomass ratio	BIOP	0.005
Nitrogen to biomass ratio	BION	0.08
Carbon to biomass ratio	BIOC	0.45
Phosphorus		
Sediment release rate (fraction of SOD)	PO4R	0.015

Table 7. Final Water Quality Coefficient Calibration Values. (concluded)

Coefficient	Variable	J. Percy Priest
Water Quality		
Ammonium		
Ammonium decay rate	NH4DK	0.12 day^{-1}
Sediment release rate (fraction of SOD)	NH4R	0.20
Lower temperature for ammonium decay	NH4T1	5 °C
Upper temperature for ammonium decay	NH4T2	25 °C
Lower temperature rate multiplier for ammonium decay	NH4K1	0.1
Upper temperature rate multiplier for ammonium decay	NH4K2	0.99
Nitrate		
Nitrate decay rate	NO3DK	0.03 day^{-1}
Lower temperature for nitrate decay	NO3T1	5 °C
Upper temperature for nitrate decay	NO3T2	30 °C
Lower temperature rate multiplier for nitrate decay	NO3K1	0.1
Upper temperature rate multiplier for nitrate decay	NO3K2	0.99
Organic matter		
Labile DOM decay rate	LDOMDK	0.30 day^{-1}
Refractory DOM decay rate	RDOMDK	0.001 day^{-1}
Labile to refractory DOM decay rate	LRDK	0.01 day^{-1}
Labile POM decay rate	LPOMDK	0.08 day^{-1}
POM settling rate	POMS	1.0 m s^{-1}
Lower temperature for organic matter decay	OMT1	2 °C
Upper temperature for organic matter decay	OMT2	30 °C
Lower temperature rate multiplier for organic matter decay	OMK1	0.1
Upper temperature rate multiplier for organic matter decay	OMK2	0.99
Sediment decay rate	SDK	-
Oxygen		
Stoichiometry for ammonium decay	O2NH4	4.57
Stoichiometry for organic matter decay	O2OM	1.4
Stoichiometry for algal respiration decay	O2AR	1.1
Stoichiometry for algal growth decay	O2AG	1.4

Application to 1976-1978

The initial calibration of the J. Percy Priest model focused on a continuous simulation of the period of January 1976 to December 1978. This period included a normal hydrologic year (1976) and two mixed years (1977 and 1978). Of the three periods of application (1976-1978, 1981, and 1994), this period had the most complete set of data for model forcings and model evaluation. See Appendix A for additional comparisons of model predictions and measured values at Stations 3JPPS20003 and 3JPPS20008. The calibration required modifications of the estimated inflow concentrations computed using relations described previously (Table 4Table 4) in order to capture observed concentrations at the most upstream reservoir monitoring station (3JPPS20008). Specifically, concentrations of LDOM, RDOM, NO_3 and PO_4 were reduced to 0.3 of their estimated value.

Water surface elevations

Water surface elevations are predicted by the model based on the interactions between inflows, outflows, evaporation, and precipitation. Since the inflows provided include the effects of evaporation and precipitation, these options were not used during calibration. Any discrepancies between computed and observed elevations were eliminated by including either positive or negative inflows in the distributed tributary inflow file. Distributed tributary inflows enter the surface layer of all segments in a branch and are apportioned according to the surface area of each segment. As shown in Figure 10, predicted elevations reasonably matched observed elevations. Greatest differences occurred during summer months, where water surface elevations were overestimated.

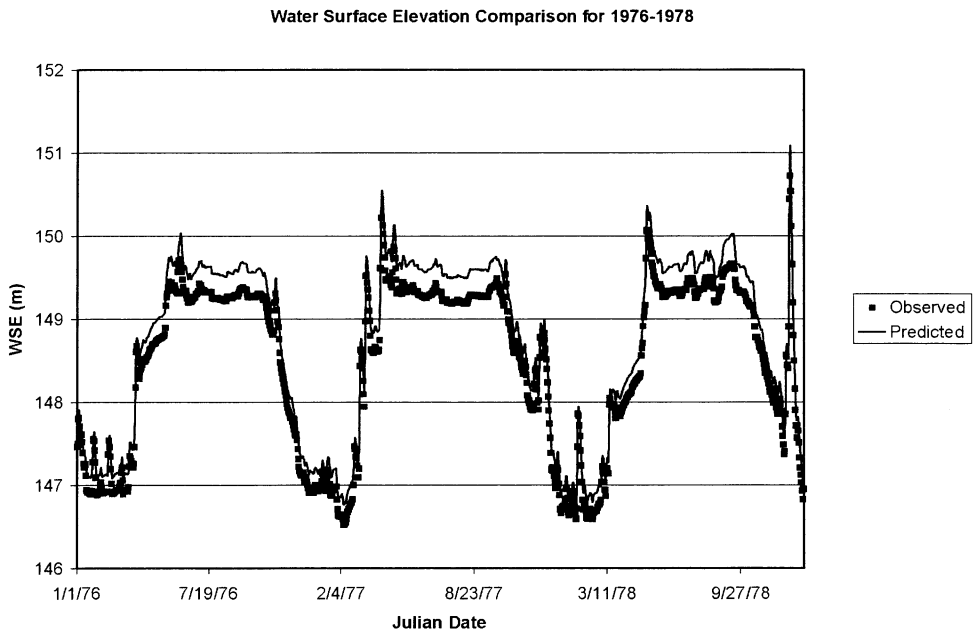

Figure 10. Computed (lines) vs. Observed (symbols) Water Surface Elevations for 1976-1978.

Water age

Water age was computed as a state variable in this application to allow evaluation of the average retention time in the reservoir. For comparison, a reservoir average water age was computed as the sum of the product of the segment water ages and volumes divided by the total reservoir volume. The computed volume-averaged water age for 1976-1978 is illustrated in Figure 11. The volume-averaged water age increased during 1976, reaching a maximum of 217 days. Water age in subsequent years was lowest in the early spring (approximately 70 days) and greatest during the month of November.

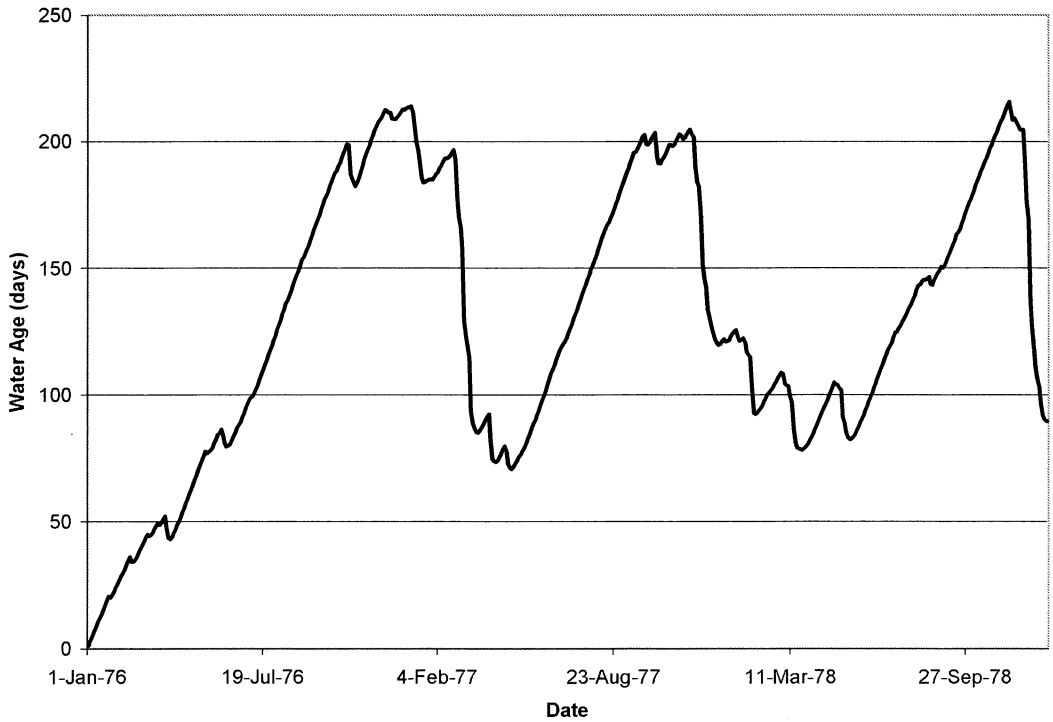

Figure 11. Computed Volume-Averaged Water Age in J. Percy Priest for 1976-1978.

Temperature

Results for temperature calibration at station 3JPPS20002, the station closest to the dam, are given in Figure 12 and Figure 13. Overall, the model closely reproduced the observed temperature profiles. Most of the discrepancies between predicted and observed temperatures occur in the epilimnion. Epilimnetic temperatures are influenced primarily by surface heat exchange, which is in turn a function of the accuracy of the meteorological data. Also, epilimnetic temperatures are influenced by the time of day the data were taken and can change several degrees over the course of a day. For 398 observations during this period, the Mean Error was -0.3, the Mean Absolute Error was 0.9, the Root Mean Square Error was 1.2 °C and the Mean Relative Absolute Error was 6 percent. The average of the observed data was 15.0 as compared to 14.7 for model predictions.

Predicted outflow temperatures are illustrated in Figure 14. For the period of 1976-1978, there were a total of 88 days during which the outflow temperatures exceeded 12.8 °C (55 °F), and 0 days during which the outflow exceeded 20 °C (68 °F); maximum temperatures in outflows were 19 °C.

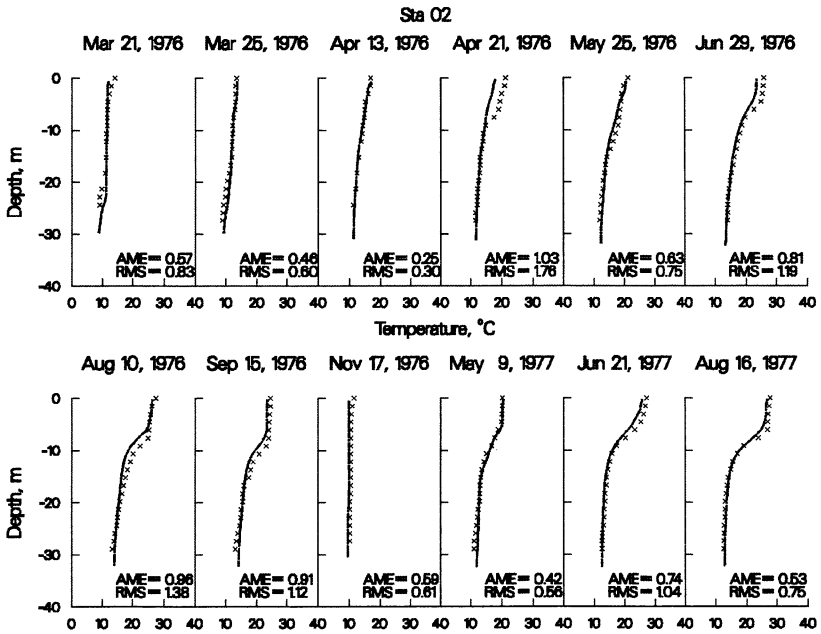

Figure 12. 1976-1978 Computed (…) vs. Observed (x) Temperatures at Station 3JPPS20002.

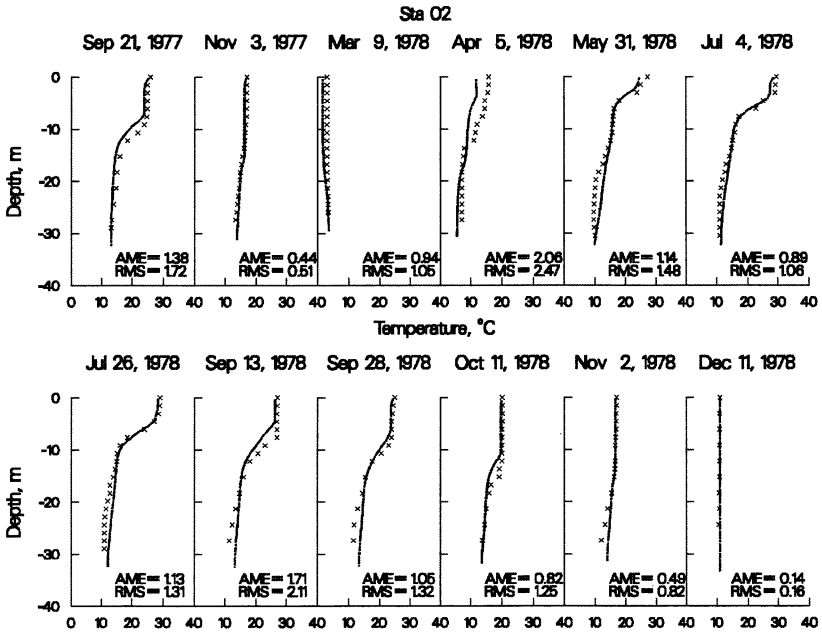

Figure 13. 1976-1978 Computed (…) vs. Observed (X) Temperatures at Station 3JPPS20002.

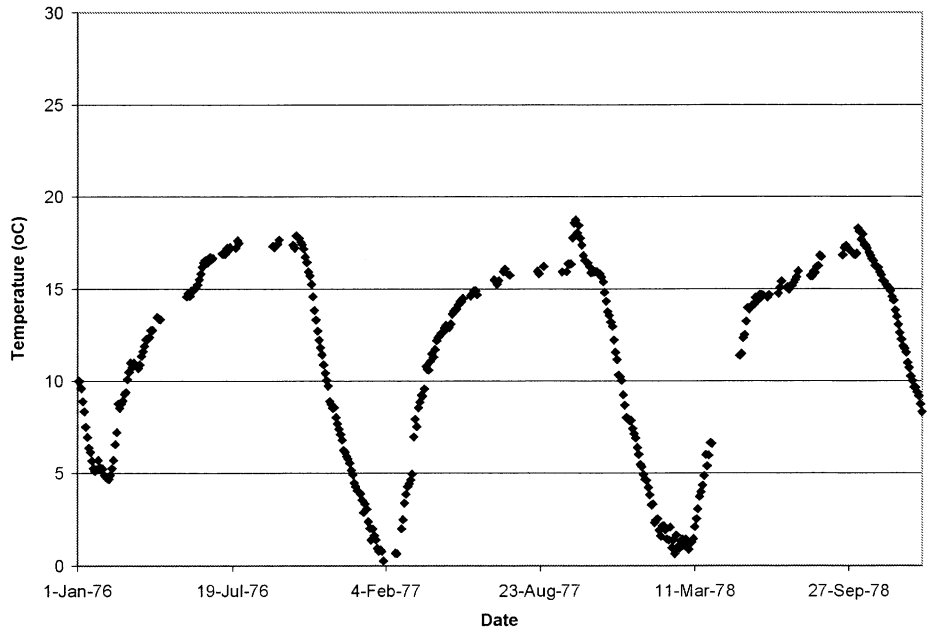

Figure 14. Predicted Outflow Temperatures for 1976-1978.

Dissolved oxygen

Calibration results at 3JPPS20002 are given in Figure 15 and Figure 16. Overall, the model did a reasonable job in reproducing the observed spatial and temporal patterns of dissolved oxygen (DO) depletion. The model generally captured the timing of the onset of oxygen depletion in the springtime, the development of hypolimnetic anoxia in summer, and the increase in DO with depth during fall overturn.

Differences in observed and predicted dissolved oxygen concentrations occurred over the three years of simulation. For 1976, hypolimnetic dissolved oxygen depletion was observed in March, with complete depletion occurring in May-June. A similar trend was apparent in 1977. However, in 1978, the observed dissolved oxygen concentrations remained high throughout the water column in April, with a less severe depletion in June. The model generally captured observed depletion during 1976 and 1977 at Station 3JPPS20002 as well as the more uniform distribution in April of 1978, with the predicted hypolimnetic depletion lagging that observed at station 3JPPS20002. The predicted depletion occurred earlier than observed at stations 3JPPS20003 and 3JPPS20008 (Appendix A). The model also captured the relatively uniform dissolved oxygen profile occurring during November of 1976 as well as the anoxic conditions persisting in November for 1977 and 1978. For a total of 398 observations, the Mean Error was 0.5, the Mean Absolute Error was 1.3, the Root Mean Square Error was 2.0 mg/l, and the Relative Mean Absolute Error was 28 percent. The mean of the observed values was 4.7 as compared to a mean predicted value of 5.1 mg/l.

Predicted dissolved oxygen concentrations averaged over the photic zone of the reservoir are illustrated in Figure 17. The depth of the photic zone was computed from the predicted light extinction coefficient and taken to be the depth of one percent of surface irradiance. Also illustrated are computed dissolved oxygen concentrations at 1.5 m (5 ft) of depth and in reservoir outflows. Note that the computed outflows do not include the effect of turbine reaeration, which at J. Percy Priest would tend to increase the outflow DO by 1- 1 ½ mg/l. The observed values interpolated to a depth of 1.5 m (5 ft) are also illustrated. The minimum predicted photic zone-averaged concentration was 5 mg/l, while the minimum predicted concentration at 1.5 m was 3.3 mg/l. Predicted concentrations in reservoir outflows approached 1 mg/l during summer months.

Nutrients

Results for ammonium, nitrate-nitrite, and dissolved inorganic phosphorus calibration are given in Figure 18-Figure 23. For ammonium and phosphorus, the model generally captures the increase in hypolimnetic concentrations during anoxia and the decrease in those concentrations during overturn. The model also generally captures the increases in nitrate-nitrite as well, but over-predicts concentrations in the epilimnion. Considerable variation occurred in nitrate concentrations between years, which appeared to be inflow related. Summary statistics for 1976-1978 nutrient predictions are provided in Table 8.

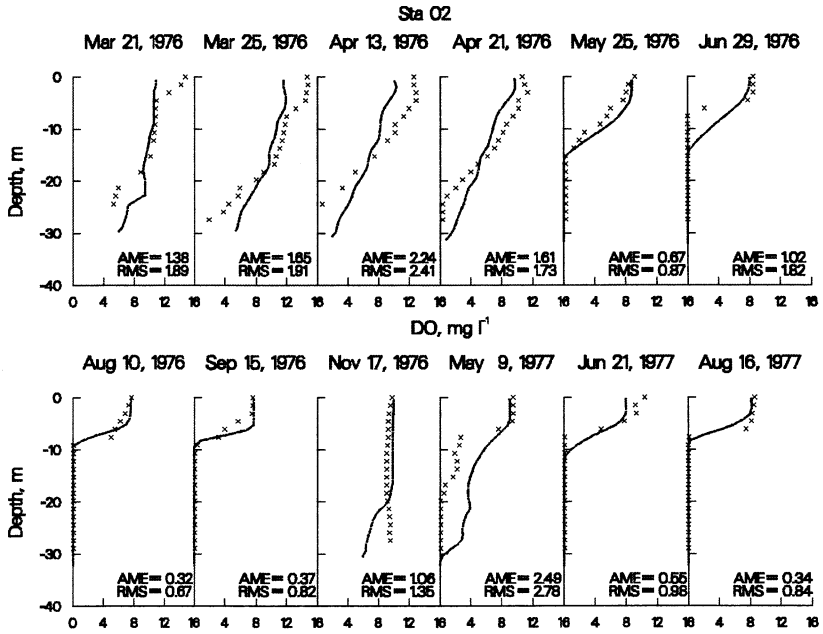

Figure 15. 1976-1978 Computed (…) vs. Observed (X) DO at Station 3JPPS20002.

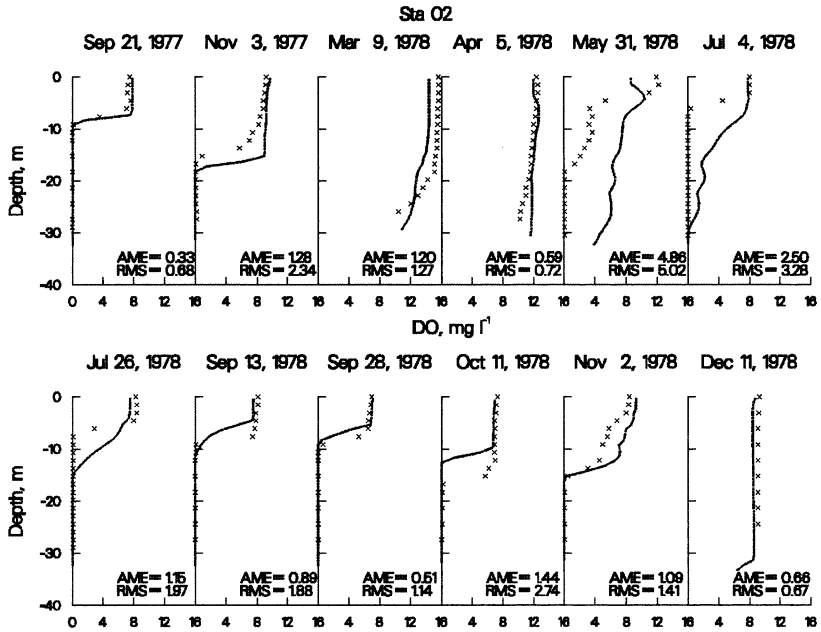

Figure 16. 1976-1978 Computed (…) vs. Observed (X) DO at Station 3JPPS20002.

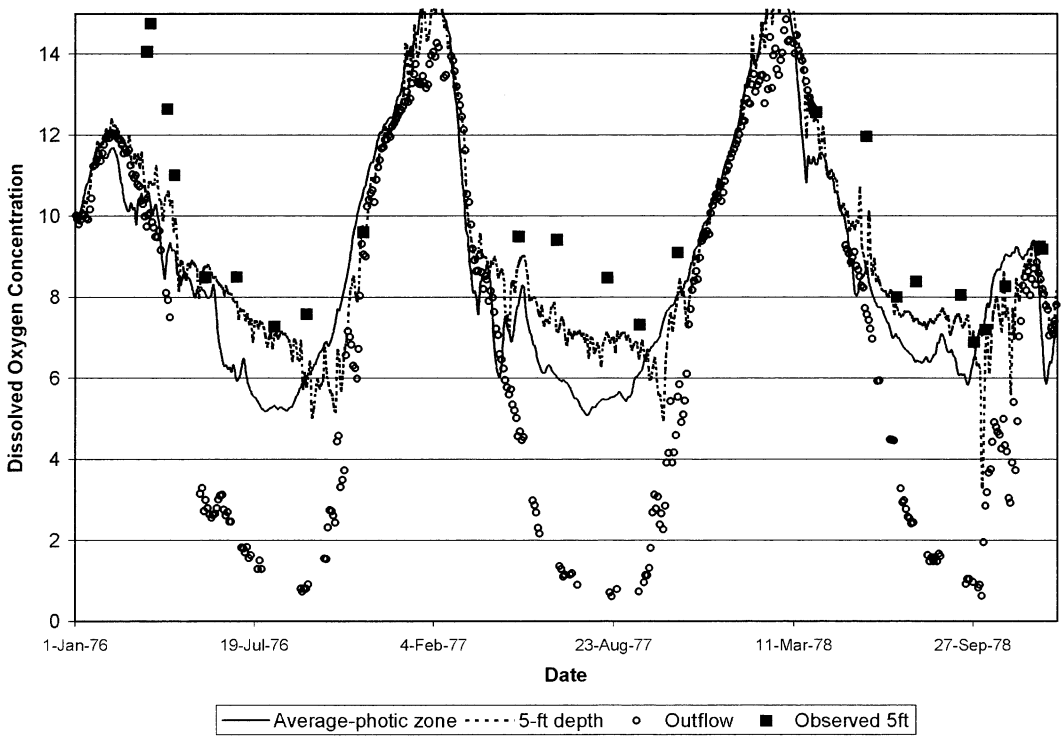

Figure 17. Predicted Average Dissolved Oxygen Concentrations (mg/l) in the Photic Zone, at 1.5 m (5 ft) Depth, and in Reservoir Outflows for 1976-1978.

Table 8. Summary Statistics for Nutrient Predictions for 1976-1978

	Ammonia	Nitrate-Nitrite	Inorganic Phosphorus
Total Observations	56	56	56
Mean Error (mg/l)	.005	-0.03	0.05
Mean Absolute Error (mg/l)	0.35	0.14	0.07
Root Mean Square Error (mg/l)	0.60	0.22	0.10
Relative Mean Absolute Error (%)	65	84	130
Mean Observations (mg/l)	.54	.17	.05
Mean Predictions (mg/l)	.55	.13	.10

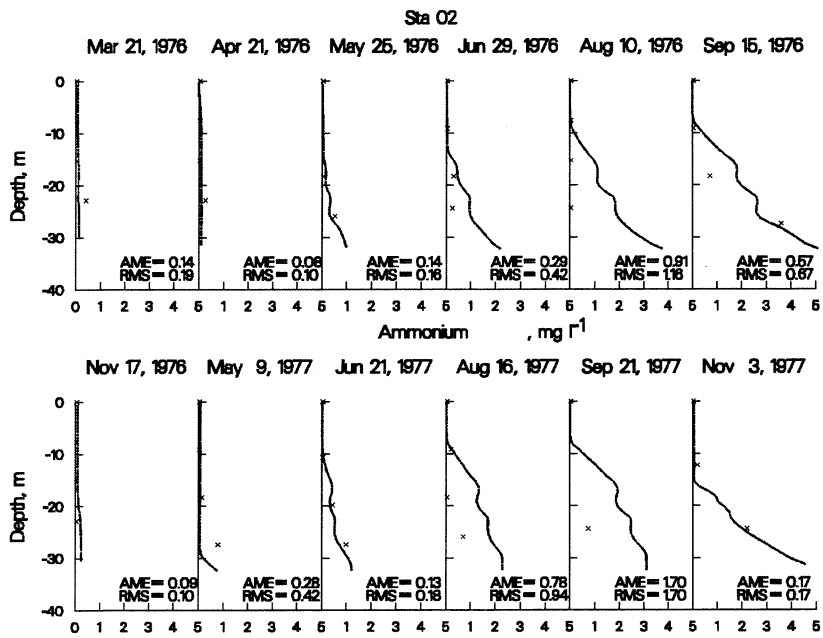

Figure 18. 1976-1978 Computed (…) vs. Observed (X) Ammonium at Station 3JPPS20002.

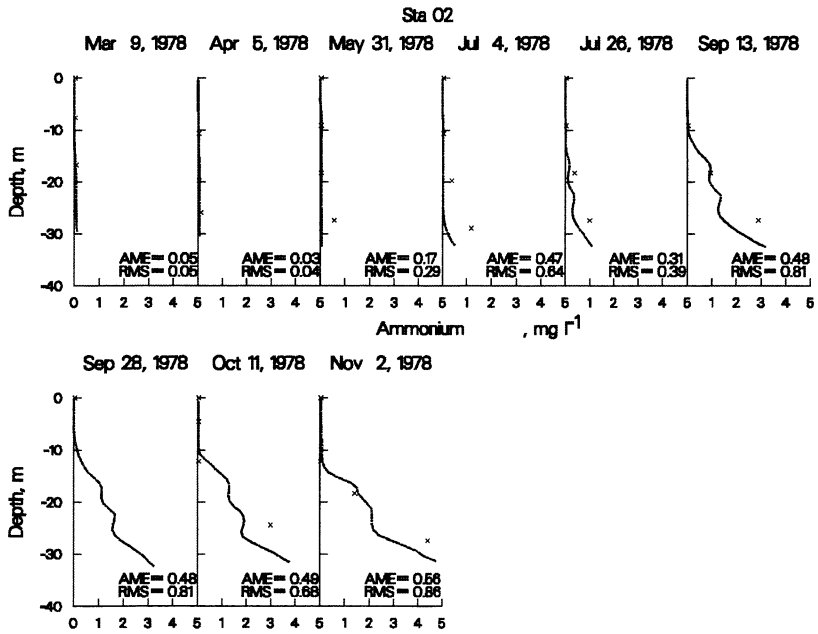

Figure 19. 1976-1978 Computed (…) vs. Observed (x) Ammonium at Station 3JPPS20002.

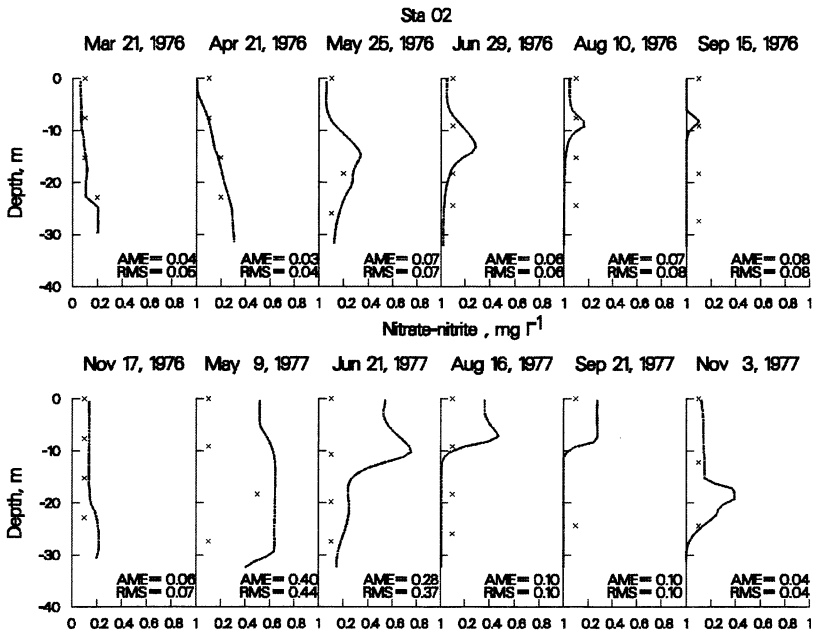

Figure 20. 1976-1978 Computed (…) vs. Observed (x) Nitrate-Nitrite at Station 3JPPS20002.

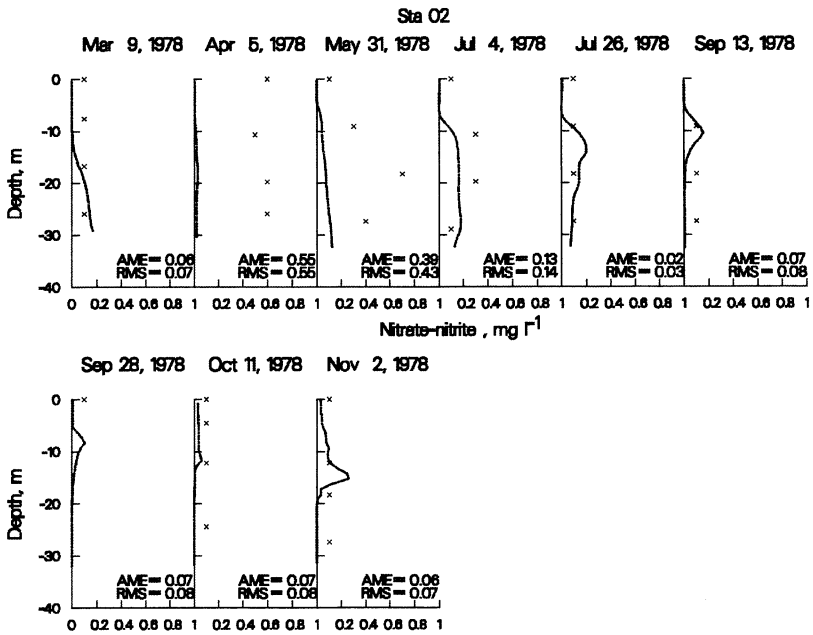

Figure 21. 1976-1978 Computed (…) vs. Observed (x) Nitrate-Nitrite at Station 3JPPS20002.

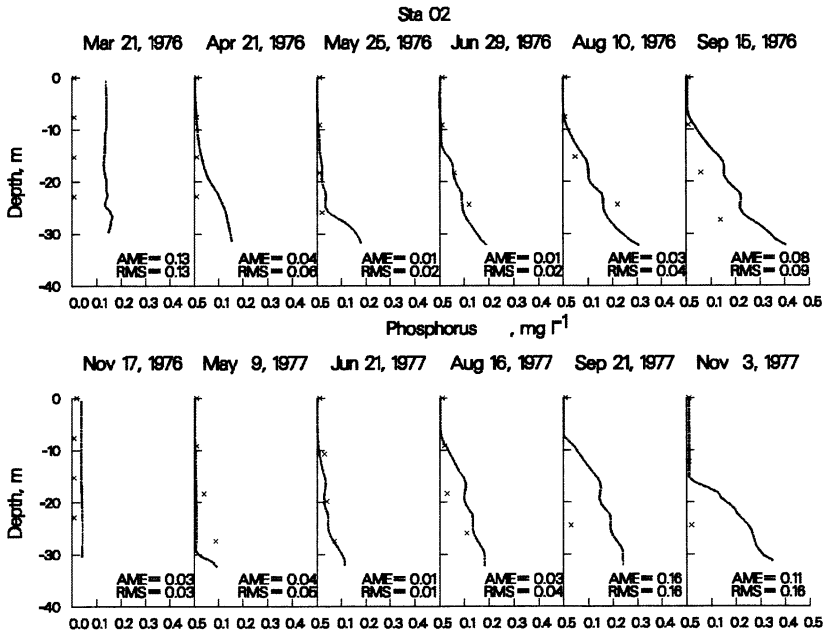

Figure 22. 1976-1978 Computed (…) vs. Observed (x) Phosphorus at Station 3JPPS20002.

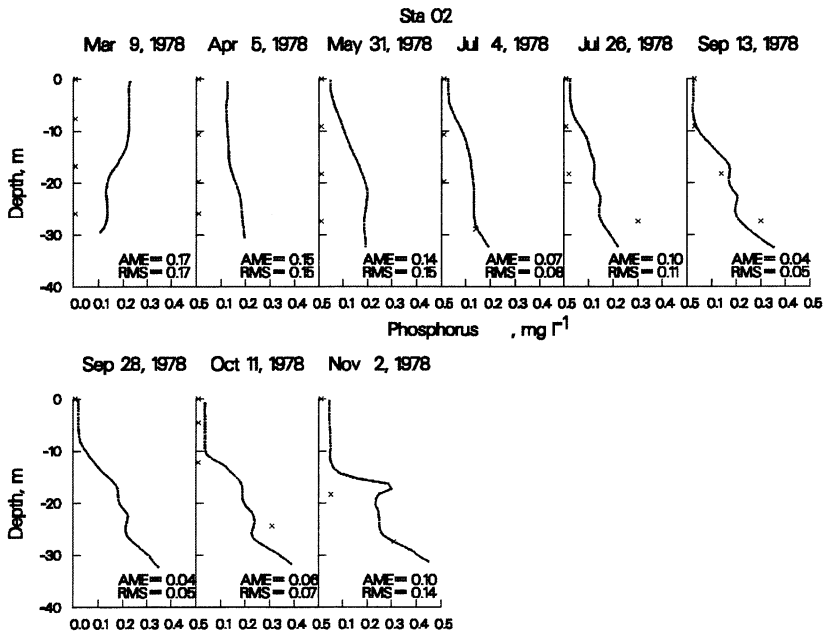

Figure 23. 1976-1978 Computed (...) vs. Observed (x) Phosphorus at Station 3JPPS20002.

Algae

Algal biomass in the CE-QUAL-W2 model is represented as grams organic matter (dry weight)/m^3 and measurements are represented as μg chlorophyll *a*/l. In order to compare the two, model output was converted to chlorophyll *a* assuming a chlorophyll *a* organic matter ratio of 65, with that ratio based on previous W2 model applications. Model predictions for 1976-1978 are compared to observed concentrations in Figure 24 and Figure 25. In general, the model captured seasonal variations in chlorophyll *a* concentrations, including spring and fall blooms. For a total of 56 observations, the Mean Error was 1.1. the Mean Absolute Error was 4.2, the Root Mean Square error was 5.5 μg chlorophyll *a*/l, and the Relative Mean Absolute Error was 48 percent. The mean of the observed values was 8.7 as compared to a mean predicted value of 9.9 μg chlorophyll *a*/l.

Predicted average, maximum and minimum chlorophyll *a* concentrations, averaged over the photic zone, are illustrated in Figure 26. Typically, maximum concentrations occurred during spring and fall months. Average predicted concentrations in the photic zone were typically less than 20 µg/l. The maximum predicted photic-zone averaged concentration was 44 µg/l.

Comparisons were also made between predicted and observed concentrations averaged over 2 m of depth. Computed and observed 2 m-averaged concentrations are illustrated in Figure 27, and indicated the model adequately captured variations in depth-averaged concentrations. A goal of a model application is to

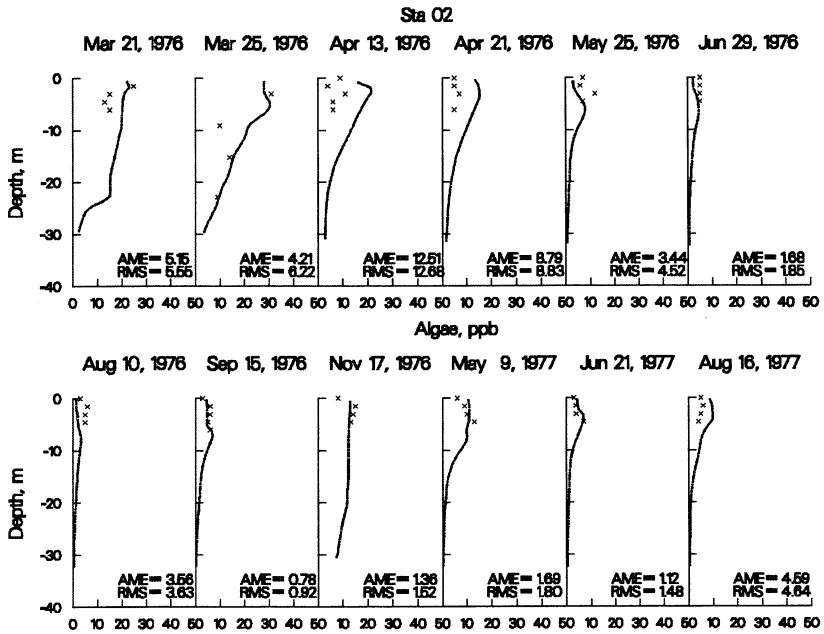

Figure 24. 1976-1978 Computed (…) vs. Observed (x) Algal Chlorophyll *a* at Station 3JPPS20002.

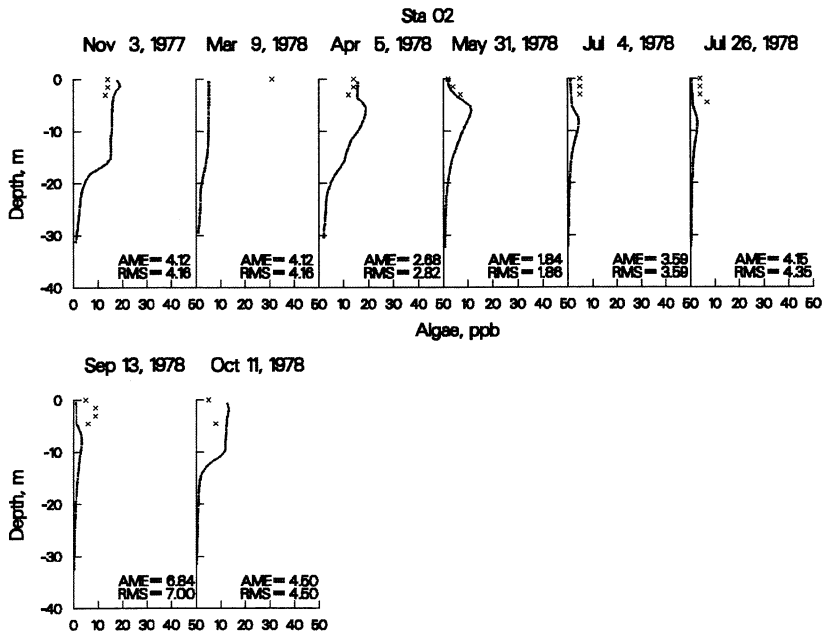

Figure 25. 1976-1978 Computed (…) vs. Observed (x) Algal Chlorophyll *a* at Station 3JPPS20002.

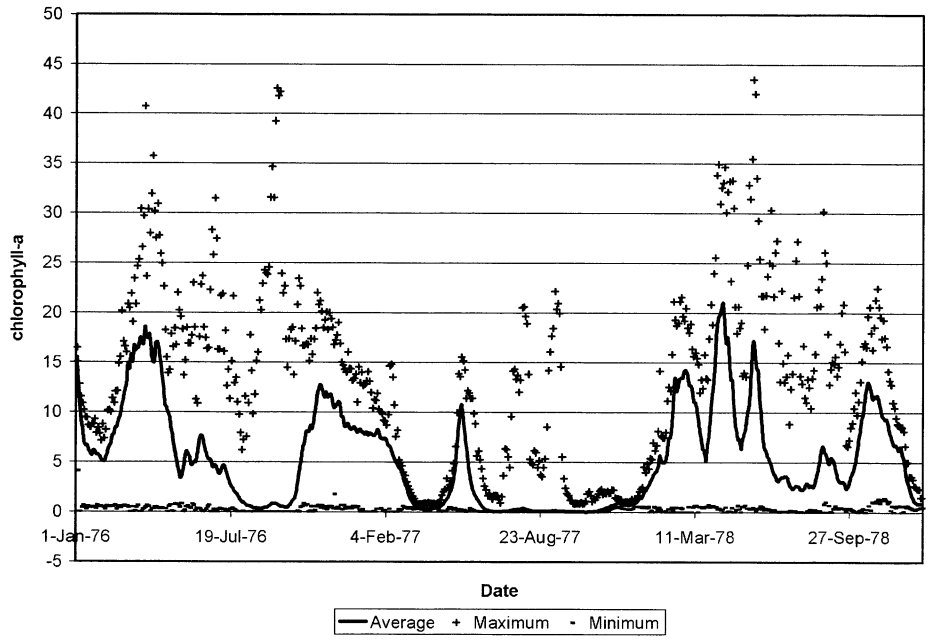

Figure 26. Predicted Average, Maximum and Minimum Chlorophyll *a* Concentrations (μg/l) in the Photic zone for 1976-1978.

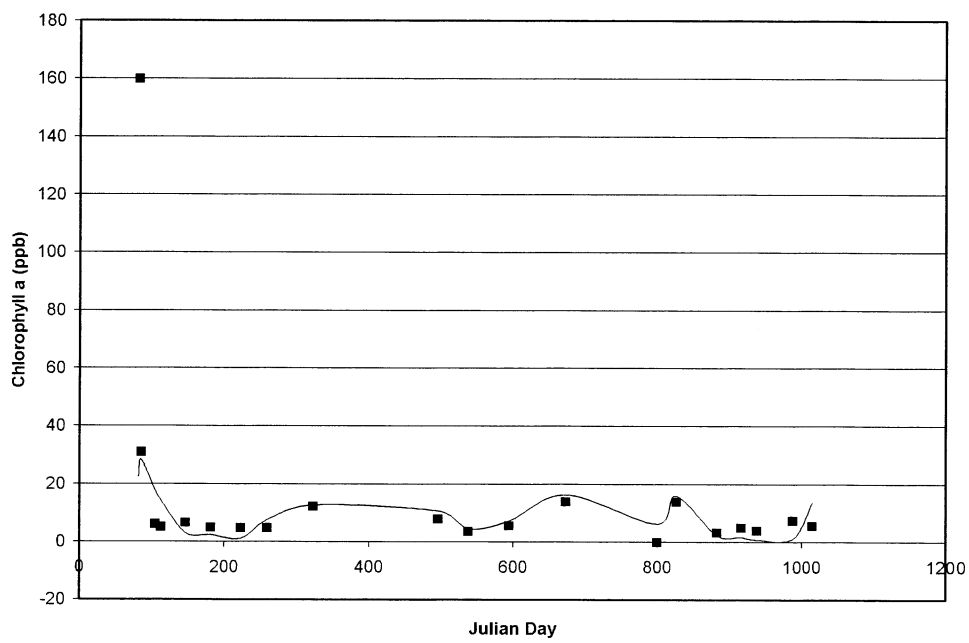

Figure 27. 1976-1978 Computed (—) vs. Observed (■) Algal Chlorophyll *a* at Station 3JPPS20002 Averaged over 2 m of Depth.

not only capture the magnitude of concentrations but to capture rates of changes in concentrations as well. For concentrations averaged over 2 m depth, temporal changes in observed and computed concentrations were computed from the difference in depth-averaged concentrations between successive observations divided by the difference in time between those observations (dC/dt). Comparison of computed and observed changes in chlorophyll *a* concentration (dChlorophyll *a*/dt) are illustrated in Figure 28 and indicate the model accurately followed observed trends in concentrations changes.

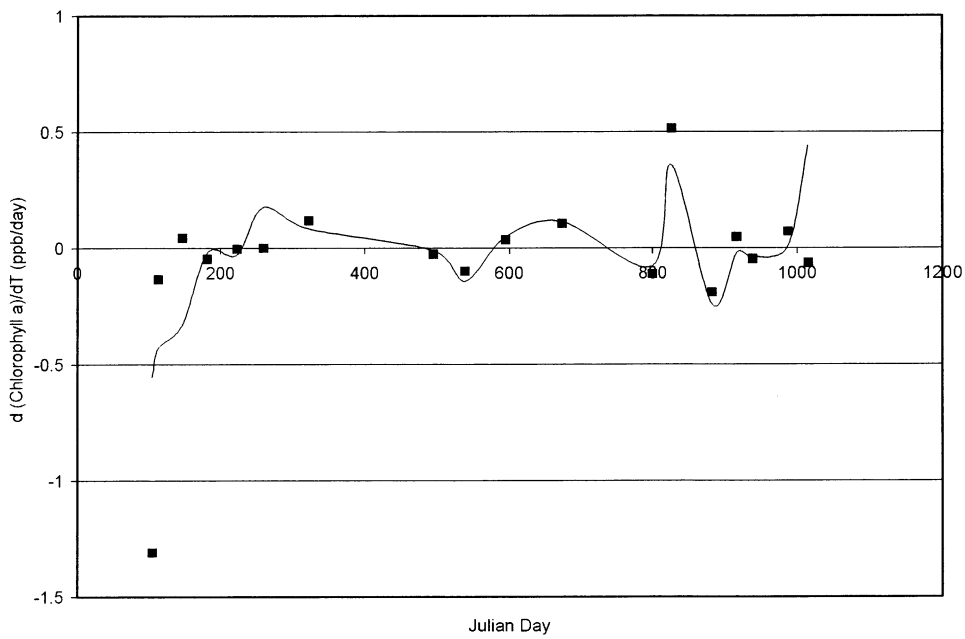

Figure 28. 1976-1978 Computed (—) vs. Observed (■) Changes in Algal Chlorophyll *a* Concentrations with Time at Station 3JPPS20002 Averaged over 2 m depth

Iron

Results for total iron calibration at station 3JPPS20002, the station closest to the dam, are given in Figure 29 and Figure 30. Overall, the model closely reproduced the observed iron profiles. Computed iron concentrations were primarily controlled by specified release rates during anoxic conditions. For a total of 48 observations, the computed Mean Error was -0.26, the Mean Absolute Error was 0.48, and the Root Mean Square error was 0.78 mg/l, and the Relative Mean Absolute Error was 60 percent. The mean of the observed values was 0.8 as compared to a mean predicted value of 0.6 mg/l.

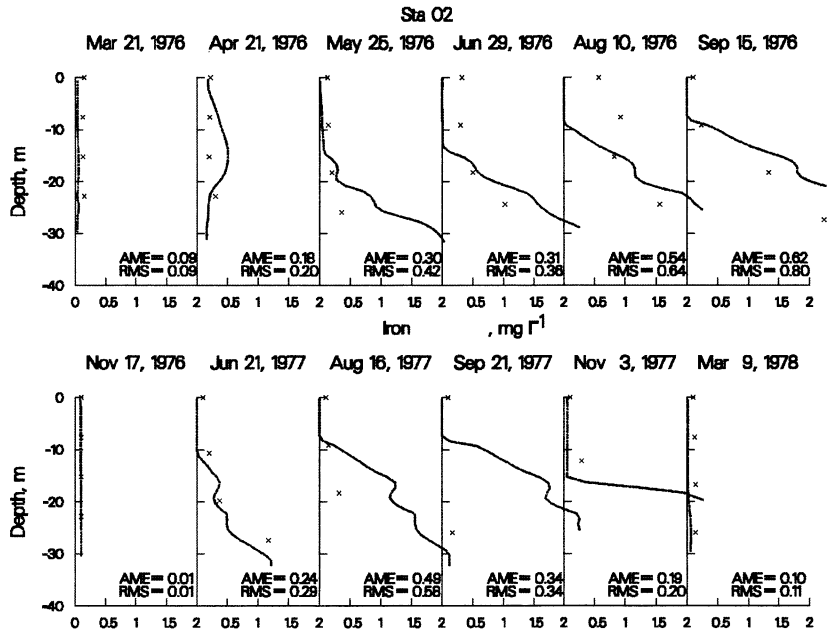

Figure 29. 1976-1978 Computed (…) vs. Observed (x) Iron Concentrations at Station 3JPPS20002.

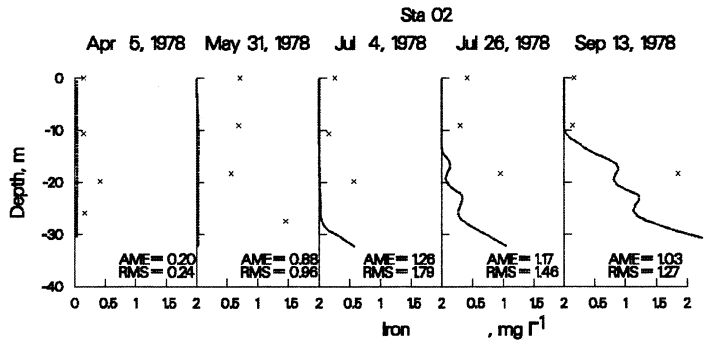

Figure 30. 1976-1978 Computed (…) vs. Observed (x) Iron Concentrations at Station 3JPPS20002.

Application to 1981

The CE-QUAL-W2 model was also applied to 1981. Data for the model application to this year were limited. There were no quality data collected for model quality forcings (boundary concentrations) during this year. Data available for comparison with model predictions were also limited. However, 1981 was selected for the application since it represented the only hydrologically dry year available. See Appendix B for additional comparisons of model predictions and measured values at station 3JPPS20008 (data were not available for station 3JPPS20003 for 1981). The calibration required modifications of the estimated inflow concentrations computed using relations described previously (Table 4) in order to capture observed concentrations at the most upstream reservoir monitoring station (3JPPS20008). Specifically, concentrations of LDOM, RDOM were reduced to 0.4 of their estimated value, while NO_3 was reduced to .01 of its estimated value.

Water surface elevations

As for the previous simulation (1976-1978), water surface elevations are predicted by the model based on the interactions between inflows, outflows, evaporation, and precipitation. Total inflows for 1981 were computed based upon the reservoir storage capacity relationships and observed water surface elevations. The inflows were distributed among major tributaries based upon either USGS records or watershed areas. Daily outflow records were available for this period, which were converted by CELRN to hourly values based upon operation rules. As shown in Figure 31, predicted elevations closely matched observed elevations.

Water age

Water age was computed as a state variable in this application to allow evaluation of the average retention time in the reservoir. The computed water age for 1981 is illustrated in Figure 32. The water age increased during 1981, reaching a maximum of 246 days.

Temperature

Results for temperature calibration at station 3JPPS20002, the station closest to the dam, are given in Figure 33. Overall, the model closely reproduced the observed temperature profiles. As with the application to 1976-1978, most of the discrepancies between predicted and observed temperatures occur in the epilimnion. For 60 observations during this period, the Mean Error was –0.9, the Mean Absolute Error was 1.0, the Root Mean Square Error was 1.3 °C, and the Relative Mean Absolute Error was 7 percent. The mean of the observations for 1981 was 15.1 as compared to the predicted mean of 14.2 °C.

Predicted outflow temperatures are illustrated in Figure 34. For 1981, the maximum temperature in outflows was 18 °C.

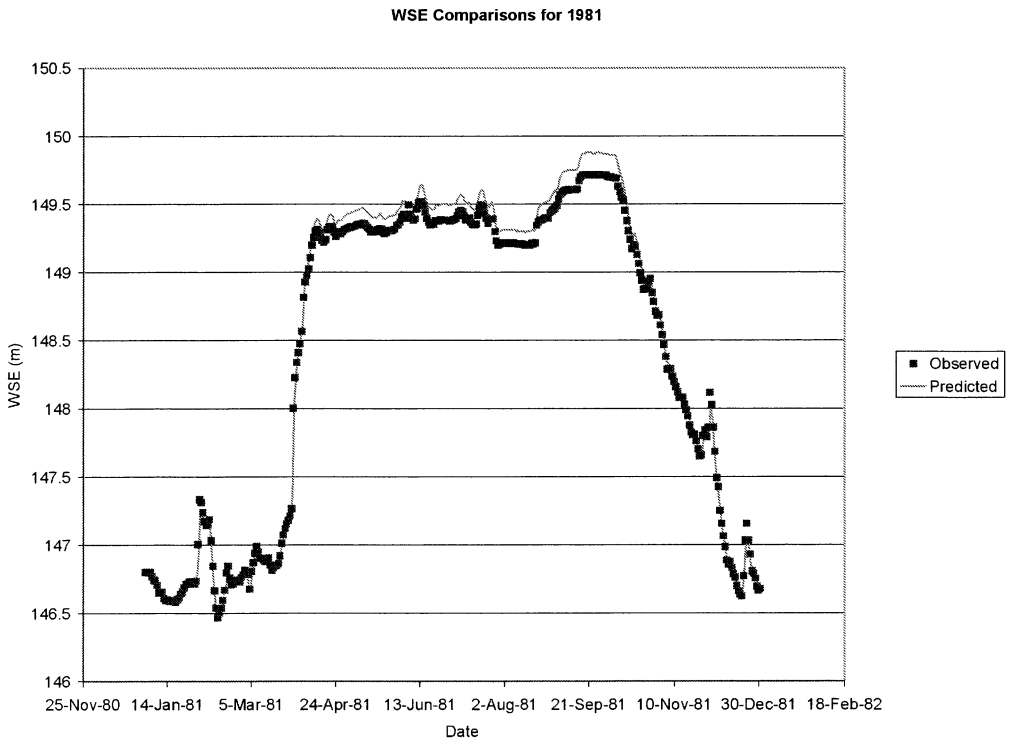

Figure 31. Computed (lines) vs. Observed (symbols) Water Surface Elevations for 1981.

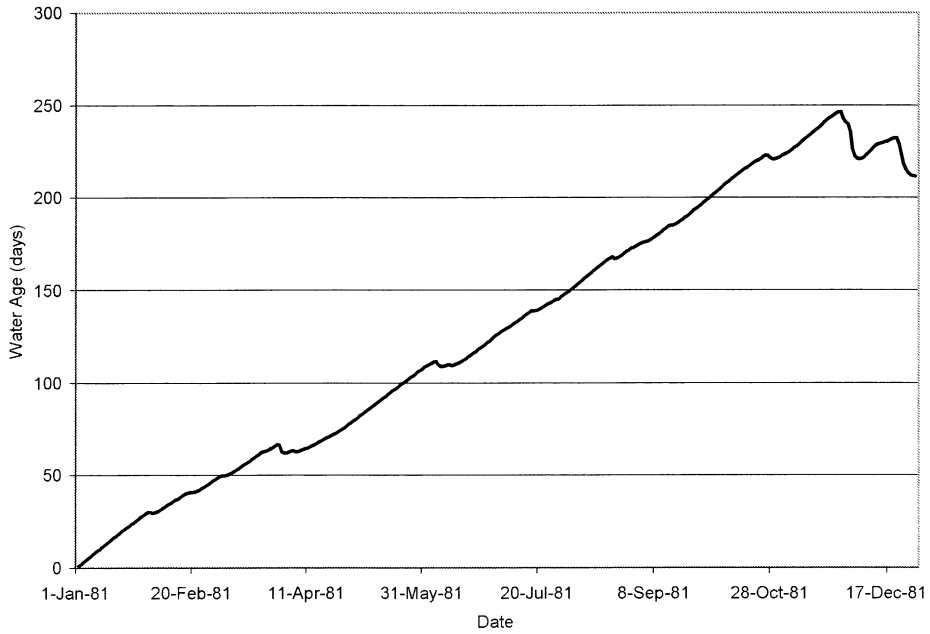

Figure 32. Computed Water Age in J. Percy Priest for 1981.

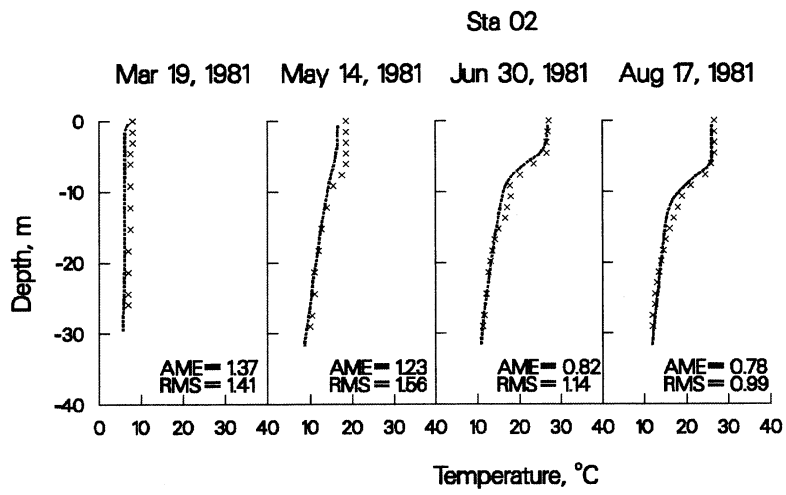

Figure 33. 1981 Computed (…) vs. Observed (x) Temperatures at Station 3JPPS20002.

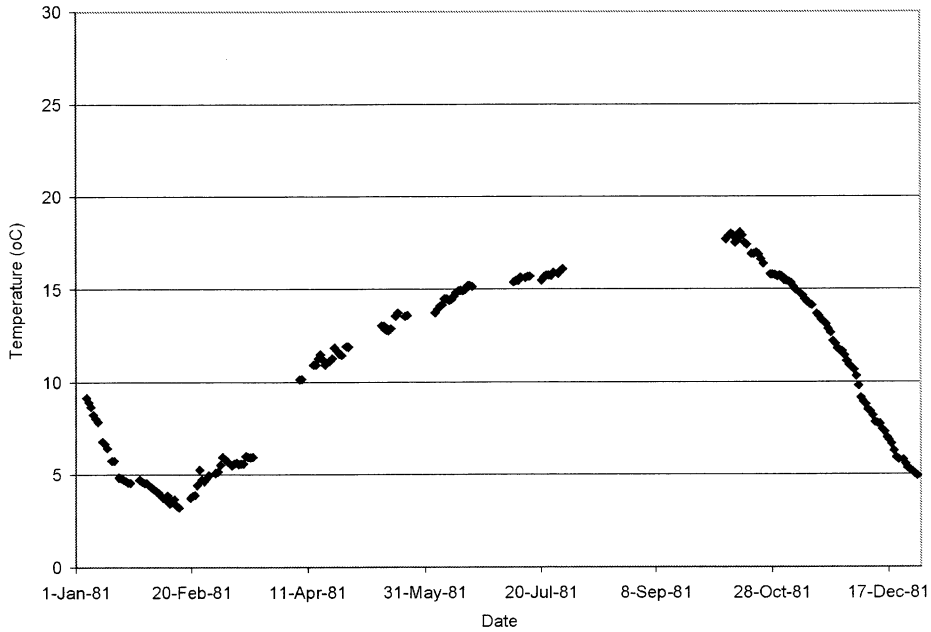

Figure 34. Predicted Outflow Temperatures for 1981.

Dissolved oxygen

Calibration results at 3JPPS20002 are given in Figure 35. Overall, the model did a reasonable job in reproducing the observed spatial and temporal patterns of dissolved oxygen (DO) depletion. The model under-predicted the timing of the onset of oxygen depletion in the springtime, but generally captured the development of hypolimnetic anoxia in summer. For a total of 60 observations, the Mean Error was 1.3, the Mean Absolute Error was 1.6, the Root Mean Square Error was 2.7 mg/l, and the Relative Mean Absolute Error was 41 percent. The mean of the observations was 4.0 as compared to a mean predicted value of 5.3 mg/l.

Predicted dissolved oxygen concentrations averaged over the photic zone of the reservoir are illustrated in Figure 36. Also illustrated are computed dissolved oxygen concentrations at 1.5 m (5 ft) of depth and in reservoir outflows. Note that the computed outflows do not include the effect of turbine reaeration. The observed values interpolated to a depth of 1.5 m (5 ft) are also illustrated. The minimum predicted photic zone-averaged concentration was 6.5 mg/l, while the minimum predicted concentration at 1.5 m was 5.1 mg/l. Note that model predictions indicated a slight increase in the minimum concentrations averaged over the photic zone and at 1.5 m depth for 1981 over the period of 1976-1978. However, there is no evidence in observed data to support this predicted increase. Predicted concentrations in reservoir outflows approached 1 mg/l during summer months.

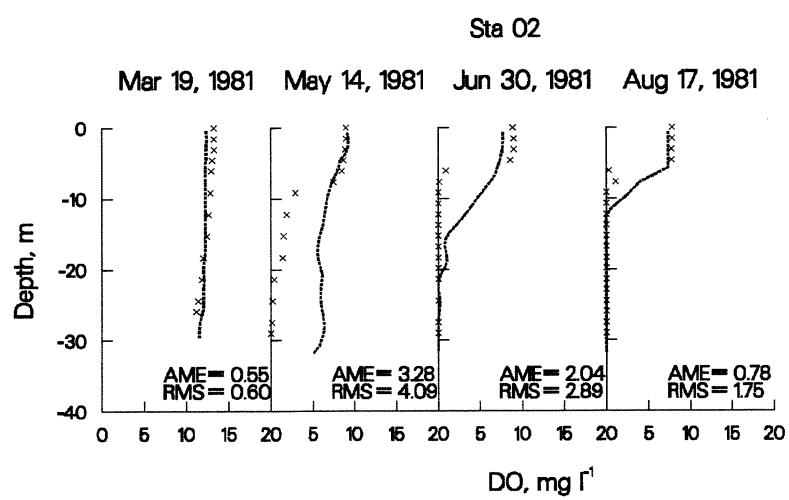

Figure 35. 1981 Computed (...) vs. Observed (x) DO at Station 3JPPS20002.

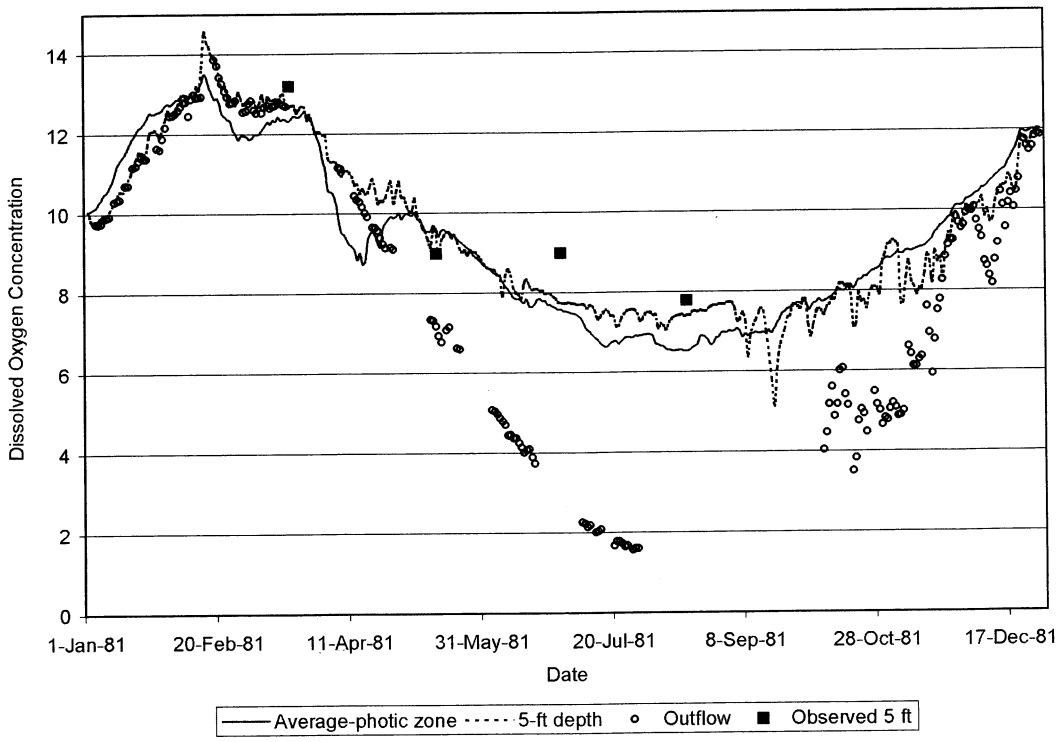

Figure 36. Predicted Average Dissolved Oxygen Concentrations (mg/l) in the Photic Zone, at 1.5 m (5 ft) Depth, and in Reservoir Outflows for 1981.

Nutrients

Results for ammonium, nitrate-nitrite, and dissolved inorganic phosphorus calibration are given in Figure 37-Figure 39. For ammonium, the model generally captures the increase in hypolimnetic concentrations during anoxia and the decrease in those concentrations during overturn. The model also generally captures the increases in nitrate-nitrite as well, but under-predicts concentrations in early months and under-predicts concentrations in the epilimnion. Only one observation was available for phosphorus. Summary statistics for 1981 nutrient predictions are provided in Table 9.

Table 9. Summary Statistics for Nutrient Predictions for 1981

	Ammonia	Nitrate -Nitrite	Inorganic Phosphorus
Total Observations	10	10	2
Mean Error (mg/l)	-0.2	-0.18	-0.06
Mean Absolute Error (mg/l)	0.2	0.22	0.06
Root Mean Square Error (mg/l)	0.3	0.28	0.07
Relative Mean Absolute Error (%)	51	86	24
Mean Observations (mg/l)	.44	.27	.03
Mean Predicted (mg/l)	.22	.08	.02

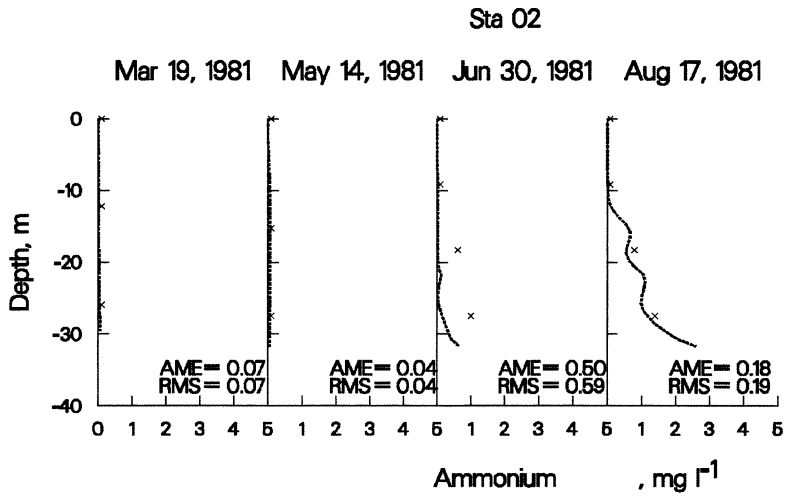

Figure 37. 1981 Computed (…) vs. Observed (x) Ammonium at Station 3JPPS20002.

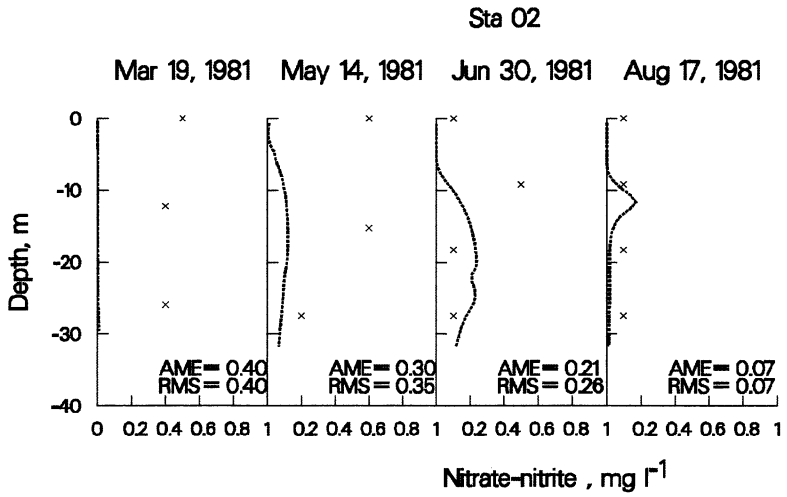

Figure 38. 1981 Computed (…) vs. Observed (x) Nitrate-Nitrite at Station 3JPPS20002.

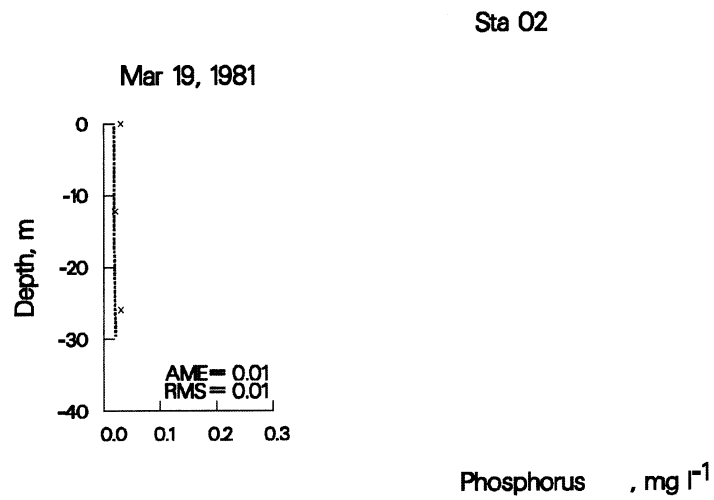

Figure 39. 1981 Computed (...) vs. Observed (x) Phosphorus at Station 3JPPS20002.

Algae

Model predictions for 1981 are compared to observed concentrations in Figure 40. In general, the model captures seasonal variations in chlorophyll *a* concentrations, including the spring bloom. The model underestimates chlorophyll *a*. For a total of 8 observations, the Mean Error was -0.9, the Mean Absolute Error was 3.7, the Root Mean Square error was 3.7 μg chlorophyll *a*/l, and the Relative Mean Absolute Error was 61 percent. The mean of the observations was 5.9 as compared to the predicted mean of 5.0 μg chlorophyll *a*/l.

Predicted average, maximum and minimum chlorophyll *a* concentrations, averaged over the photic zone, are illustrated in Figure 41. Maximum concentrations occurred during summer months. Average predicted concentrations in the photic zone were less than 20 µg/l. The maximum predicted photic-zone averaged chlorophyll *a* concentration was 44 µg/l, similar to the 1976-1978 predictions.

Comparisons were also made between predicted and observed concentrations averaged over 2 m of depth. Computed and observed 2 m-averaged concentrations are illustrated in Figure 42, and indicated the model over-predicted variations in depth-averaged concentrations. Comparison of computed and observed changes in chlorophyll *a* concentration (dChlorophyll *a*/dt) are illustrated in Figure 43 and indicate over-prediction of the summer decline.

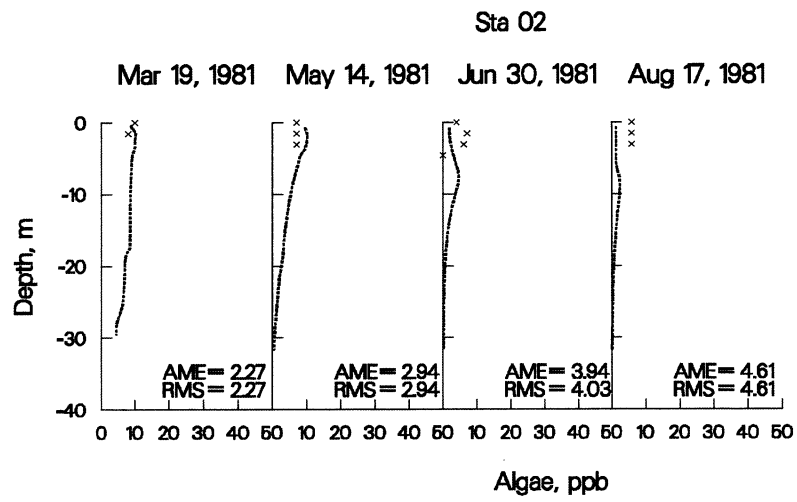

Figure 40. 1981 Computed (...) vs. Observed (x) Algal Chlorophyll *a* at Station 3JPPS20002.

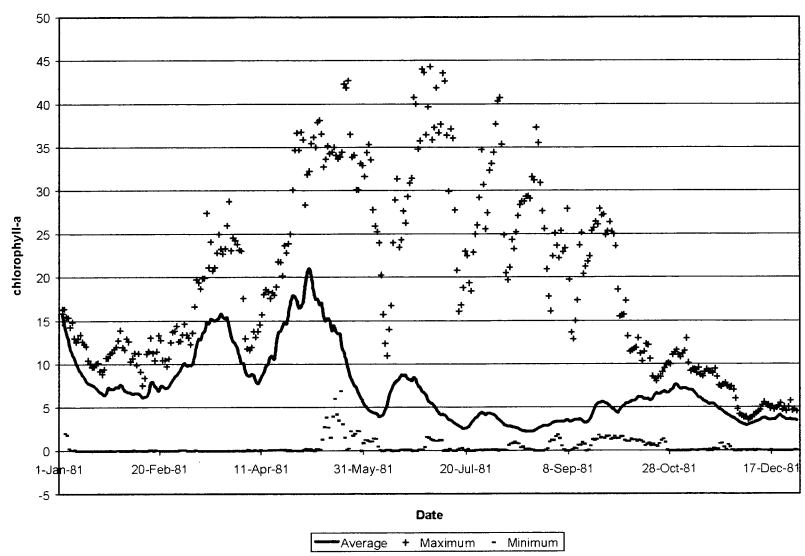

Figure 41. Predicted Average, Maximum and Minimum Chlorophyll *a* Concentrations (μg/l) in the Photic Zone for 1981.

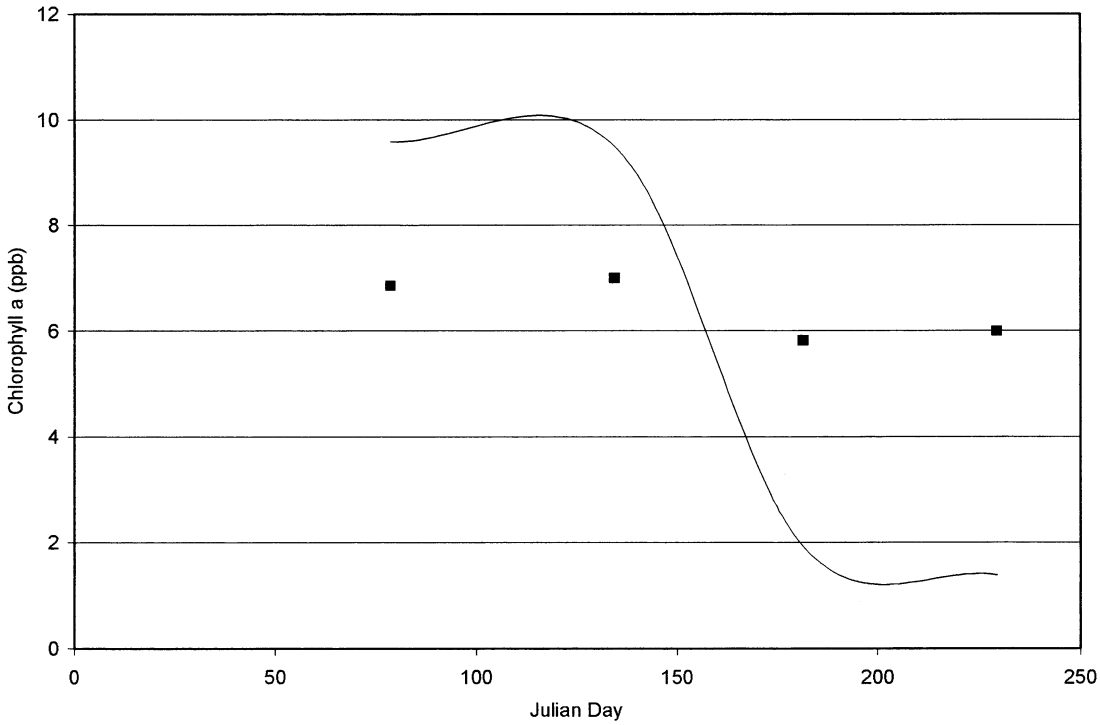

Figure 42. 1981 Computed (—) vs. Observed (■) Algal Chlorophyll *a* at Station 3JPPS20002 Averaged Over 2 m of Depth.

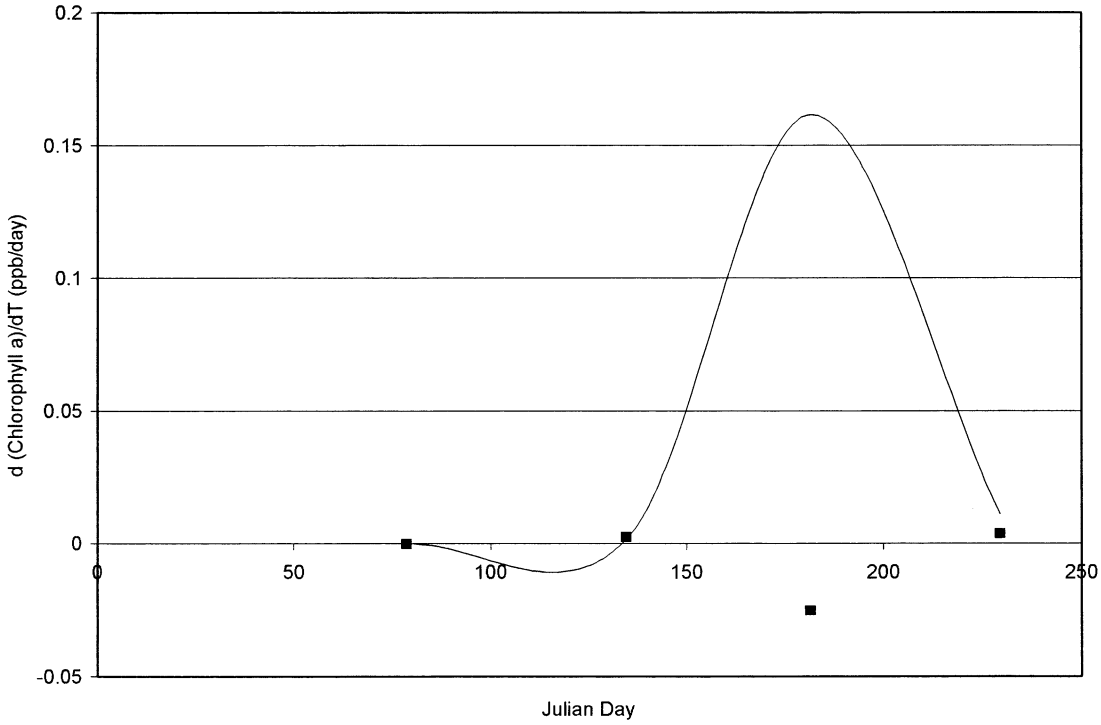

Figure 43. 1981 Computed (—) vs. Observed (■) Changes in Algal Chlorophyll *a* Concentrations with Time at Station 3JPPS20002 Averaged Over 2 m of Depth.

Iron

Results for total iron calibration at station 3JPPS20002, the station closest to the dam, are given in Figure 44. Overall, the model closely reproduced the observed iron profiles. Computed iron concentrations were primarily controlled by specified release rates during anoxic conditions. For a total of 10 observations, the computed Mean Error was -0.5, the Mean Absolute Error was 0.5, the Root Mean Square error was 0.8 mg/l, and the Relative Mean Absolute Error was 70 percent. The mean of the observations was 0.7 as compared to a predicted mean of 0.2 mg/l.

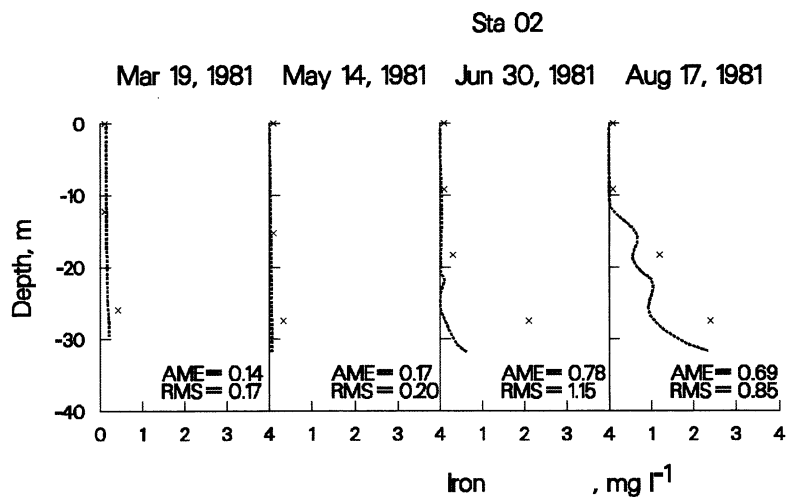

Figure 44. 1981 Computed (...) vs. Observed (x) Iron Concentrations at Station 3JPPS20002.

Application to 1994

The final period to which the model was applied was 1994. This year represented a hydrologically wet year. As with the application to 1981, data available for model forcings (water quality boundary conditions), and for comparison with model predictions were limited. Model quality forcings were based upon empirical relationships developed from data collected in the 1970's. Comparisons to the limited data available suggested that concentrations predicted with these relationships were reasonable. See Appendix C for additional comparisons of model predictions and measured values. The calibration required modifications of the estimated inflow concentrations computed using relations described previously (Table 4) in order to capture observed concentrations at the most upstream reservoir monitoring station (3JPPS20008). Specifically, concentrations of LDOM, RDOM, and LPOM were reduced to 0.1 of their estimated value.

Water surface elevations

Water surface elevations are predicted by the model based on the interactions between inflows, outflows, evaporation, and precipitation. Inflows were computed similarly to those for previous years of application. There were hourly outflow records available for this period, which were used in the simulations. As shown in Figure 45, predicted elevations closely matched observed elevations.

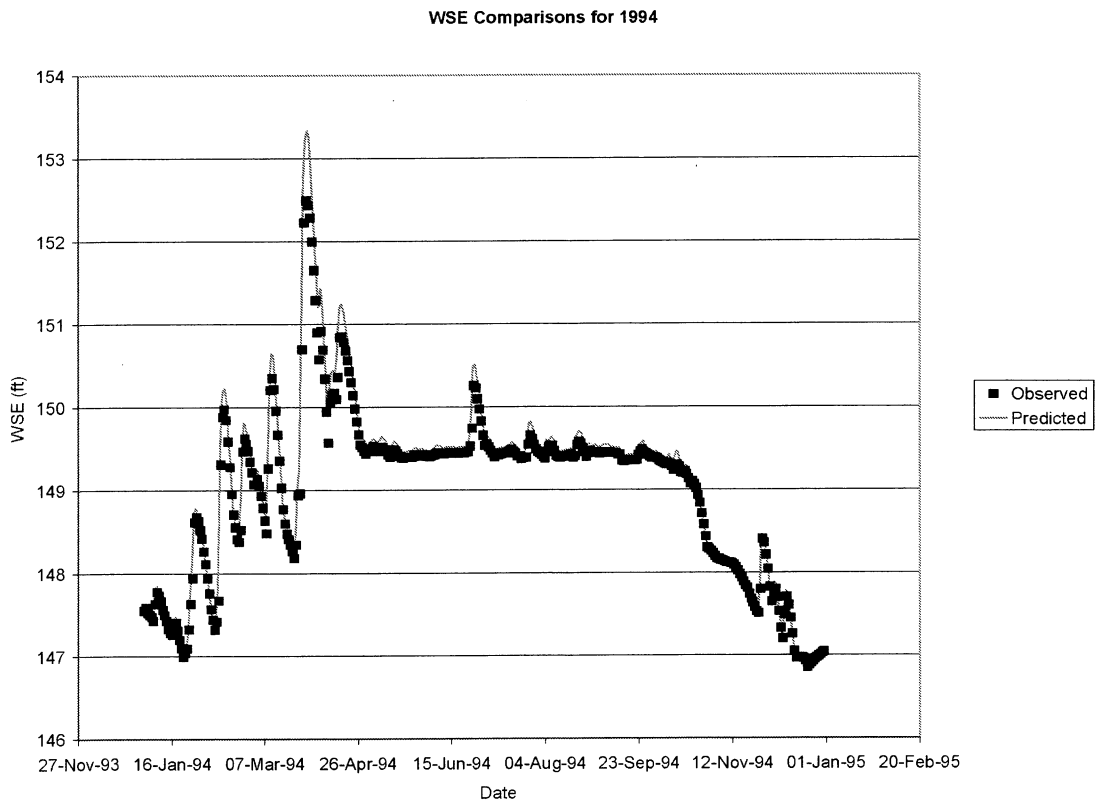

Figure 45. Computed (lines) vs. Observed (symbols) Water Surface Elevations for 1994.

Water age

Water age was computed as a state variable in this application to allow evaluation of the average retention time in the reservoir. The computed water age for 1994 is illustrated in Figure 46. The water age increased during 1994, reaching a maximum of 176 days.

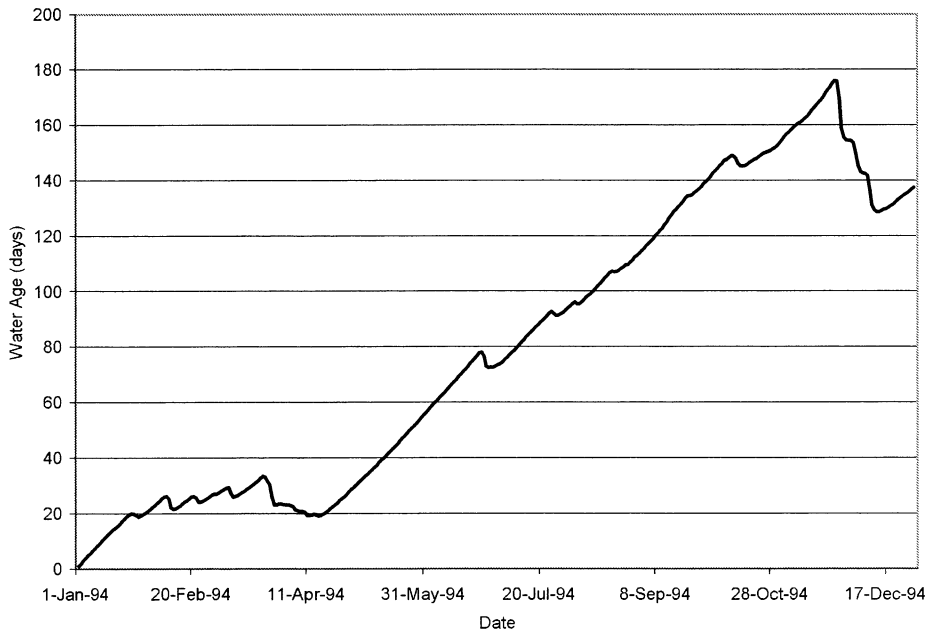

Figure 46. Computed Water Age in J. Percy Priest for 1994.

Temperature

Results for temperature calibration at station 3JPPS20002, the station closest to the dam, are given in Figure 47. Overall, the model closely reproduced the observed temperature profiles. Most of the discrepancies between predicted and observed temperatures occur in the epilimnion. Discrepancies also occurred in the hypolimnion for this year of application, with predicted temperatures being consistently colder than those observed. This is attributed to the meteorological data, which did not seem to accurately represent conditions for this year. For 106 observations during this period, the Mean Error was –1.1, the Mean Absolute Error was 1.2, the Root Mean Square Error was 1.5 °C, and the Relative Mean Absolute Error was 8 percent. The mean of the observations was 14.5 and compared to a predicted mean of 13.4 °C.

Predicted outflow temperatures are illustrated in Figure 48. The maximum temperature in 1994 outflows was 20.2 °C.

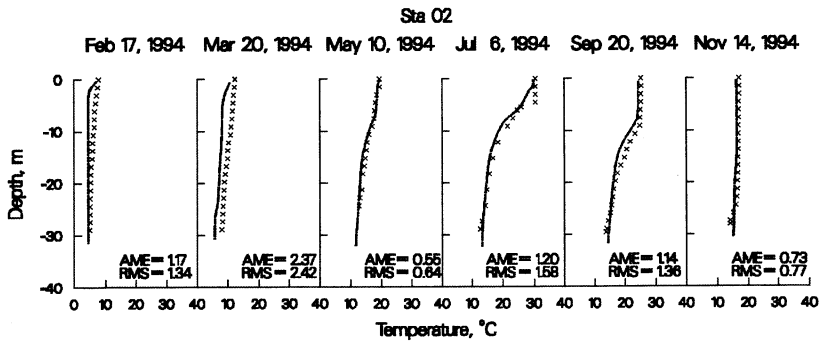

Figure 47. 1994 Computed (…) vs. Observed (x) Temperatures at Station 3JPPS20002.

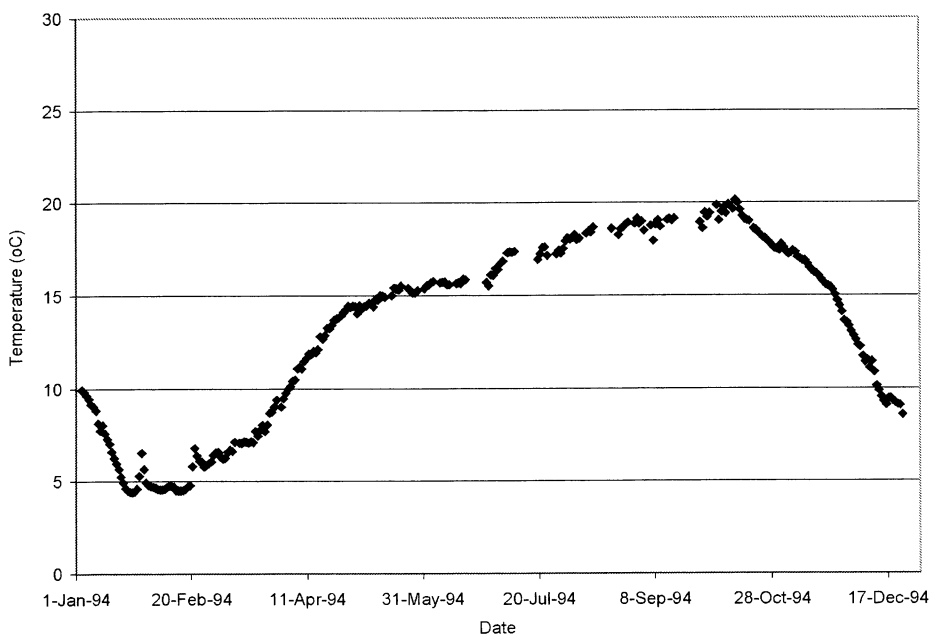

Figure 48. Predicted Outflow Temperatures for 1994.

Dissolved oxygen

Calibration results at 3JPPS20002 are given in Figure 49. Overall, the model did a reasonable job in reproducing the observed spatial and temporal patterns of dissolved oxygen (DO) depletion. The model generally captured the timing of the onset of oxygen depletion in the springtime, the development of hypolimnetic anoxia in summer, and the increase in DO with depth during fall overturn. For a total of 106 observations, the Mean Error was 0.9, the Mean Absolute Error was 1.2, the Root Mean Square Error was 1.7 mg/l, and the Relative Mean Absolute Error was 20 percent. The mean of the observations was 6.2 mg/l as compared to a predicted mean of 7.0 mg/l.

Predicted dissolved oxygen concentrations averaged over the photic zone of the reservoir are illustrated in Figure 50. Also illustrated are computed dissolved oxygen concentrations at 1.5 m (5 ft) of depth and in reservoir outflows. Note that the computed outflows do not include the effect of turbine reaeration. The observed values interpolated to a depth of 1.5 m (5 ft) are also illustrated. The minimum predicted photic zone-averaged concentration was 7.3 mg/l, while the minimum predicted concentration at 1.5 m was 5.4 mg/l. Note that model predictions indicated a slight increase in the minimum concentrations averaged over the photic zone and at 1.5 m depth for 1994 over 1981 and 1976-1978 predictions. However, there is no evidence in observed data to support this predicted increase. Predicted concentrations in reservoir outflows approached 1 mg/l during summer months.

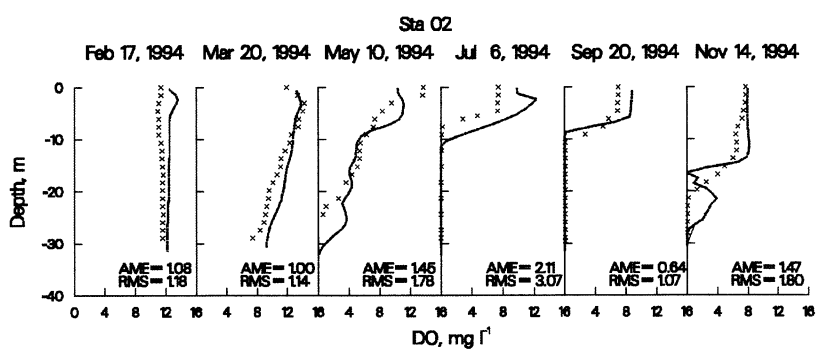

Figure 49. 1994 Computed (...) vs. Observed (x) DO at Station 3JPPS20002.

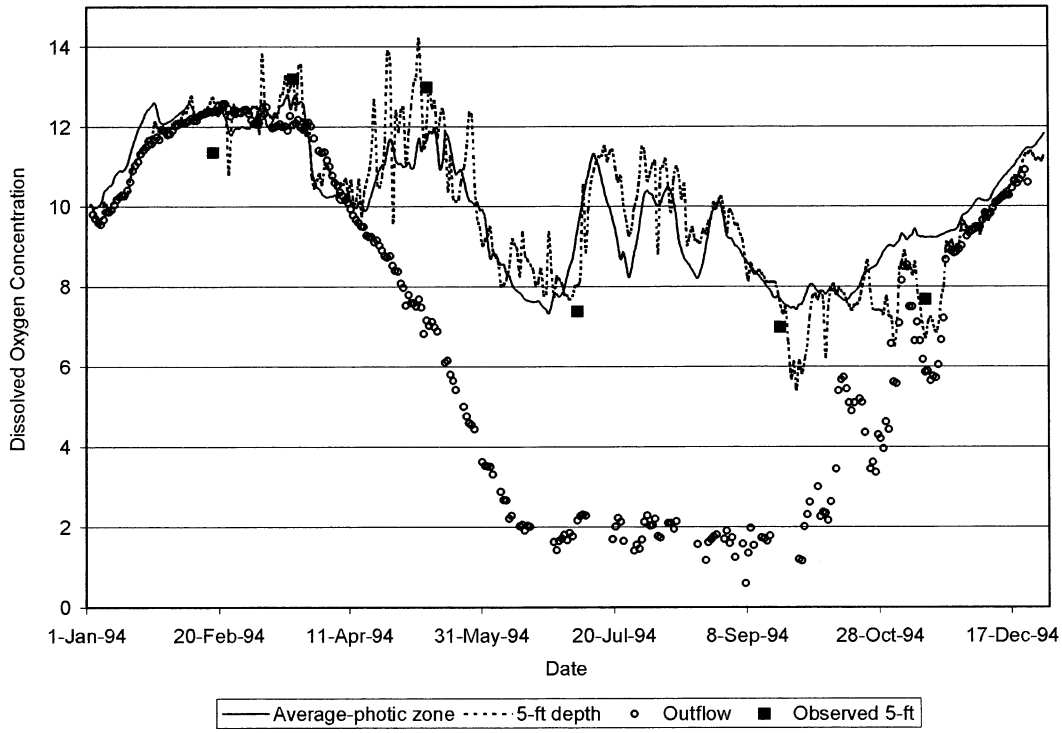

Figure 50. Predicted Average Dissolved Oxygen Concentrations (mg/l) in the Photic Zone, at 1.5 m (5 ft) Depth, and in Reservoir Outflows for 1994.

Nutrients

Results for ammonium, nitrate-nitrite, and dissolved inorganic phosphorus calibration are given in Figure 51-Figure 53. For ammonium, the model generally captures the increase in hypolimnetic concentrations during anoxia and the decrease in those concentrations during overturn. The model also generally captures the increases in nitrate-nitrite as well. Phosphorus concentrations are over-predicted during fall months, particularly as a result of an inflow event in July, suggesting inappropriate boundary forcings. This may be attributed to sediment release rates being less in 1994 than previous years. However, in the absence of supporting data, the release rates for all years were held the same for consistency. Summary statistics for 1994 nutrient predictions are provided in Table 10.

Table 10. Summary Statistics for Nutrient Predictions for 1994

	Ammonia	Nitrate-Nitrite	Inorganic Phosphorus
Total Observations	18	18	14
Mean Error (mg/l)	0.4	-0.2	0.2
Mean Absolute Error (mg/l)	0.5	0.3	0.2
Root Mean Square Error (mg/l)	0.7	0.4	0.3
Relative Mean Absolute Error (%)	105	79	380
Mean Observations (mg/l)	0.4	0.4	0.1
Mean Predicted (mg/l)	0.8	0.2	0.2

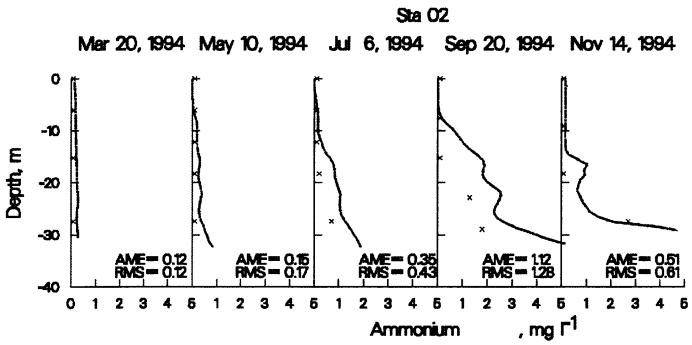

Figure 51. 1994 Computed (…) vs. Observed (x) Ammonium at Station 3JPPS20002.

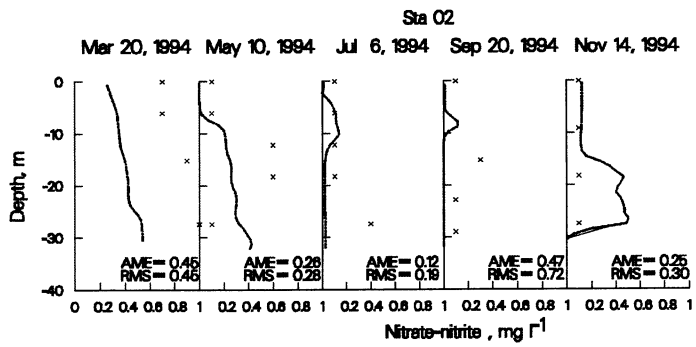

Figure 52. 1994 Computed (…) vs. Observed (x) Nitrate-Nitrite at Station 3JPPS20002.

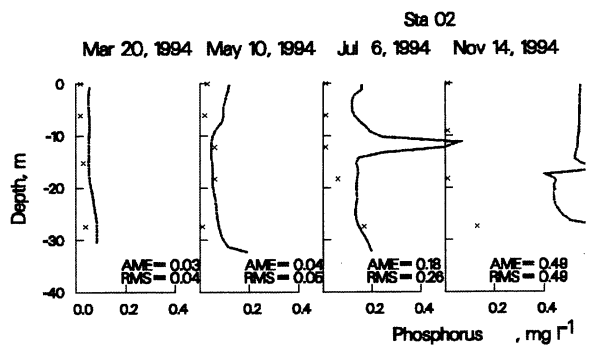

Figure 53. 1994 Computed (…) vs. Observed (x) Phosphorus at Station 3JPPS20002.

Algae

Model predictions for 1994 are compared to observed concentrations in Figure 54. In general, the model captured seasonal variations in chlorophyll *a* concentrations, including spring and fall blooms. For a total of 17 observations, the Mean Error was 6, the Mean Absolute Error was 13, the Root Mean Square error was 16 μg chlorophyll *a*/l, and the Relative Mean Absolute Error was 84 percent. The mean of the observations was 16 as compared to a predicted mean of 22 μg chlorophyll *a*/l. The relatively poor statistical comparison is attributed, in part, to the over-prediction of chlorophyll *a* during late summer and early fall, partially a result of the over-prediction of phosphorus.

Predicted average, maximum and minimum chlorophyll *a* concentrations, averaged over the photic zone, are illustrated in Figure 55. Typically, maximum concentrations occurred during summer. Average predicted concentrations in the photic zone were at times greater than 30 µg/l. The maximum predicted photic-zone averaged concentration was 64 µg/l. Predictions for 1994 were higher than other modeled years. However, the model over-predicted concentrations during summer months as compared to observed data.

Comparisons were also made between predicted and observed concentrations averaged over 2 m of depth. Computed and observed 2 m-averaged concentrations are illustrated in Figure 56, and indicated the model under-predicted concentrations during the spring and over-predicted concentrations during the fall. Comparison of computed and observed changes in chlorophyll *a* concentration (dChlorophyll *a*/dt) are illustrated in Figure 57 and indicate the model under-predicted a rapid decline in concentrations during 1994 and their subsequent recovery.

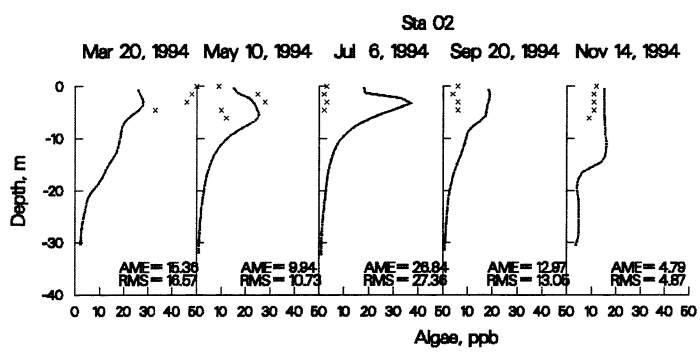

Figure 54. 1994 Computed (...) vs. Observed (x) Algal Chlorophyll *a* at Station 3JPPS20002.

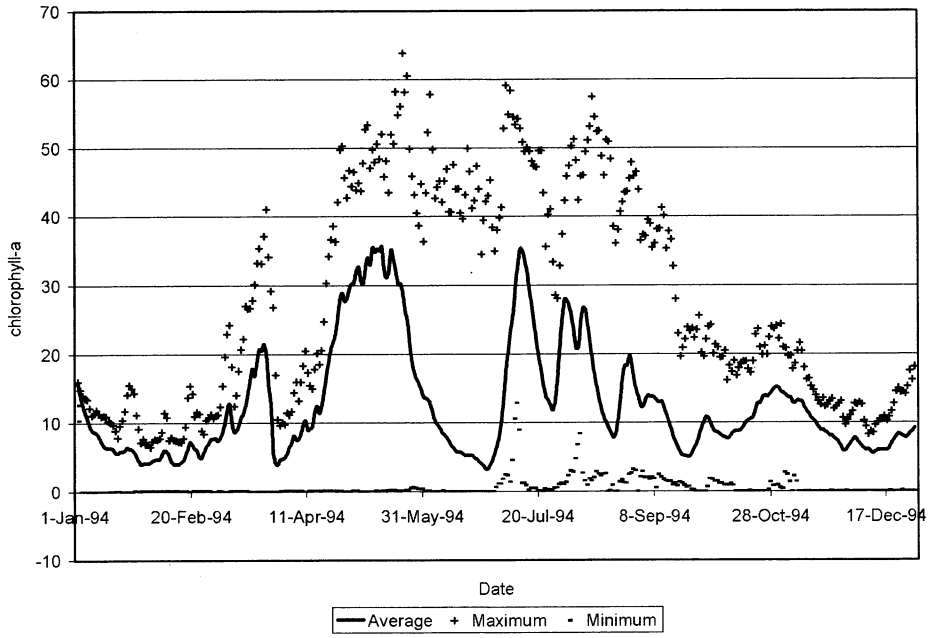

Figure 55. Predicted Average, Maximum and Minimum Chlorophyll *a* Concentrations (μg/l) in the Photic Zone for 1994.

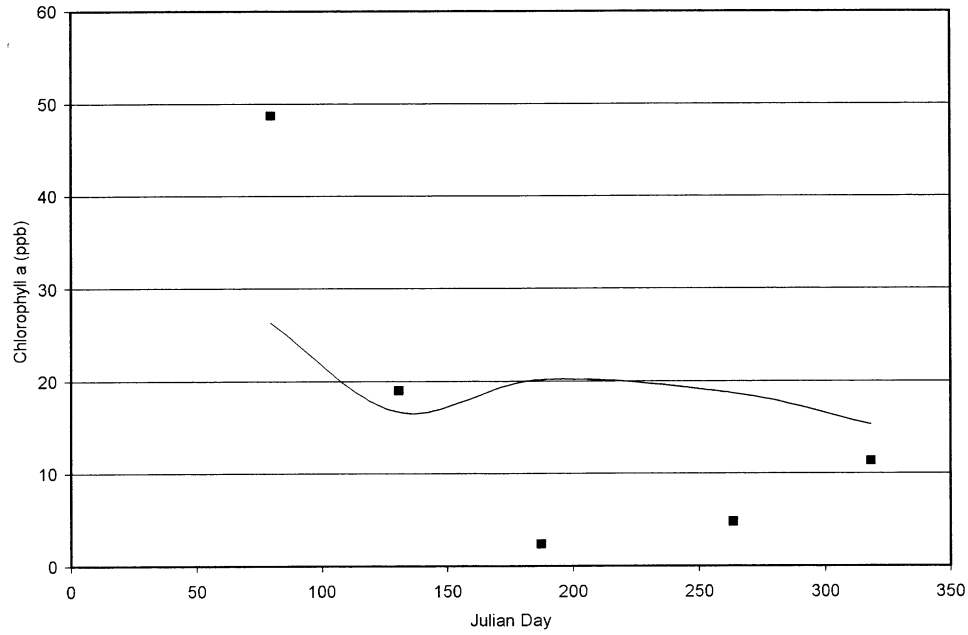

Figure 56. 1994 Computed (—) vs. Observed (■) Algal Chlorophyll *a* at Station 3JPPS20002 Averaged Over 2 m of Depth.

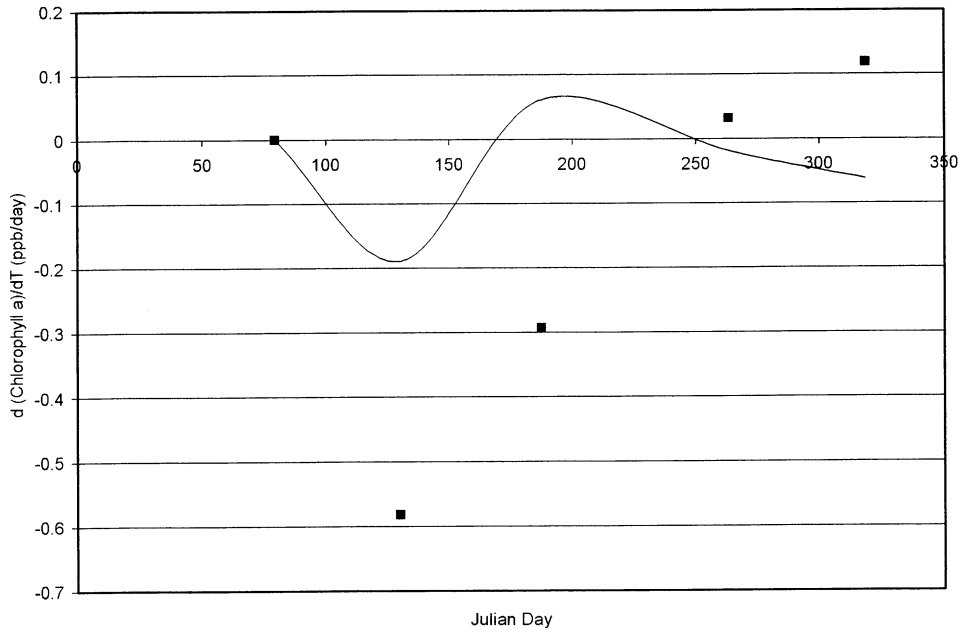

Figure 57. 1994 Computed (—) vs. Observed (■) Changes in Algal Chlorophyll *a* Concentrations with Time at Station 3JPPS20002 Averaged Over 2 m of Depth.

Iron

Results for total iron calibration at station 3JPPS20002, the station closest to the dam, are given in Figure 58. Overall, the model closely reproduced the observed iron profiles in spring and summer, but over-predicted concentrations in the fall. Computed iron concentrations were primarily controlled by specified release rates during anoxic conditions. For a total of 15 observations, the computed Mean Error was 0.4, the Mean Absolute Error was 0.5, the Root Mean Square error was 0.7 mg/l, and the Relative Mean Absolute Error was 112 percent. The mean of the observations was 0.4 in comparison to a predicted mean of 0.8 mg/l.

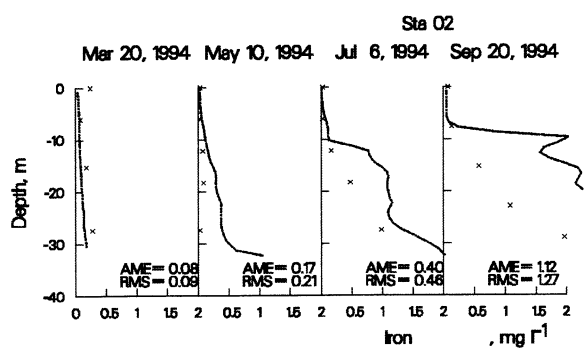

Figure 58. 1994 Computed (...) vs. Observed (x) Iron Concentrations at Station 3JPPS20002.

5 Evaluation of Model Scenarios

Wastewater Treatment Plants

The CE-QUAL-W2 model developed for J. Percy Priest was applied to assess the potential impact of the existing and hypothetical wastewater discharges on the water quality of the reservoir. To assess the impact of the existing facility, model runs were completed with and without flows and loadings from the Smyrna STP (TN0020541, see Point sources). To assess the impact of a new hypothetical discharge, the model was run with the combination of the Smyrna discharges and an additional wastewater discharge of 0.44 m^3/s (10 mgd). The hypothetical discharge was assumed to have the following wastewater characteristics: temperature, 20 °C; labile DOM, 15.0 mg/L; phosphate, 6.6 mg/l; ammonia, 10.0 mg/l; and dissolved oxygen concentration, 6.0 mg/l. These discharges were based upon representative concentrations for secondary effluents. Simulations were completed where the hypothetical discharge was arbitrarily placed in model segments 10, 20, 30, and 36 of the main channel. In addition, simulations included discharges from the hypothetical facility into these segments as a density placed inflow and where the inflow was placed into the hypolimnion. For the scenarios simulated with and without the Smyrna facility and with the combined Smyrna and hypothetical facility, the distributed inflows were adjusted to maintain the water balance.

The discharge of wastewater into the facility is expected to have localized effects. However, since the placement of the hypothetical discharge was arbitrary, it was considered that assessment of the relative reservoir-wide impacts of the discharge on dissolved oxygen concentrations could make a more meaningful evaluation of potential impacts. For this analysis, the CE-QUAL-W2 model code was modified to provide three additional forms of output:

- Volume days that dissolved oxygen concentrations were less than 5 mg/l in the reservoir.
- Volume days that dissolved oxygen concentrations were less than 2 mg/l in the photic zone.
- Volume-days that dissolved oxygen concentrations were less than 2 mg/l in the aphotic zone.

These model output were computed as the sum of the product of the computed volumes and dissolved oxygen concentrations for these conditions over the course of the simulation. The location of the photic and aphotic zone was determined from the model computed light extinction and assuming that 1 percent of surface light defined the photic zone depth. The 1981 (dry year) conditions were used as the basis for all of these evaluations.

The results of these simulations are illustrated in Figure 59 to Figure 61. The removal of the Smyrna facility (average discharge 0.09 m^3/s), was projected to produce a slight (approximately 1 percent) decrease in the reservoir-wide conditions where dissolved oxygen concentrations were less that 5 gm/l. The Smyrna facility was projected to have a negligible impact on the period during which the reservoir-wide concentrations were less than 2 mg/l. For the hypothetical discharge, a density placed discharge was estimated to produce a 4-6 percent increase in the time volume-days during which the dissolved oxygen concentrations were less than 5 mg/l. Larger increases were computed in the volume-days that the reservoir concentrations were less than 2 mg/l (72-83 percent increase in the photic zone and 8 to 14 percent increase in the aphotic zone). Discharges into the hypolimnion typically cause a reduction in the volume-days during which dissolved oxygen concentrations were less than 5 mg/l in the reservoir, and 2 mg/l in the aphotic zone due to hypolimnetic injection of aerobic effluent. However, the hypolimnetic discharges simulated all resulted in an increase in the volume days during which the dissolved oxygen concentrations were less than 2 mg/l in the photic zone, attributed to the upward mixing of additional oxygen consuming materials.

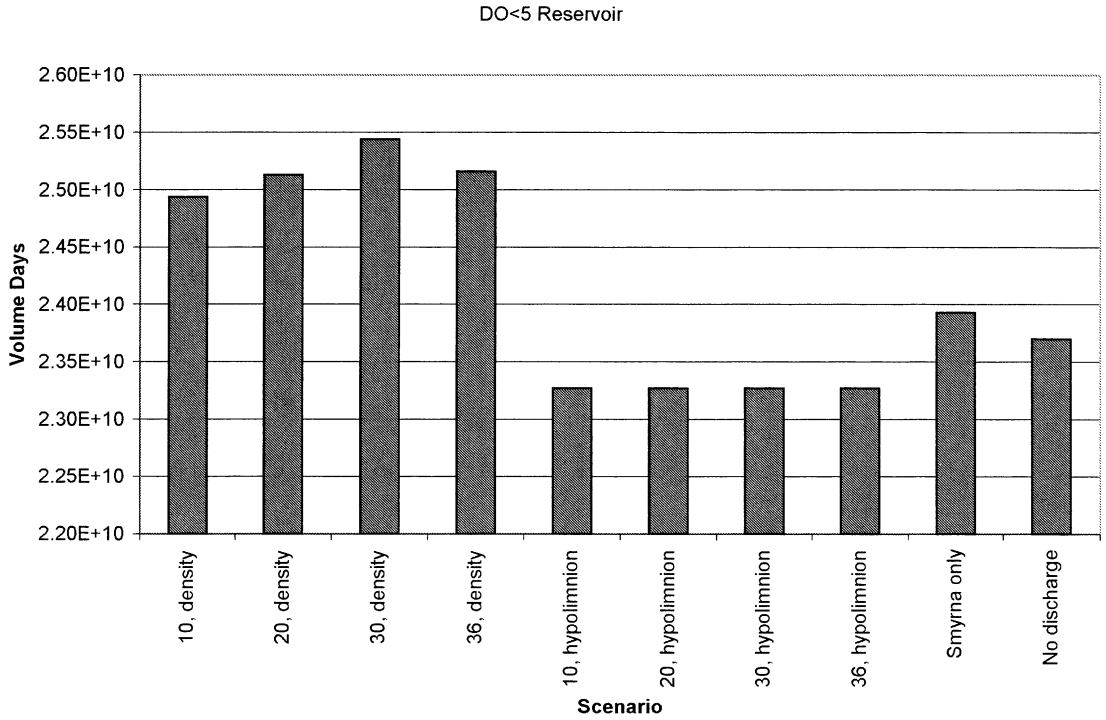

Figure 59. 1981 Cumulative Volume-days during which Dissolved Oxygen Concentrations were Less Than 5 mg/l in J. Percy Priest for Different Wastewater Conditions.

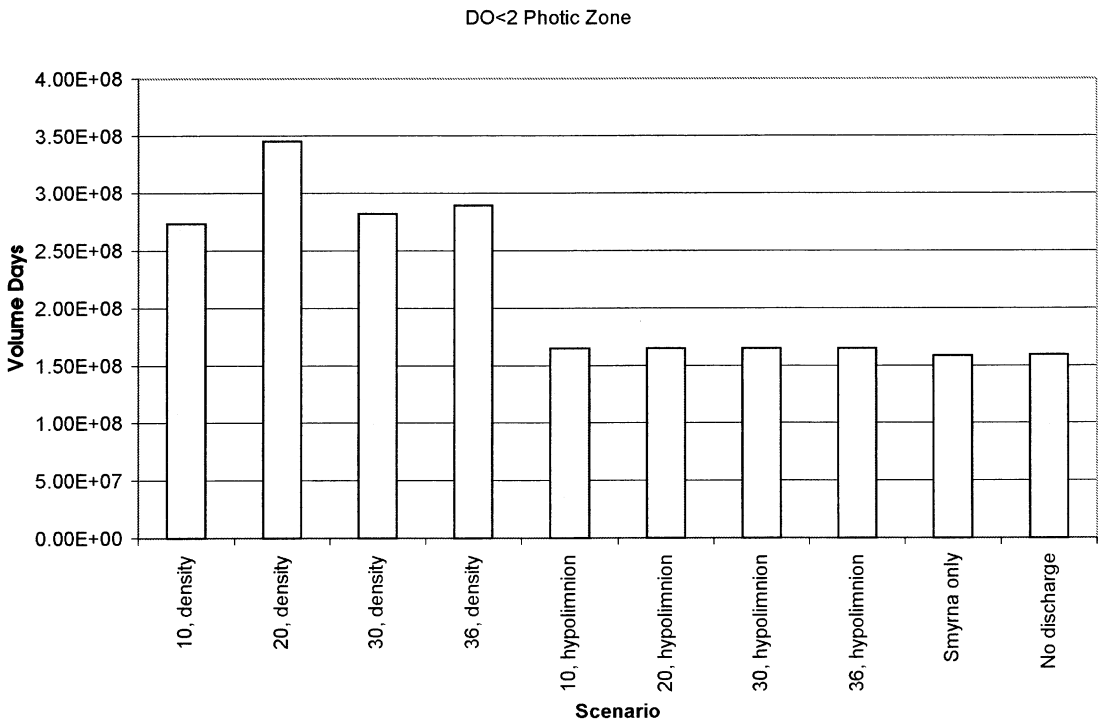

Figure 60. 1981 Cumulative Volume-days when Dissolved Oxygen Concentrations were Less Than 2 mg/l in the Photic Zone of J. Percy Priest for Different Wastewater Conditions.

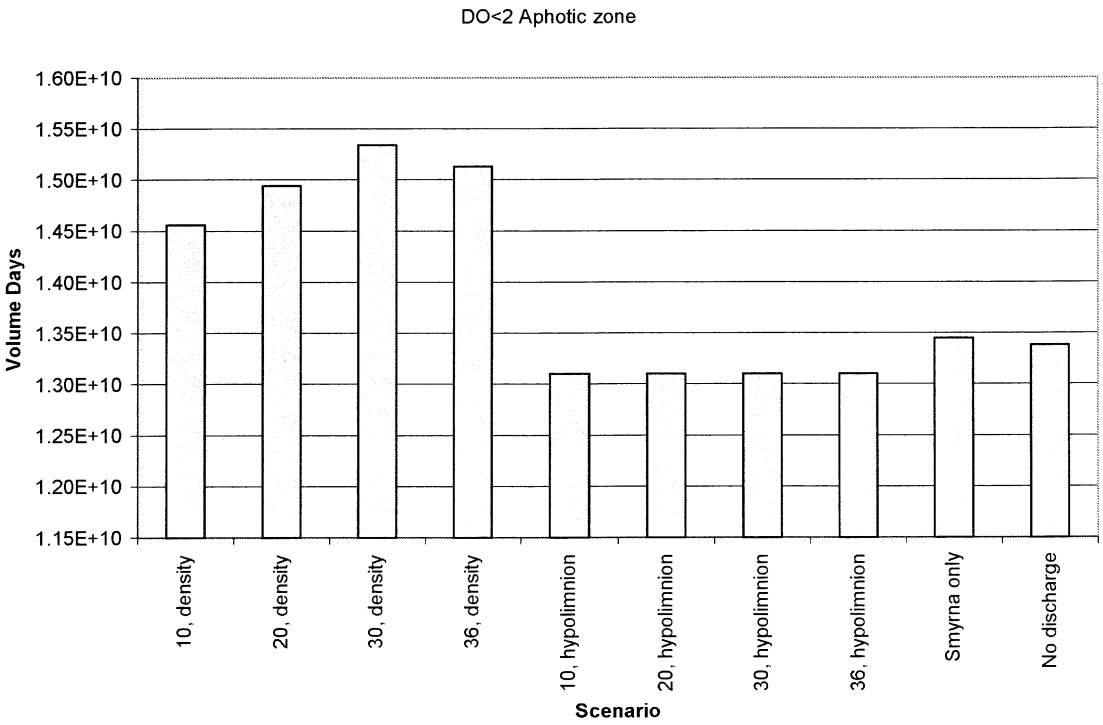

Figure 61. 1981 Cumulative Volume-days when Dissolved Oxygen Concentrations were less than 2 mg/l in the Aphotic Zone of J. Percy Priest for Different Wastewater Conditions.

Dissolved Oxygen Injection

As part of the model application, modifications to CE-QUAL-W2 were made to allow evaluation of a dissolved oxygen injection system. The modifications were based upon the previous application of an oxygenation system at Richard B. Russell Reservoir (RBR), a Corps facility bordering Georgia and South Carolina.

Model theory

When a continuous release of bubbles occurs at a depth in a water column, the passage of bubbles through the water column entrains ambient water. The transfer of gasses from the bubbles to the surrounding water ensues. The gas in the bubbles is exposed to the local hydrostatic pressures, which are directly proportional to the saturation concentration of the gas bubble at the gas-water interface. The saturation concentration of oxygen under 4 atmospheres of pressure (42 m), will be 4 times the saturation concentration at the surface. The molar fraction is also proportional to the local saturation concentration of the gas. In the case of molecular oxygen, the saturation concentration of oxygen will be 5 times that of the atmospheric composition of oxygen in air. The saturated concentration in equilibrium with the gas at any depth is:

$$C_S = \frac{Y\,P_t}{H} = \frac{Y}{H}\left[1 + \frac{\rho_t\,(D - z)}{P}\right]$$

where C_s is the saturated gas concentration (mg/l), Y the mole fraction of the gas, P_t the total hydrostatic pressure (atm), H is Henry's law constant (atm/mole fraction), D the total depth of the diffuser (m), Z the height above the diffuser (m), g the acceleration of gravity (m^2/s), and ρ_t the density of the fluid (kg/m^3).

The mass flux of the gas across the gas-liquid interface can be formulated as a first-order process. The rate of gas transfer is proportional to the difference between the exiting concentration and the equilibrium concentration of the gas in solution. This relationship can be expressed as

$$\frac{dm}{dt} = K_g\ A\,(C_S - C)$$

where dm/dt the mass flux of gas, K_g the mass exchange coefficient (m^2/s), A the interfacial area (m^2), C_s the saturation concentration of the gas in solution (mg/l), and C the concentration of gas in solution (mg/l).

The exchange of both nitrogen and oxygen is required in this formulation to determine the molar fraction of gases in each bubble as it rises through the water column. The concentration potential for oxygen will be large for conditions where the initial molar fraction of oxygen is unity. A small concentration potential of nitrogen exists since the saturation concentration of the bubble is initially zero. The injection rate determines the total number of bubbles in a

given computational cell. This computation is sensitive to the rise velocity, the bubble diameter, and the mass exchange coefficient. This calculational procedure assumed that the rise velocity of a bubble remains constant throughout the water column. As the bubble changes volume in response to the exchange of mass and changing hydrostatic pressure, the rise velocity will also change. However, in the RBR application, it was assumed that the rise velocity was relatively insensitive to the bubble sizes under consideration, and held constant.

The steps in the analysis are described below:

1. The number of bubbles in each computational cell is determined as a fraction of the mass flux of injected gas, mean bubble diameter, and the rise velocity of the bubbles. The number of bubbles will remain constant in each computational cell if the injection rate is constant, but may vary between computational cells if the heights vary. The effective rise velocity of a bubble will be a function of the velocity of the entrained water, and the size of the bubble. The terminal rise velocity of bubbles in the size class generated by fine pore diffusers is relatively insensitive to bubble size, and a constant rise velocity was assumed for this and the RBR application.

2. The initial mass in a bubble is determined by dividing the mass flux of the injected gas by the flux of bubbles.

3. The volume and surface area of a single bubble plume is determined assuming a spherical bubble shape, the local hydrostatic pressure, and the mass retained in the bubble.

4. The saturation concentration for oxygen and nitrogen is determined from the local hydrostatic pressure, molar fraction within the bubble, and Henry's law constant.

5. The oxygen and nitrogen mass flux is determined in a given computational cell for a single bubble. The detention time of the bubble in each computation cell is used to estimate the bubble mass flux. The total mass in a single bubble is recalculated based on the flux estimate.

6. The molar fraction is determined using the updated bubble mass for oxygen and nitrogen. This value is used in the calculation of mass exchange in the adjoining computational cell by repeating steps 3-6, starting at the depth of the diffuser and stopping at the water surface.

The total mass flux in each cell is computed by applying the total number of bubbles in each computational cell to the mass flux of a single cell during the current time step. The change in mass is divided by the volume of the current cell to obtain the change in concentration in a given cell.

Implementation in CE-QUAL-W2

The algorithm described above was implemented in CE-QUAL-W2 based upon routines developed for the RBR application. The code and model input

were modified and then tested using the input developed for the 1981 and 1994 application years.

The model input was modified to specify whether the option was to be implemented and then to specify the number of injections that were to occur. For each diffuser, variables required for the analysis, summarized in Table 11, were then input as illustrated below

OXYGEN INJ	**O2C**	**NINJ**
	ON	1

OXYGEN INJ	**IDIF**	**KTO**	**KBO**	**BDIA**	**RVEL**	**MFRAC**	**KL**
	37	27	35	2.0	0.30	1.0	1.0E-6

Table 11. Variables Required for Computation of Bubble Mass Exchange

Variable	Definition	Description
IDIF	Horizontal location of diffuser	Horizontal Segment number
KTO, KBO	Vertical location	Top and bottom cell numbers
BDIA	Mean bubble diameter	Determined by diffuser type (mm)
RVEL	Rise velocity	effective rise velocity of the bubble plume (m/s)
MFRAC	Molar fraction of injected gas	1.0 for molecular O2, 0.21 for air
KL	Mass exchange coefficient for oxygen	exchange rate (m/s)

In addition to the above input, the time variable mass flux of injected gas (g/s) was specified in an additional time series file (note 1g/s = 0.95 T/day), the format of which follows the format of all CE-QUAL-W2 time series input. The main control file (W2_con.npt) was modified to allow specification of the internal file (oxygen file set to do_jpp.npt), and whether the time varying mass flux input were to be lineraly interpolated (O2IC set to ON), as illustrated below.

INTERPOL	**QINIC**	**TRIC**	**DTIC**	**HDIC**	**QOUTIC**	**WDIC**	**METIC**	**O2IC**
	ON	ON	ON	OFF	OFF	OFF	ON	ON

OXY FILE..... **OXYFN**.....
do_jpp.npt

The modified CE-QUAL-W2 was then applied, using the variable values specified above, to J. Percy Priest for the years 1981, and 1994. DO injections of 5 and 10 g/s for 1981 and 1994, respectively, were specified to occur between Julian days 150 to 250. For 1981, the resulting profiles near the dam are illustrated in Figure 62, and outflow concentrations in Figure 63. Similarly, for 1994 the resulting profiles near the dam are illustrated in Figure 64, and outflow concentrations in Figure 65. The two applications demonstrate the increase in hypolimnetic dissolved oxygen concentrations and outflow concentrations that could result from a dissolved oxygen injection. The predictions also demonstrate the variations in the magnitude of the injection that may be required between dry (1981) and wet (1994) hydrologic years.

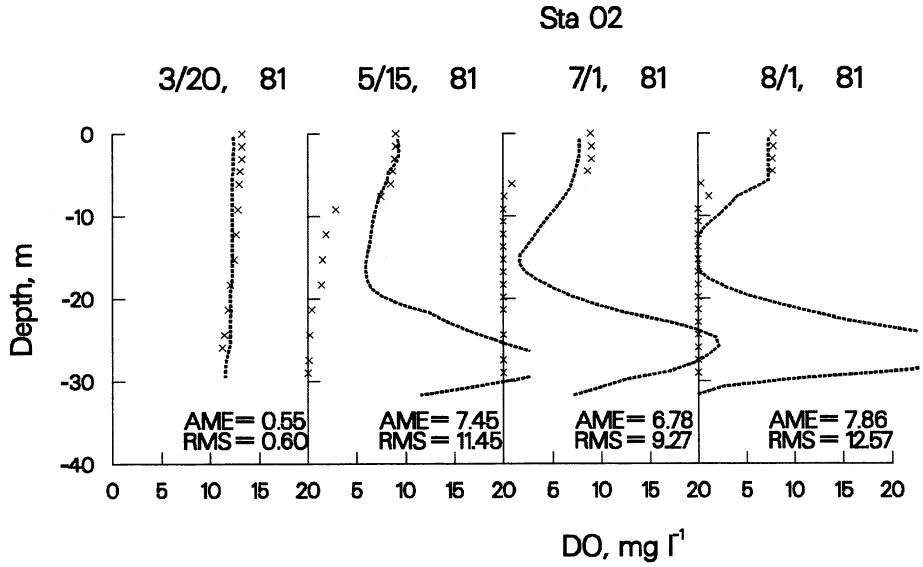

Figure 62. Predicted Dissolved Oxygen Profiles for 1981 at Station 20002 for a DO Injection of 5 g/s for the period of Julian Day 150 to 250.

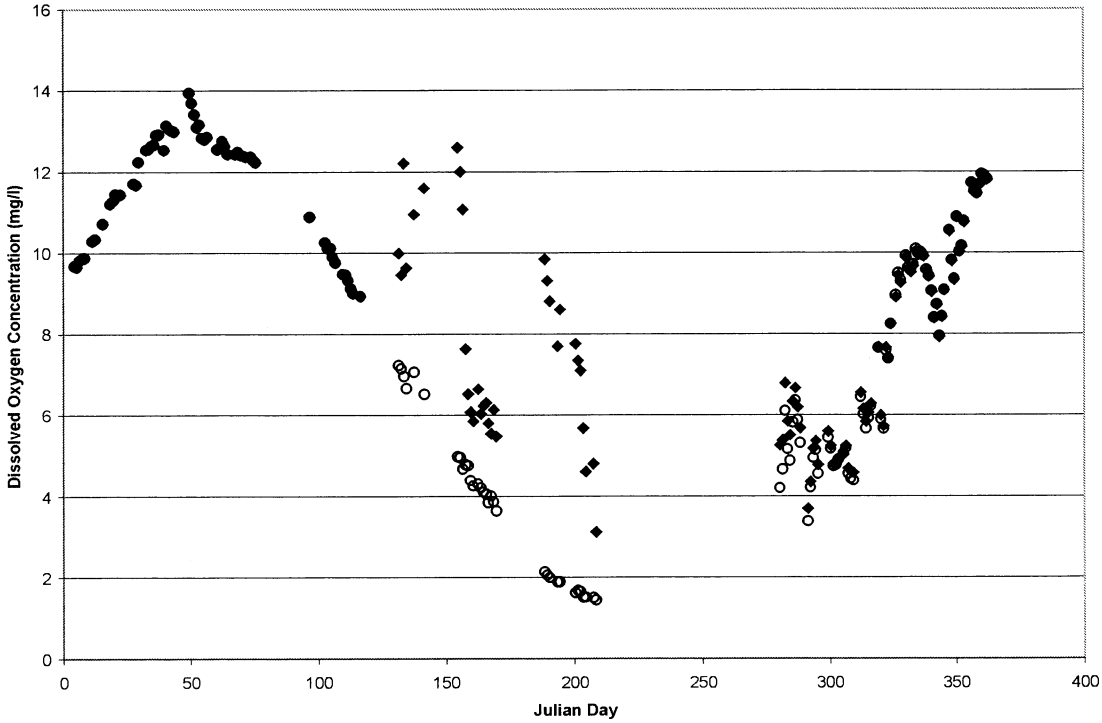

Figure 63. Predicted Dissolved Oxygen Outflow Concentrations for 1981 with (◆) and without (○) a DO Injection of 5 g/s for the period of Julian Day 150 to 250.

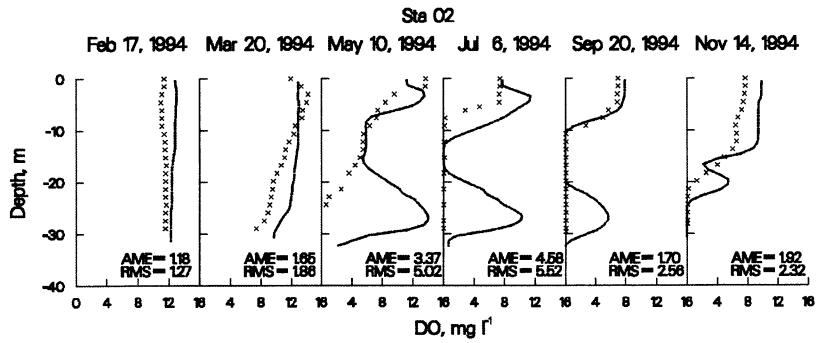

Figure 64. Predicted Dissolved Oxygen Profiles for 1994 at Station 20002 for a DO Injection of 10 g/s for the period of Julian Day 150 to 250.

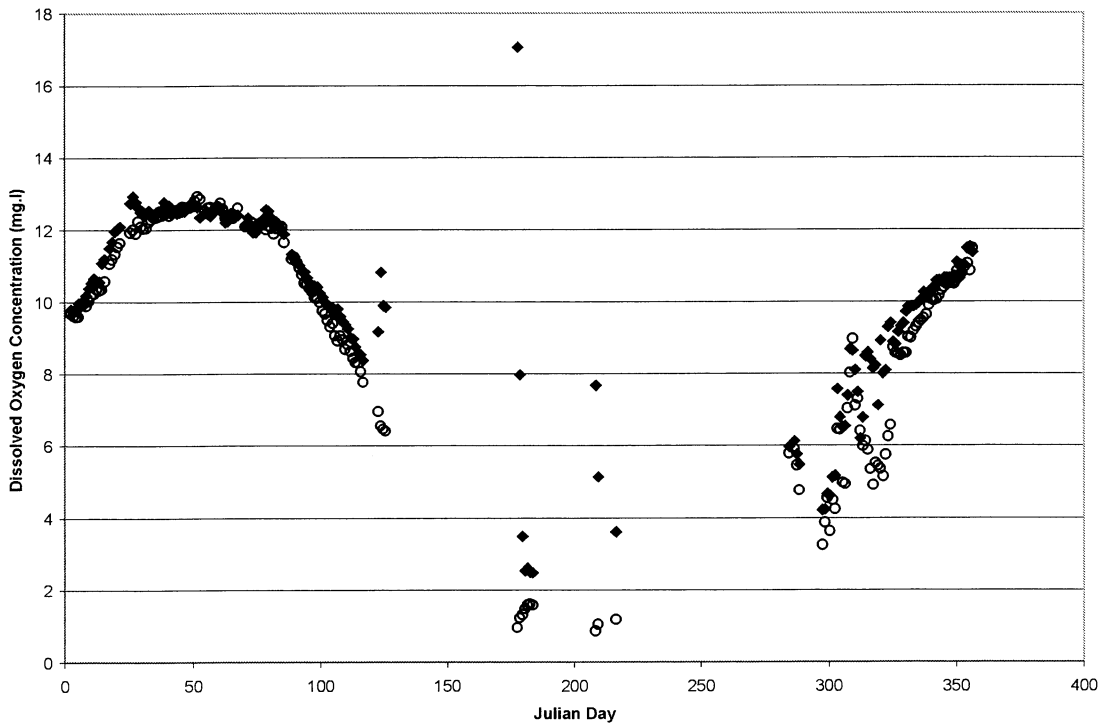

Figure 65. Predicted Outflow Dissolved Oxygen Concentrations for 1994 for a DO Injection of 10 g/s for the period of Julian Day 150 to 250.

6 Conclusions and Recommendations

A calibrated CE-QUAL-W2 model of J. Percy Priest has been developed suitable for addressing a variety of management related issues. The water quality model, while only a simplified description of what in reality is a very complex system, generally accurately predicted variations in temperature, dissolved oxygen concentrations, iron and nutrients, in comparison to observed data for the 5 years of simulation (1976-1978, 1981 and 1994). The 5 years represented hydrologic conditions ranging from dry (1981) to wet (1994). The model was then used to demonstrate two potential management related issues: an additional wastewater discharge to the reservoir, and a dissolved oxygen injection system. For the later scenario, the model was modified based upon a previous application to Richard B. Russell Reservoir.

For this application, none of the kinetic coefficients were varied between simulation years. Rather, a considerable portion of the effort required for the application consisted of determining a consistent set of kinetic coefficients for all years simulated. However, it is not entirely reasonable to assume that algal populations, sediment release rates, and other processes would be constant over the 18 year time span between the 1976 and 1994 applications. The collection of more recent data may provide a basis for additional calibration to present conditions.

While model predictions were in reasonable agreement with observed data, predictions were responsive to changes in loadings. However, inflows and loadings to the system were generally based on estimated, rather than measured, values. Errors in loadings were potentially greatest for the 1981 and 1994 simulation years, since the methods used to estimate the loadings were developed using data collected in the 1970's. Until such time as more recent data are collected, it is suggested that the best use of the model as a management tool would be to assess relative rather than absolute impacts of alternative management scenarios.

References

American Public Health Association, American Water Works Association, and Water Pollution Control Federation. (1981). *Standard Methods for the Examination of Water and Wastewater. 16th ed.,* Washington, DC.

Cole, T. M., and Buchak, E. M. (1995). "CE-QUAL-W2: A Two-Dimensional, Laterally Averaged, Hydrodynamic and Water Quality Model, Version 2.0," Instruction Report EL-95-1, US Army Engineer Waterways Experiment Station, Vicksburg, MS.

CELRN. (1978). "Water Quality Conditions in J. Percy Priest Reservoir, Nashville District, U.S. Army Corps of Engineers.

CELRN. (1999). J. Percy Priest Lake Cultural Resource Management Plan (Overview), U.S. Army Corps of Engineers, Nashville District's web site (http://www.orn.usace.army.mil/culture/cultural/jppv.htm)

Appendix A

The following plots are included to provide a more complete assessment of how well the model is capturing temporal and spatial trends in the water quality data. Plots in this section are provided for Station 3JPPS20003 and 3JJS20008 for the years 1976-1978.

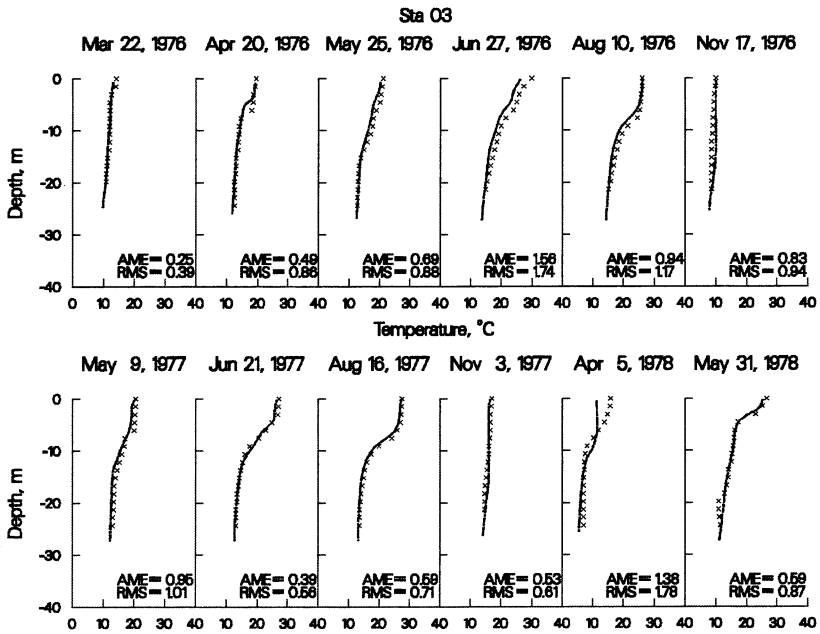

Figure A1. 1976-1978 Computed (...) vs. Observed (x) Temperatures at Station 3JPPS20003.

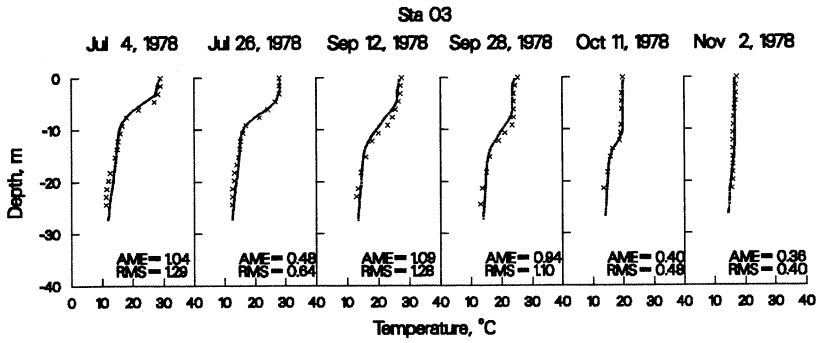

Figure A2. 1976-1978 Computed (…) vs. Observed (x) Temperatures at Station 3JPPS20003.

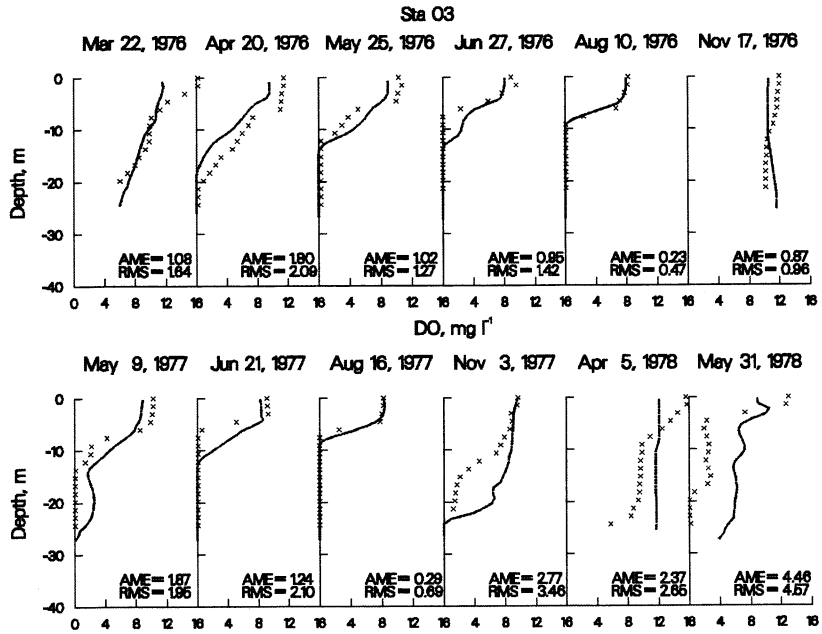

Figure A3. 1976-1978 Computed (…) vs. Observed (x) DO at Station 3JPPS20003.

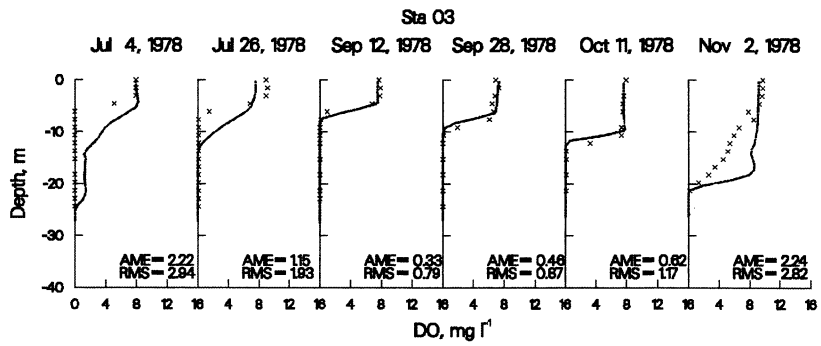

Figure A4. 1976-1978 Computed (…) vs. Observed (x) DO at Station 3JPPS20003.

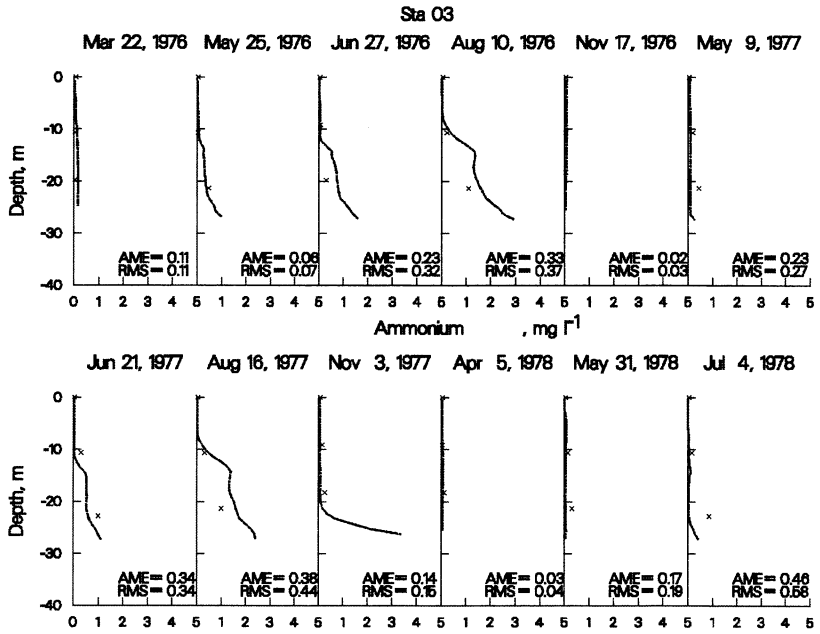

Figure A5. 1976-1978 Computed (…) vs. Observed (x) Ammonium at Station 3JPPS20003.

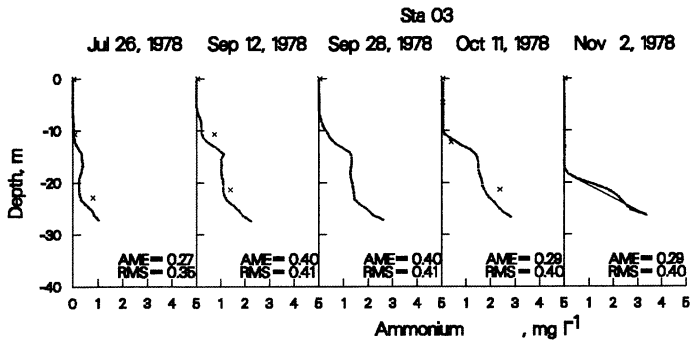

Figure A6. 1976-1978 Computed (…) vs. Observed (x) Ammonium at Station 3JPPS20003.

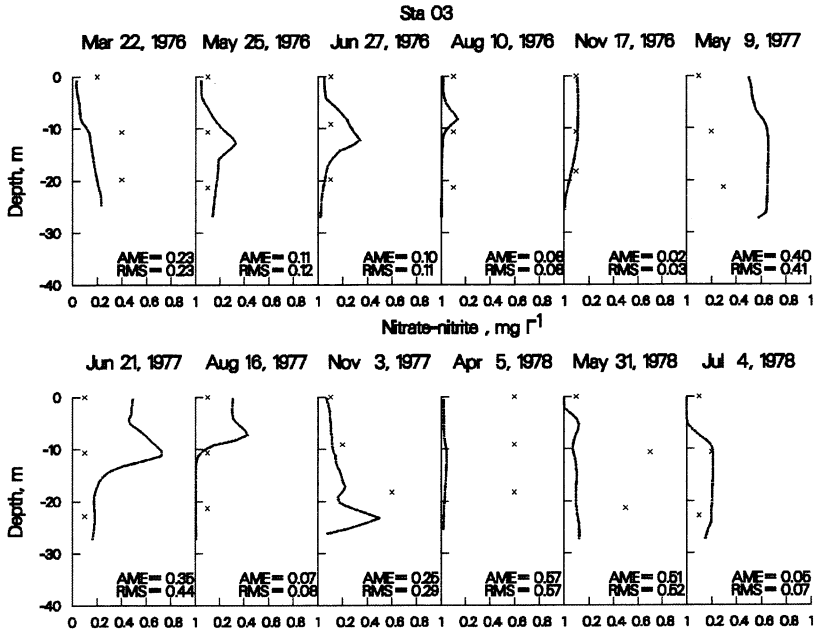

Figure A7. 1976-1978 Computed (…) vs. Observed (x) Nitrate-Nitrite at Station 3JPPS20003.

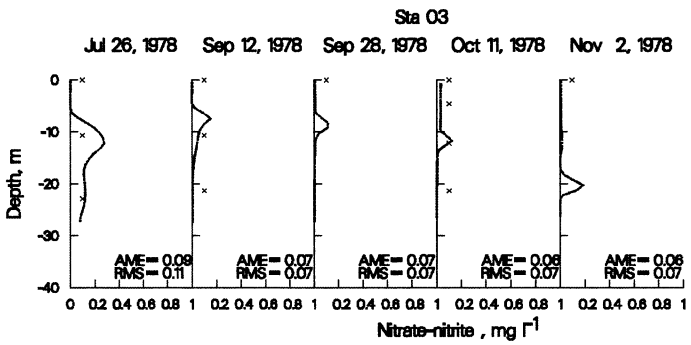

Figure A8. 1976-1978 Computed (…) vs. Observed (x) Nitrate-Nitrite at Station 3JPPS20003.

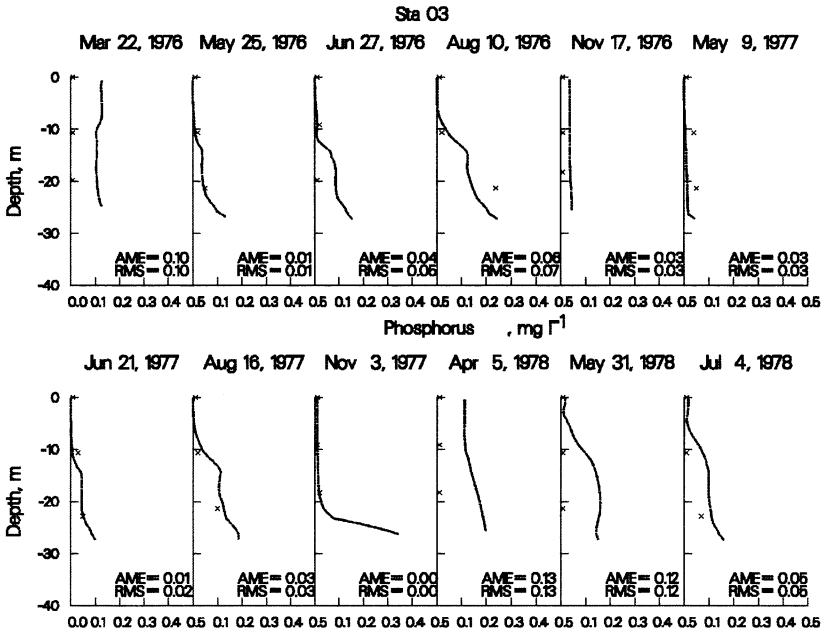

Figure A9. 1976-1978 Computed (…) vs. Observed (x) Phosphorus at Station 3JPPS20003.

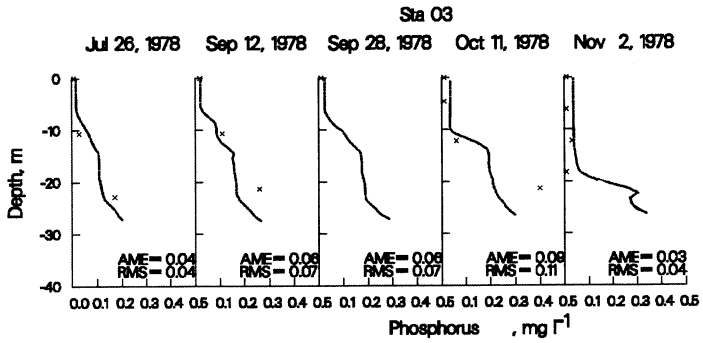

Figure A10. 1976-1978 Computed (…) vs. Observed (x) Phosphorus at Station 3JPPS20003.

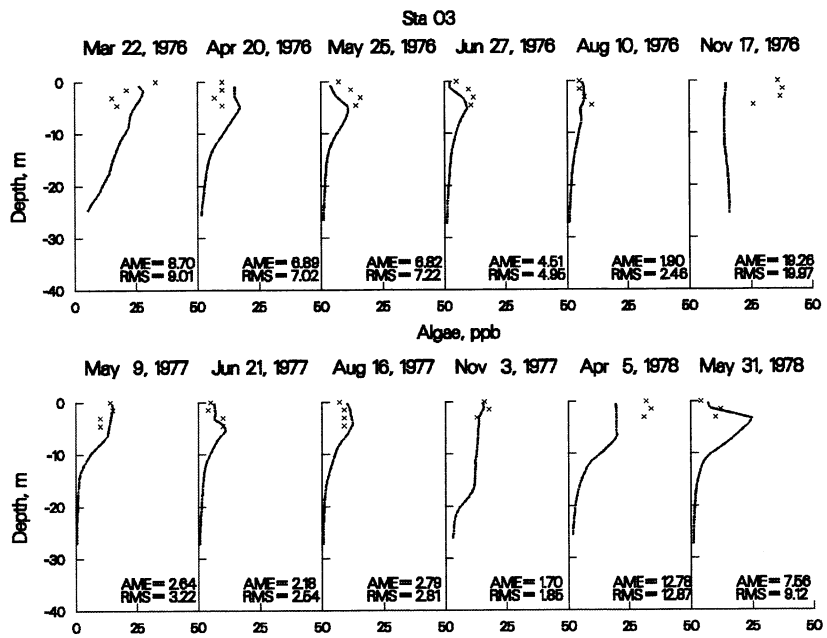

Figure A11. 1976-1978 Computed (…) vs. Observed (x) Algal Chlorophyll *a* at Station 3JPPS20003.

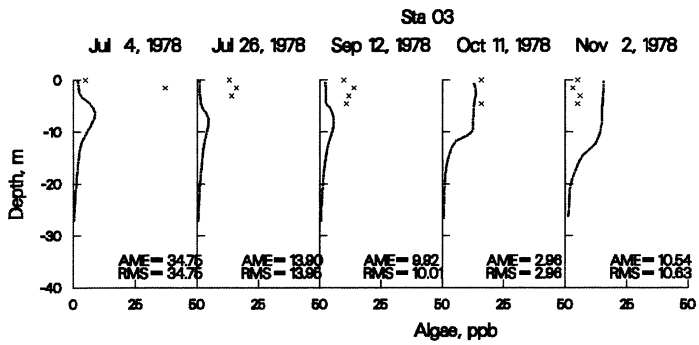

Figure A12. 1976-1978 Computed (…) vs. Observed (x) Algal Chlorophyll *a* at Station 3JPPS20003.

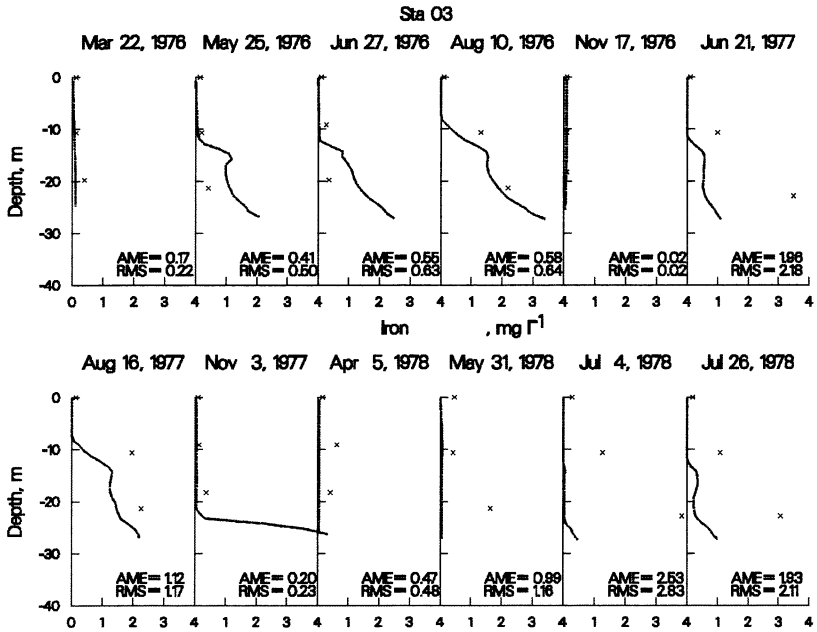

Figure A13. 1976-1978 Computed (…) vs. Observed (x) Iron Concentrations at Station 3JPPS20003.

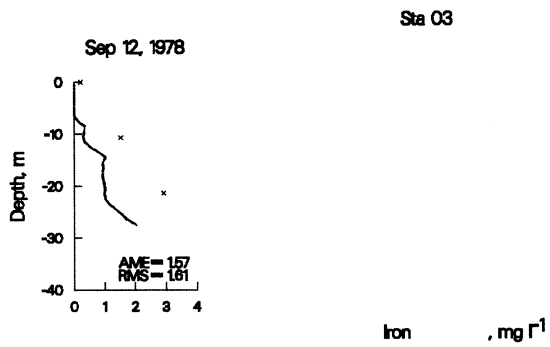

Figure A14. 1976-1978 Computed (…) vs. Observed (x) Iron Concentrations at Station 3JPPS20003.

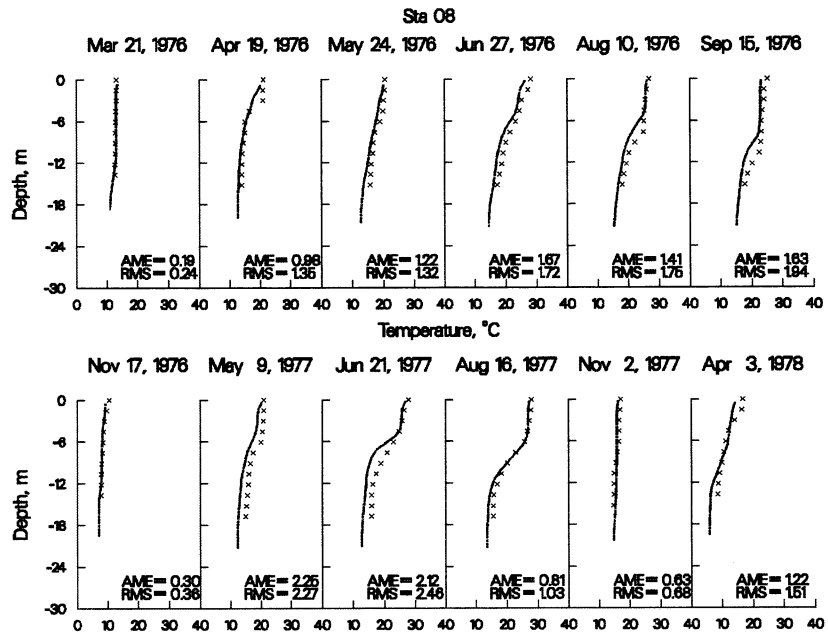

Figure A15. 1976-1978 Computed (…) vs. Observed (x) Temperatures at Station 3JPPS20008.

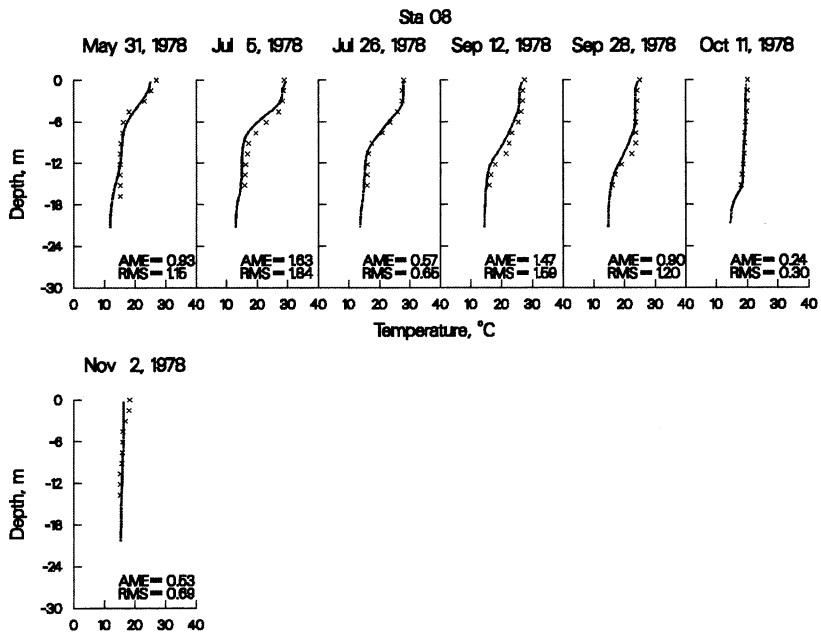

Figure A16. 1976-1978 Computed (…) vs. Observed (x) Temperatures at Station 3JPPS20008.

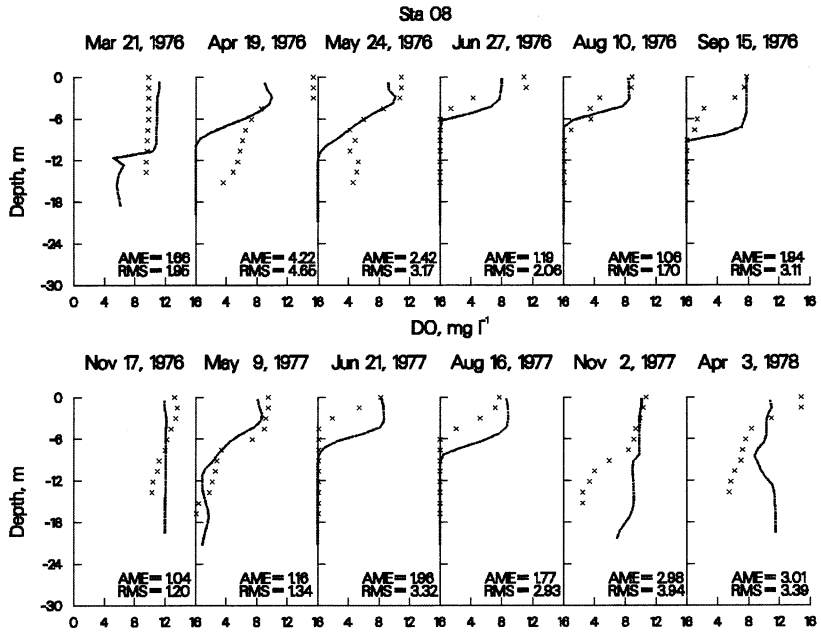

Figure A17. 1976-1978 Computed (…) vs. Observed (x) DO at Station 3JPPS20008.

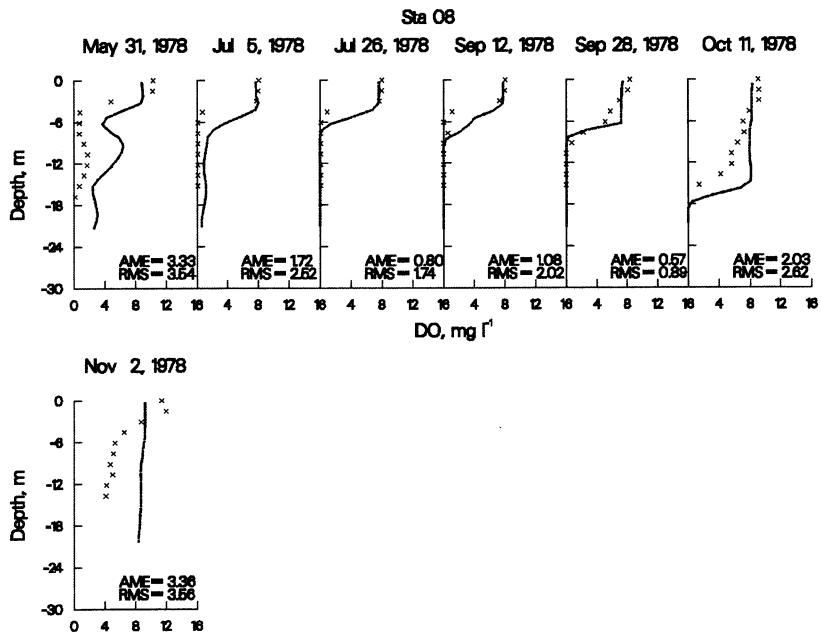

Figure A18. 1976-1978 Computed (…) vs. Observed (x) DO at Station 3JPPS20008.

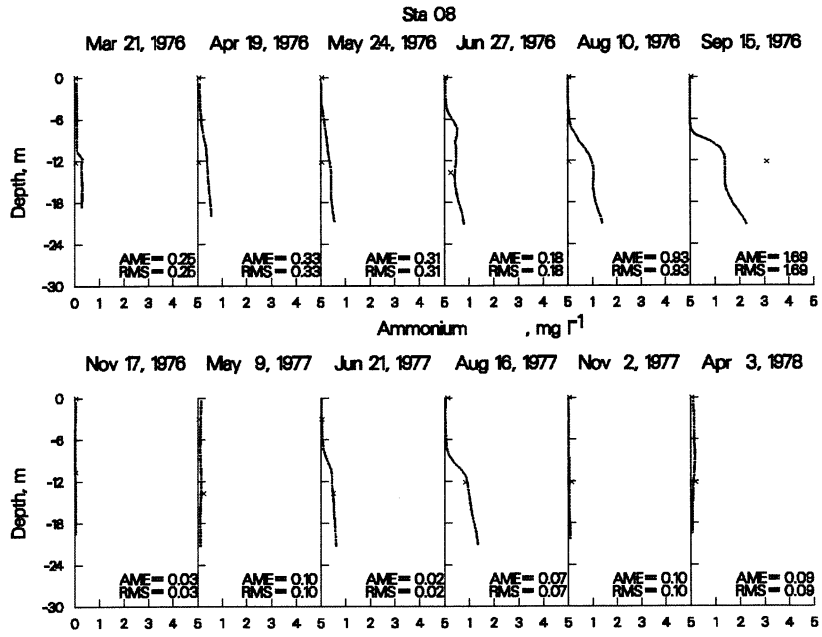

Figure A19. 1976-1978 Computed (…) vs. Observed (x) Ammonium at Station 3JPPS20008.

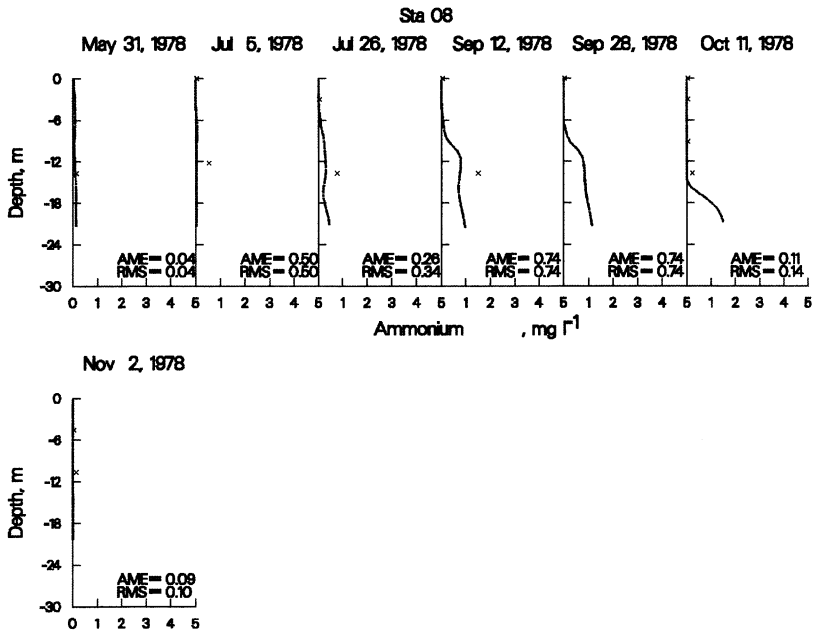

Figure A20. 1976-1978 Computed (…) vs. Observed (x) Ammonium at Station 3JPPS20008.

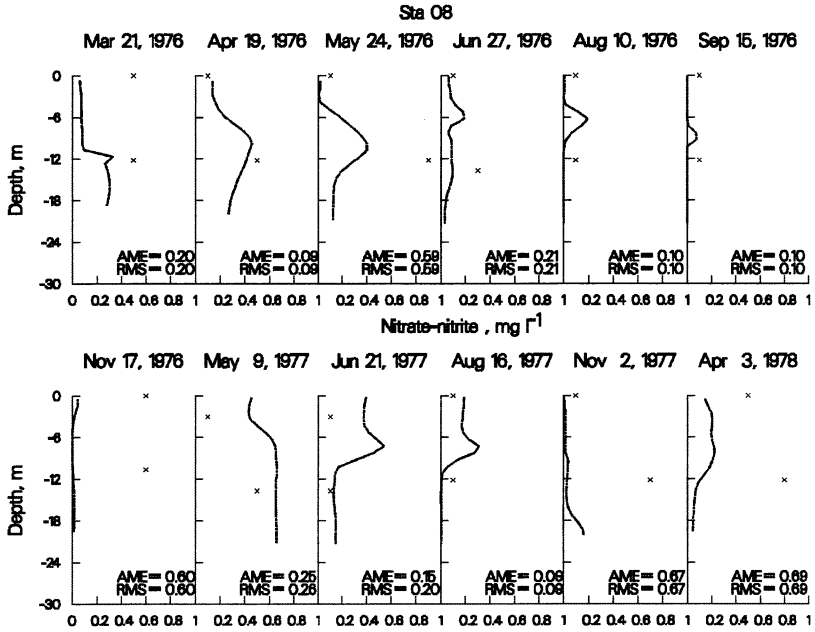

Figure A21. 1976-1978 Computed (…) vs. Observed (x) Nitrate-Nitrite at Station 3JPPS20008.

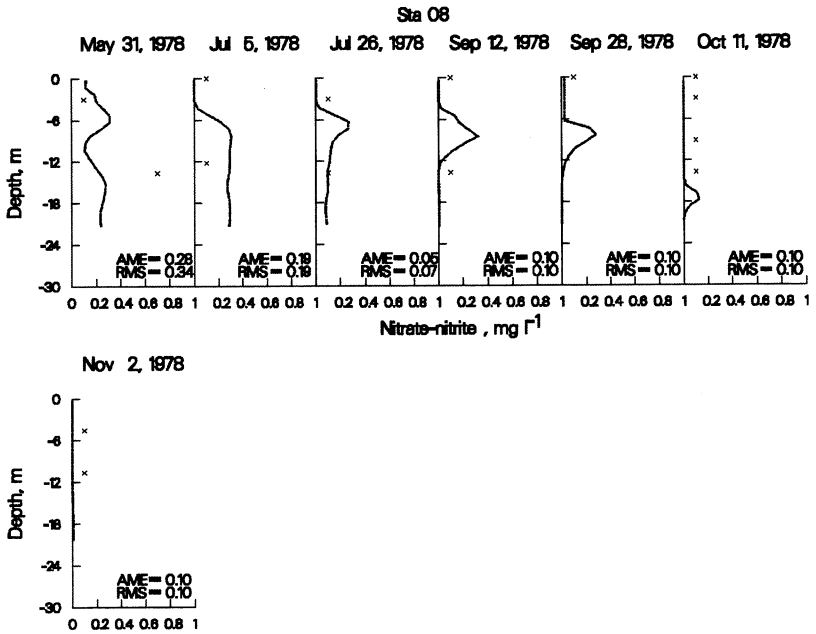

Figure A22. 1976-1978 Computed (…) vs. Observed (x) Nitrate-Nitrite at Station 3JPPS20008.

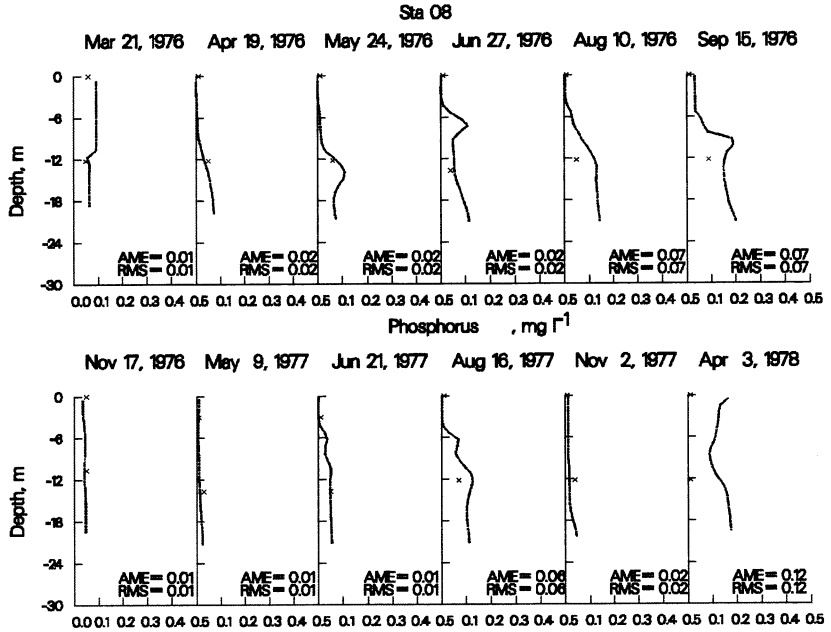

Figure A23. 1976-1978 Computed (…) vs. Observed (x) Phosphorus at Station 3JPPS20008.

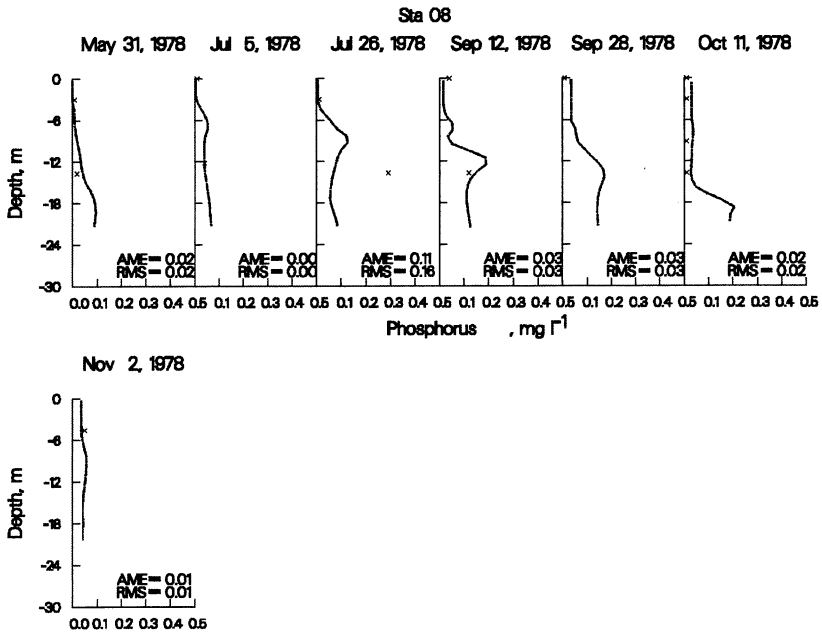

Figure A24. 1976-1978 Computed (…) vs. Observed (x) Phosphorus at Station 3JPPS20008.

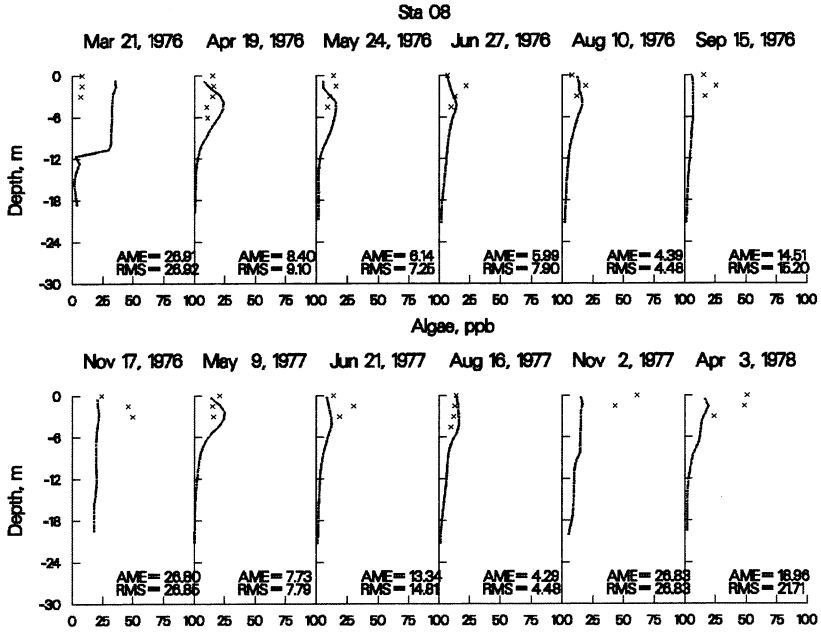

Figure A25. 1976-1978 Computed (…) vs. Observed (x) Algal Chlorophyll *a* at Station 3JPPS20008.

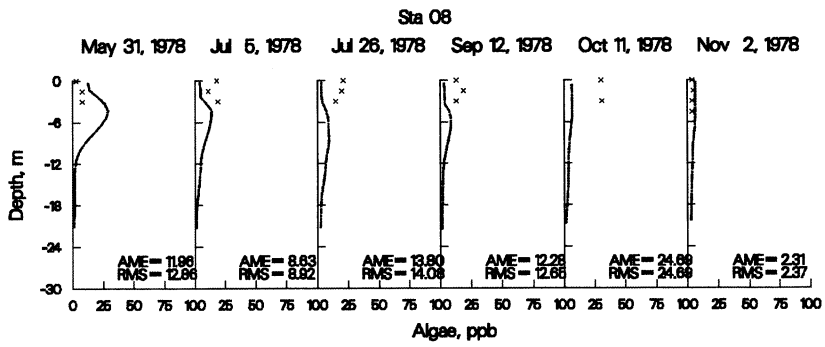

Figure A26. 1976-1978 Computed (…) vs. Observed (x) Algal Chlorophyll *a* at Station 3JPPS20008.

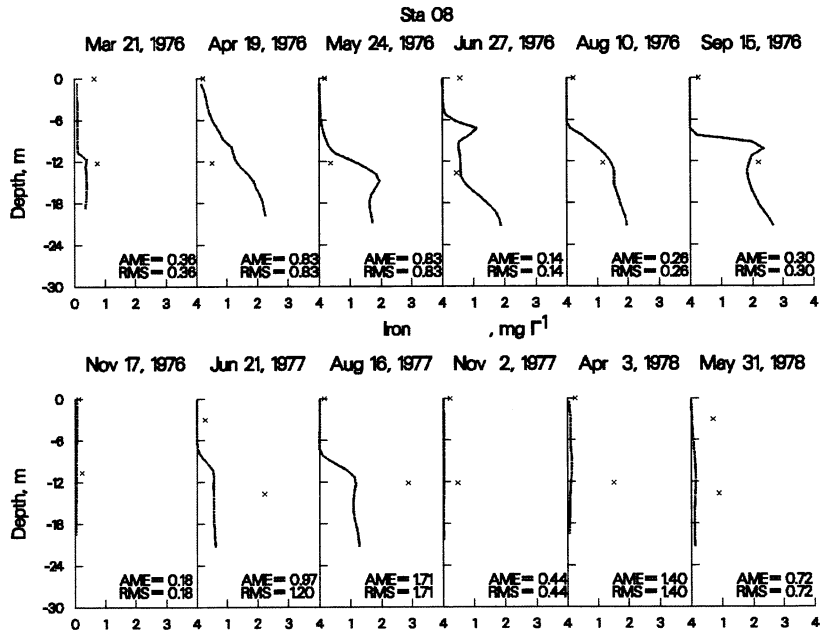

Figure A27. 1976-1978 Computed (…) vs. Observed (x) Iron Concentrations at Station 3JPPS20008.

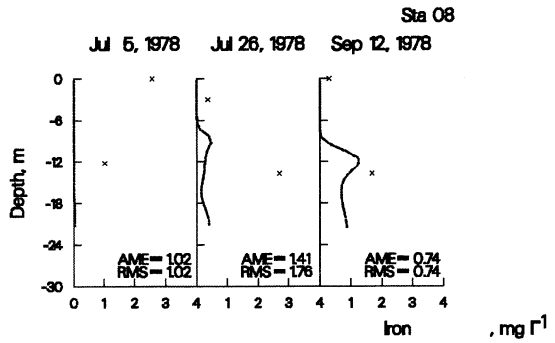

Figure A28. 1976-1978 Computed (…) vs. Observed (x) Iron Concentrations at Station 3JPPS20008.

Appendix B

The following plots are included to provide a more complete assessment of how well the model is capturing temporal and spatial trends in the water quality data. Plots in this section are provided for stations 3JPPS20003 and 3JPPS20008 for the year 1981.

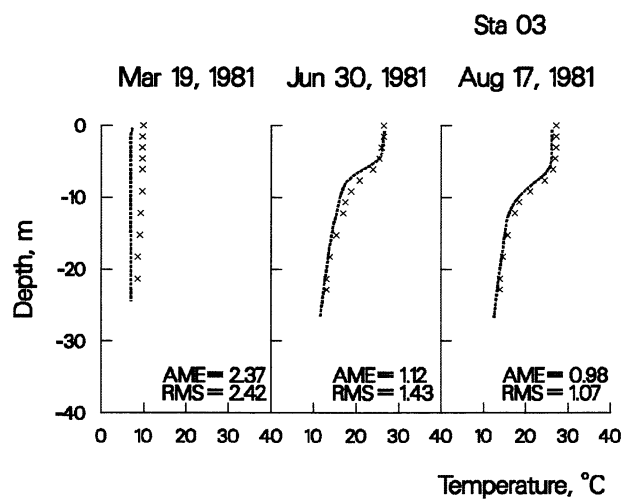

Figure B1. 1981 Computed (...) vs. Observed (x) water Temperatures at Station 3JPPS20003.

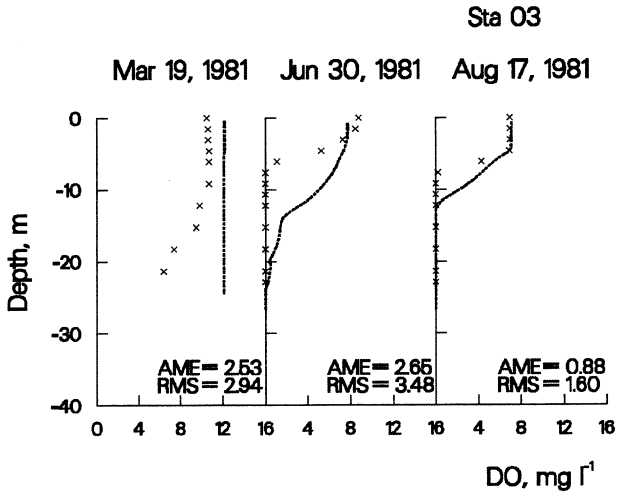

Figure B2. 1981 Computed (…) vs. Observed (x) DO at Station 3JPPS20003.

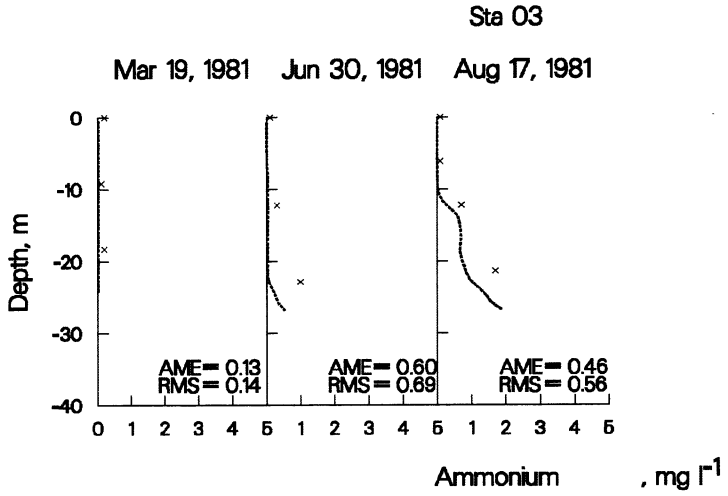

Figure B3. 1981 Computed (…) vs. Observed (x) Ammonium at Station 3JPPS20003.

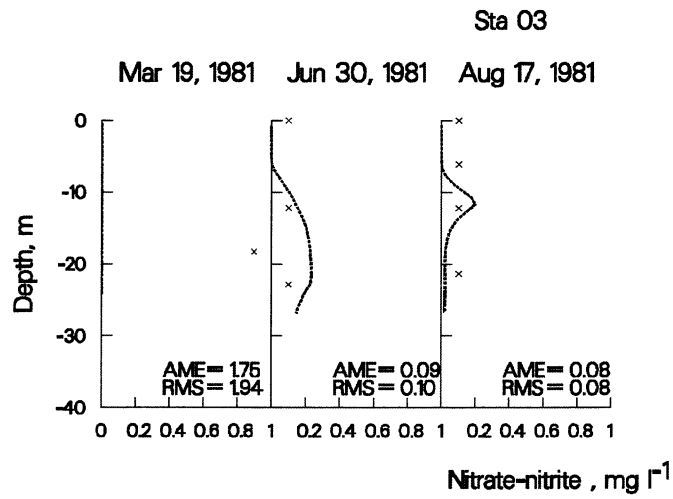

Figure B4. 1981 Computed (…) vs. Observed (x) Nitrate-Nitrite at Station 3JPPS20003.

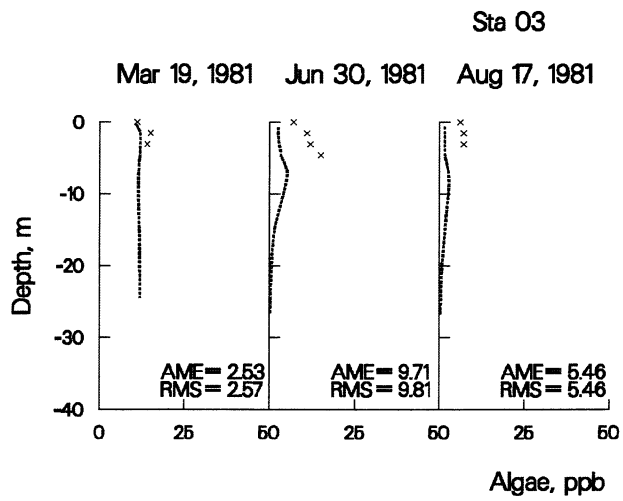

Figure B5. 1981 Computed (…) vs. Observed (x) Algal Chlorophyll *a* at Station 3JPPS20003.

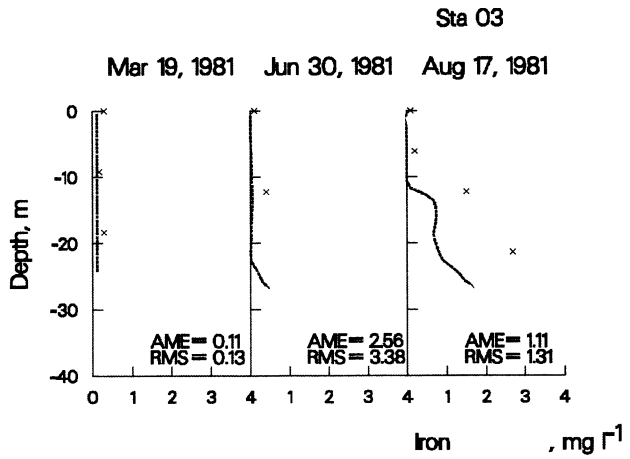

Figure B6. 1981 Computed (…) vs. Observed (x) Iron Concentrations at Station 3JPPS20003.

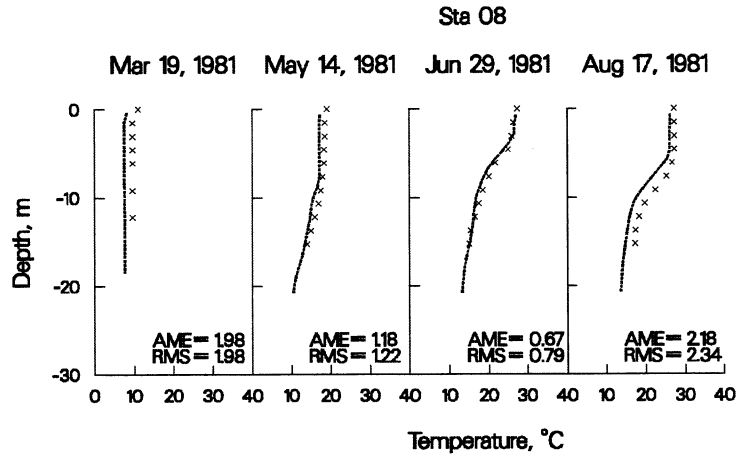

Figure B7. 1981 Computed (…) vs. Observed (x) water Temperatures at Station 3JPPS20008.

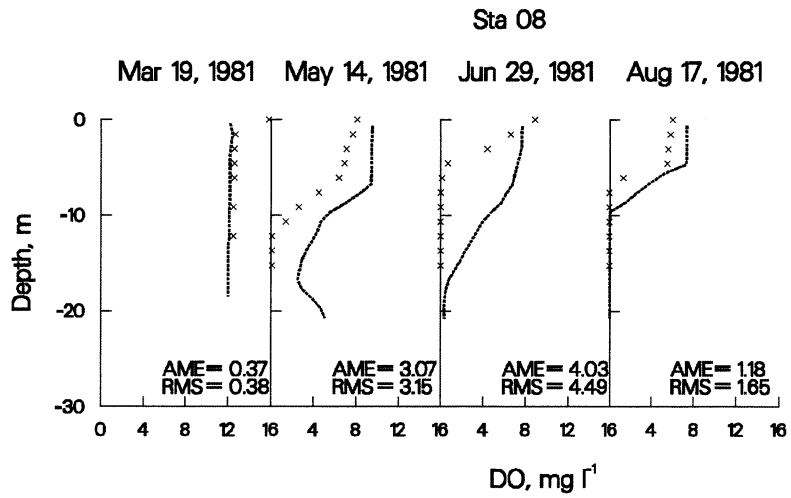

Figure B8. 1981 Computed (…) vs. Observed (x) DO at Station 3JPPS20008.

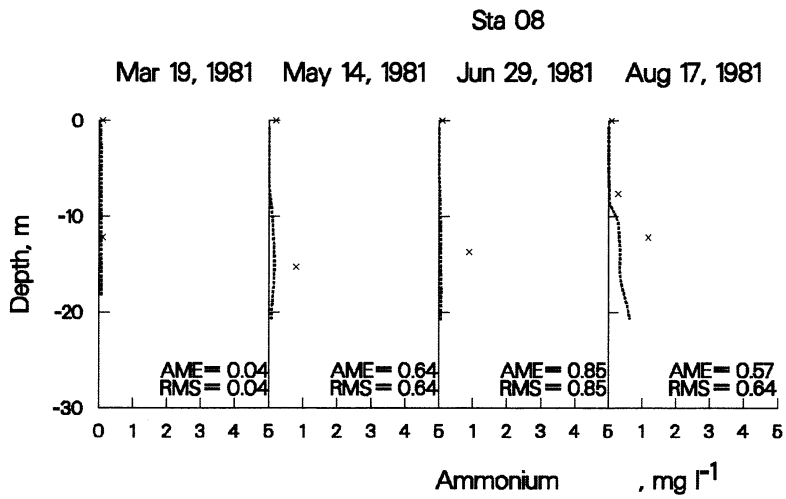

Figure B9. 1981 Computed (…) vs. Observed (x) Ammonium at Station 3JPPS20008.

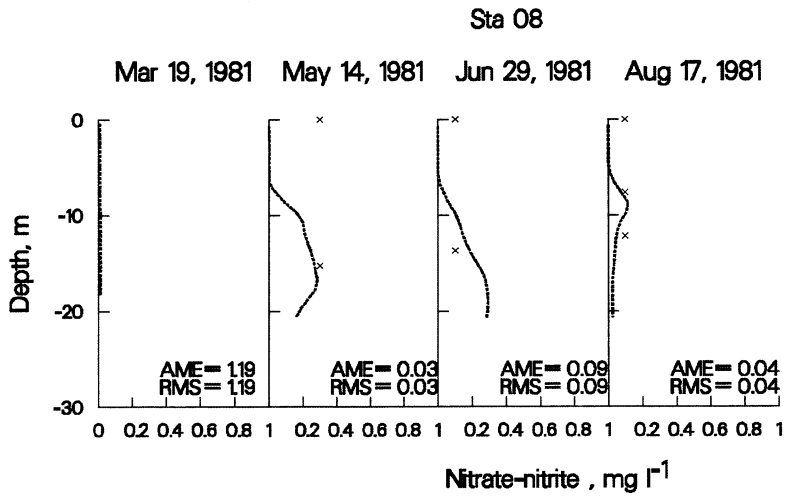

Figure B10. 1981 Computed (...) vs. Observed (x) Nitrate-Nitrite at Station 3JPPS20008.

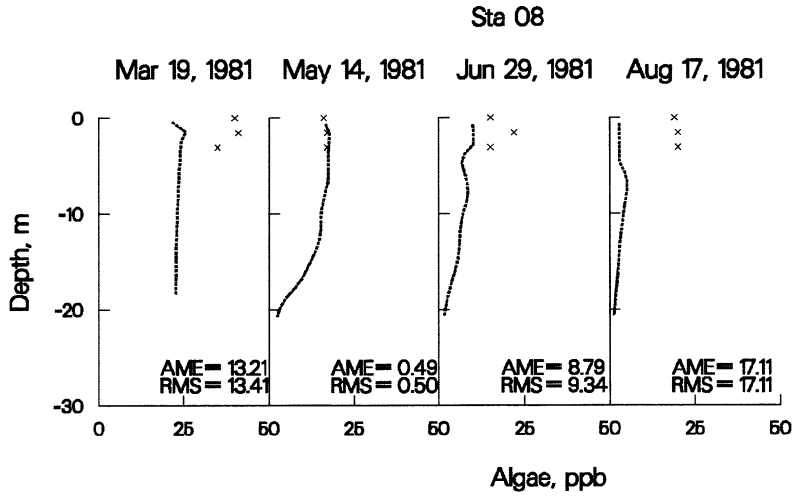

Figure B11. 1981 Computed (...) vs. Observed (x) Algal Chlorophyll *a* at Station 3JPPS20008.

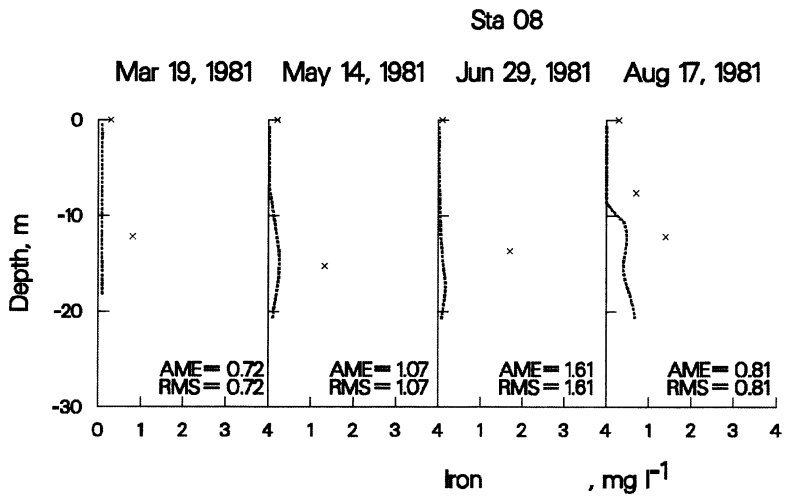

Figure B12. 1981 Computed (…) vs. Observed (x) Iron Concentrations at Station 3JPPS20008.

Appendix C

The following plots are included to provide a more complete assessment of how well the model is capturing temporal and spatial trends in the water quality data. Plots in this section are provided for Station 3JPPS20003 and 3JPPS20008 for the year 1994.

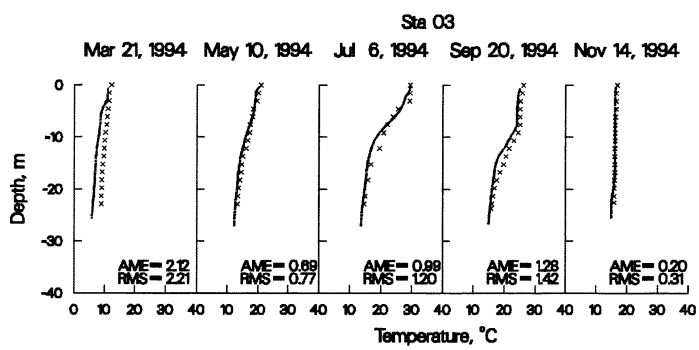

Figure C1. 1994 Computed (…) vs. Observed (x) Temperatures at Station 3JPPS20003.

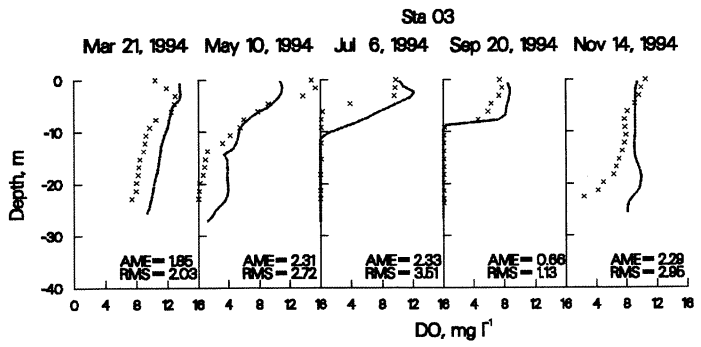

Figure C2. 1994 Computed (…) vs. Observed (x) DO at Station 3JPPS20003.

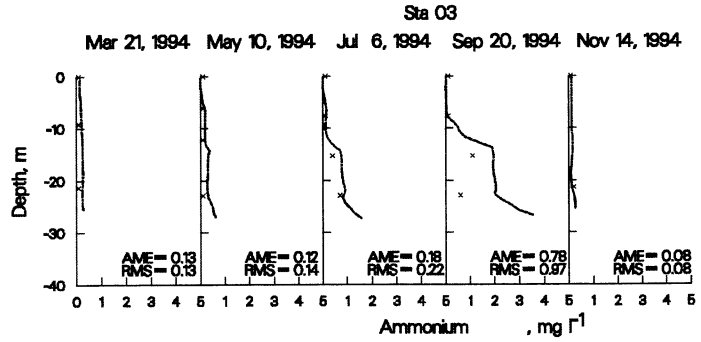

Figure C3. 1994 Computed (…) vs. Observed (x) Ammonium at Station 3JPPS20003.

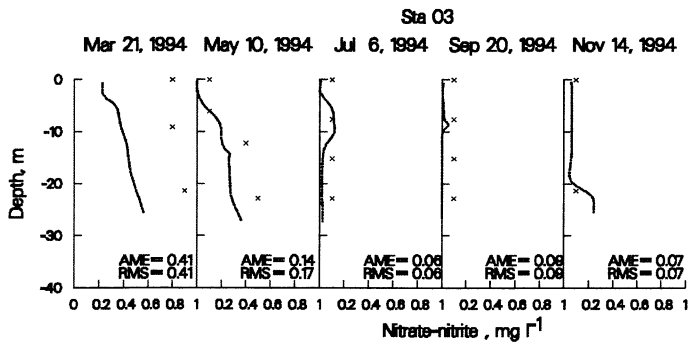

Figure C4. 1994 Computed (…) vs. Observed (x) Nitrate-Nitrite at Station 3JPPS20003.

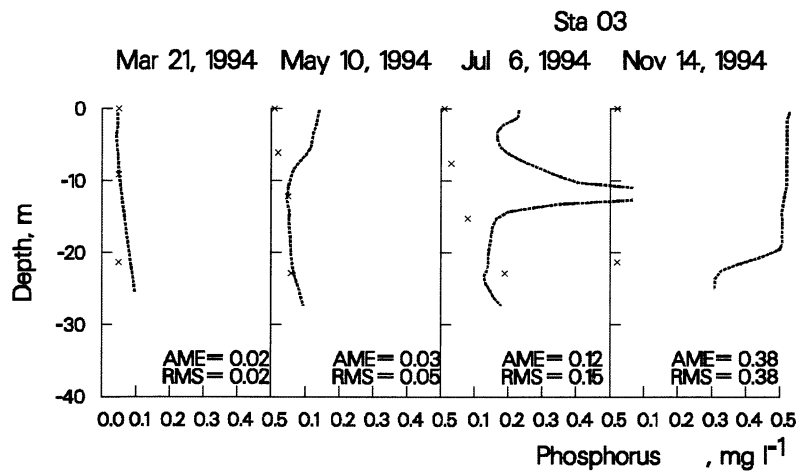

Figure C5. 1994 Computed (…) vs. Observed (x) Phosphorus at Station 3JPPS20003.

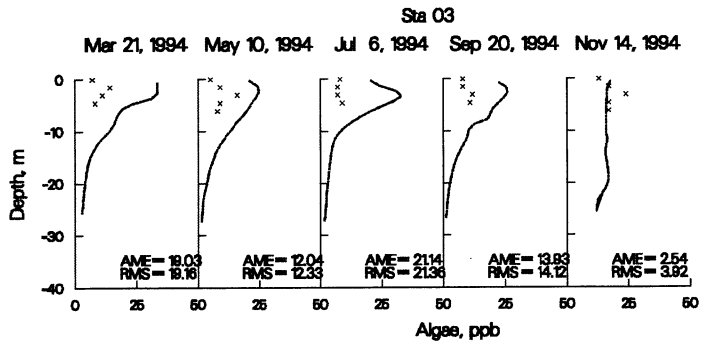

Figure C6. 1994 Computed (…) vs. Observed (x) Algal Chlorophyll *a* at Station 3JPPS20003.

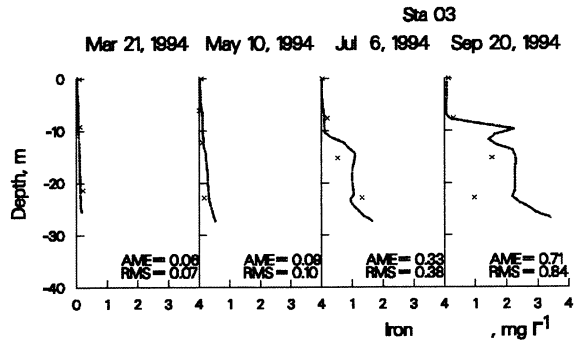

Figure C7. 1994 Computed (…) vs. Observed (x) Iron Concentrations at Station 3JPPS20003.

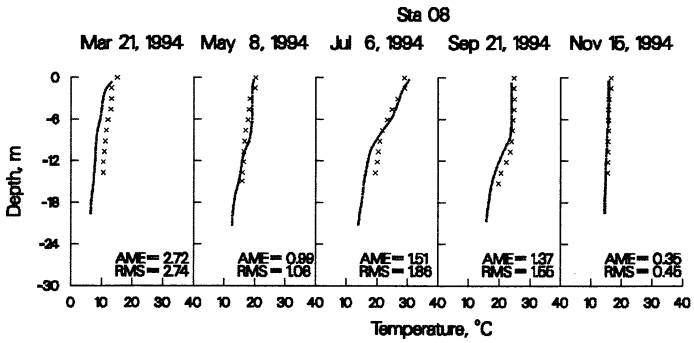

Figure C8. 1994 Computed (…) vs. Observed (x) Temperatures at Station 3JPPS20008.

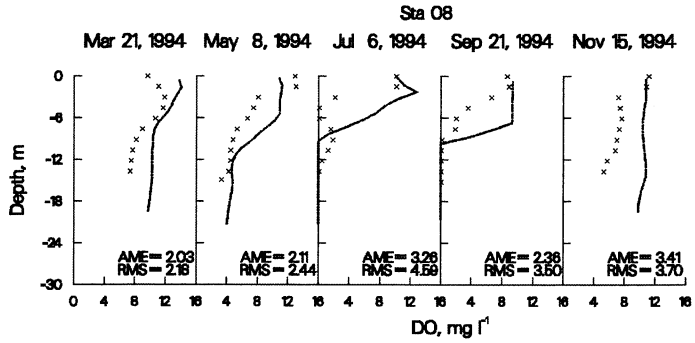

Figure C9. 1994 Computed (…) vs. Observed (x) DO at Station 3JPPS20008.

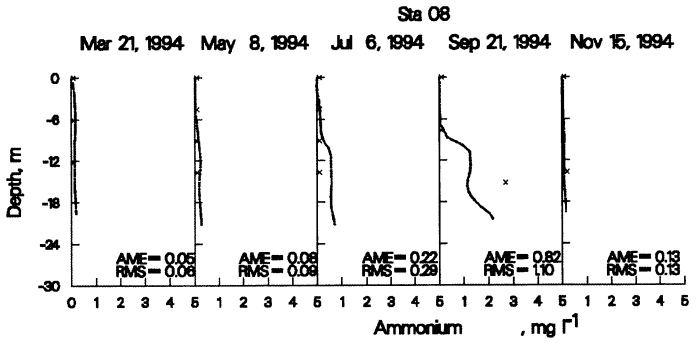

Figure C10. 1994 Computed (…) vs. Observed (x) Ammonium at Station 3JPPS20008.

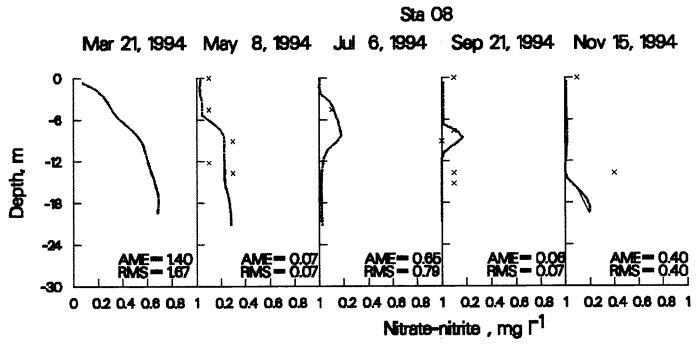

Figure C11. 1994 Computed (…) vs. Observed (x) Nitrate-Nitrite at Station 3JPPS20008.

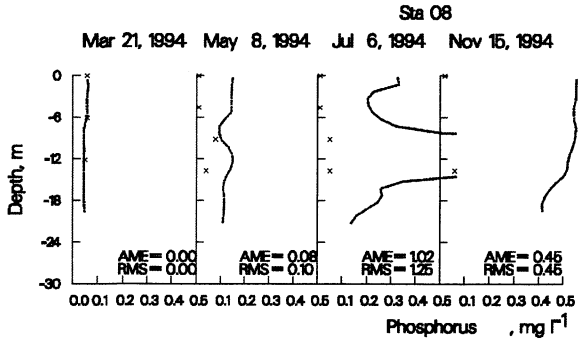

Figure C12. 1994 Computed (…) vs. Observed (x) Phosphorus at Station 3JPPS20008.

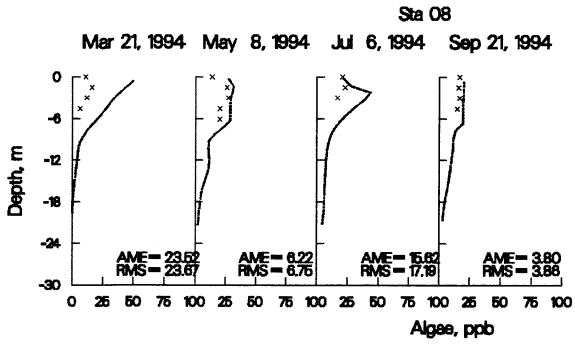

Figure C13. 1994 Computed (…) vs. Observed (x) Algal Chlorophyll *a* at Station 3JPPS20008.

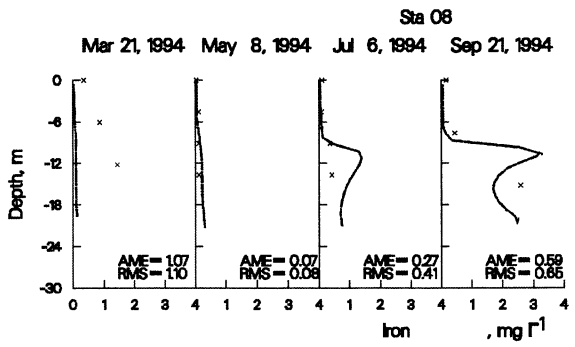

Figure C14. 1994 Computed (…) vs. Observed (x) Iron Concentrations at Station 3JPPS20008.